공학박사학위논문

Improvement of Hydrologic Model Parameter Estimation Using Hydrograph Section Separation and Uncertainty Analysis

수문곡선 구간분리와 불확실성 분석을 통한 수문 모형의 매개변수 추정 개선

2015 년 2 월

서울대학교 대학원

건설환경공학부

김 충 수

ABSTRACT

Improvement of Hydrologic Model Parameter Estimation Using Hydrograph Section Separation and Uncertainty Analysis

by Kim, Chung-Soo

Department of Civil and Environmental Engineering

Seoul National University

Prof. Kim, Young-Oh, Advisor

It is well known that parameter estimation in model simulation is an essential procedure that significantly affects simulation outputs. Nevertheless, there has not been a standardized methodology and procedure for parameter estimation. It is difficult to select and present the most optimal technique and scenarios for parameter estimation because of the uncertainties and variability in parameters. For these reasons, parameter estimation depends on a selected model, rainfall event, or a model user.

For estimating the parameters of a rainfall-runoff model, the problem that is of primary concern is to find the optimal solution accurately, but it is difficult to find the solution because an objective function would not be defined clearly or estimated parameters that use only a few number of rainfall events are not reliable.

Therefore, a generalization of parameter estimation procedure is necessary, and it should be able to consider the correlation of parameters and provide constant results without reference to model users and used models. In addition, the generalized procedure should consider the different characteristics of each rainfall event, such as the size of rainfall and the features of runoff, because the response modality of each model to each rainfall event is quite distinguished.

First, the existing parameter estimation used in practice was examined. In Korea, the initial value of parameters estimated by a “trial-and error” method based on each event for historical data has been used for flood forecasting. By examining the existing approach, the necessity of an improved parameter estimation method that could secure reliability in flood forecasting was raised.

In this study, a problem in parameter estimation for flood forecasting in Korea has been determined. In practical works, a conventional trial-and error method has been

used to estimate parameters based on historical data, and they are applied to a model as initial inputs for flood forecasting. The parameter estimation procedure urgently needs to be improved to enhance reliability in flood forecasting.

In order to resolve the problems, this study examined the efficiency in parameter estimation by using time-series input data rather than focusing on each event narrowly. Moreover, depending on a trial-and-error method was avoided, and instead, Shuffled Complex Evolution Metropolis of the University Arizona (SCE-UA), a global optimization method that provides the optimal parameter by estimating parameter sets, was used, and its results were analyzed and compared.

In particular, a hydrograph analysis that could reflect the characteristics of runoff as parameter estimation was proposed. For a more accurate and reliable parameter estimation, a hydrograph was divided into three sections at each inflection point: rising limb, crest, and falling limb. A proposed method in this study aims to provide a solution to a problem that has fluctuated in parameter estimation in accordance with the characteristics of rainfall events and runoff. In addition, Generalized Likelihood Uncertainty Estimators (GLUE), an uncertainty analysis method, was applied to present a range of parameters, and it was expected to contribute to the improvement of

estimation accuracy and to the enhancement of the applicability of estimated parameters.

The ultimate objective of this study is to improve the parameter estimation procedure, and the proposed methodology shows finding the optimal parameter that can satisfy the objectives of both peak discharge and discharge volume at the same time in consideration of the size of runoff and the discharge moving behavior.

Keywords: parameter estimation, global optimization, SCE-UA, hydrograph section separation, GLUE, optimal parameter

***Student Number*: 2005-30253**

TABLE OF CONTETNS

LIST OF TABLES

LIST OF FIGURES

LIST OF SYMBOLES

Latin Uppercase

A	Basin area (km^2)
E	Nash−Sutcliffe model efficiency coefficient
F_{sa}	Saturated runoff ratio
Ii	Inflow from the upstream of a river channel (m^3/s)
K , P	Coefficients of the storage function
K_r	Regression constant
N	Number of response variable sets
O	Direct runoff in consideration of lag time (m^3/s)
Q_o^i	Observed discharge at time i
$\overline{Q_o}$	Average of observed discharge
$Q_{obs,peak}$	Observed peak flow
$Q_{obs,vol}$	Observed total volume
Q_s^i	Simulated discharge at time i
$Q_{sim,peak}$	Simulated peak flow
$Q_{sim,vol}$	Simulated total volume

R_{sa}	Saturated rainfall at the saturation point
RE_p	Relative error of peak flow
RE_v	Relative error of volume
S	Actual storage in a river channel (m^3)
T	Temperature
T_l	Lag time
W_i	Weighting factor
$\overline{Y}$	Average of observed data
Y_t	Observed data

Latin Lowercase

f	Coefficient of average inflow
f_1	Rate of primary runoff prior to saturated runoff
n	Total number of observed data
p	Number of complexes
r_{ave}	Basin averaged rainfall per unit time (mm/hr)
t , t_i	Time
y_o	Observed discharge

$\overline{y_o}$	Average of observed discharge
y_c	Simulated discharge

Greek Uppercase

Θ	Feasible parameter space

Greek Lowercase

α	Rainfall multiplication ratio
θ	Parameter set

1. Introduction

1.1 Research Background

It should be preceded to estimate discharge and flood in a target basin for flood forecasting, water resources planning, and infrastructure design. Hydrologic techniques, such as a unit hydrograph derived from the relationship between historical rainfall and discharge data, can be used to estimate discharge and flood volume. In general, it is commonly accepted that flood estimation through the application of a rainfall-runoff model can be more reasonable and appropriate because a model simulation is based on the nature. To simulate natural phenomenon accurately, it is required to improve a limitation which is a model based on mathematical and physical theories that could not reproduce the nature perfectly. In case of a conceptual model used a concept of parameters to improve this limitation that a model simulation has. Since the 2000s, a rainfall-runoff model based on a physical theory has been able to reproduce the nature, and it can reflect improved geographical information and

hydrological variables in a basin to minimize the uncertainties of parameters and a bias of simulations.

Although there have been efforts to simplify parameter estimation in a physics-based distributed model, it is still highly important to verify and adjust the initial parameters estimated by geomorphological data and hydrological characteristics because these initial parameters definitely affect the accuracy and reliability of model simulation outputs. Nowadays, to estimate parameters, a trial-and-error method in the early stage of development of a rainfall-runoff model has been generally used, and there are several other methodologies, such as Genetic Algorithm (GA) and Neural Network Algorithm. Nevertheless, there is no standardized technique and procedure for parameter estimation, and it is likely to be applied differently according to a selected model, rainfall events, or a model users as it is difficult to select and present the most optimal technique and scenarios for parameter estimation because of the uncertainty and variability of parameters.

For estimating parameters, the problem that is of primary concern is to find the optimal solution accurately, but it is difficult to find the solution because an objective function would not be defined clearly or estimated parameters that use only a few

number of rainfall events are not reliable. Even if an objective function is configured properly, typical methods that are used generally, such as the trial-and-error method, are able to bring about local problems. For these reasons, the results of parameter estimation are different, depending on the model users or the characteristics of rainfall events.

The sensitivity analysis is a part of the parameter estimation procedure and a primary factor for each model. Sensitivity analysis is an important step for the improvement of the reliability of parameter estimation results. A general method of sensitivity analysis is to quantify how the sensitivity and uncertainty in the model outputs can be apportioned to each of the estimated parameters; however, this approach does not consider the correlation of parameters and the propagation impacts in a model. These problems hinders finding the optimal solution and causes local problems in parameter estimation.

Therefore, an improved parameter estimation that can consider the correlation of parameters and provide constant results without reference to model users and used models is necessary. In addition, an improved methodology should be able to consider the different characteristics of each rainfall event, such as the size of rainfall, runoff,

and the features of runoff because the response modality of each model to each rainfall event is quite distinguished.

In short, the ultimate goal of this research is to improve the results of parameter estimations for a hydrologic model. For this, a global optimization method that reflects the correlation among parameters is used to present the optimal parameter set. Moreover, uncertainty analysis is conducted to improve the reliability in parameter estimation. Furthermore, Hydrograph Section Separation (HSS), a newly proposed methodology, is introduced. In brief, HSS is a new approach for parameter estimation, which can satisfy both peak flow and total discharge by simulating a rainfall-runoff model and, at the same time, reflect the characteristics of runoff on a hydrograph.

1.2 Research Objectives and Scope

The objectives of this research are to examine the existing problems in parameter estimation for flood forecasting in field-works and suggest a methodology to provide a solution to those problems. In detail, this research show finding optimal parameters

and aims to present a reasonable range for the parameters that are actually used for flood forecasting. Moreover a new method is proposed to estimate appropriate parameters, which can be applied constantly without being affected by the features of rainfall events.

Briefly, the objectives of this research are described as follows:

(1) Determine current problems in the existing parameter estimation approach for flood forecasting in field practices, and propose a parameter estimation methodology to improve them

(2) Estimate the parameters for each divided section (rising limb, crest, and falling limb) on a hydrograph to reflect the characteristics of runoff according to change in time and verify the superiority of the proposed methodology

(3) Estimate the optimal parameter by applying a global optimization method and present their reasonable range by conducting an uncertainty analysis so that model users would have a choice on parameters for practical works

In Korea, for practical works, a trial-and-error method has been applied to estimate the initial values of parameters based on each historical rainfall event, and these values are used for flood forecasting. However, this approach does not consider the uncertainties in parameter estimation and only depends on each fragmentary event without taking into consideration time-series data. The current approach would lower the reliability of estimated parameters.

In this research, time-series data for all the historical observations were used to extend the scope of applicable rainfall events for parameter estimation instead of using each single event individually. Moreover, instead of the trial-and-error method, a global optimization method that could estimate the parameter set simultaneously was used to provide the optimal parameter, and uncertainty analysis was conducted to present the range for the optimal parameter set.

In addition, a hydrograph is examined by dividing it into three sections according to two inflection point on a hydrograph. It is expected that this proposed methodology can improve reliability in parameter estimation for a rainfall-runoff model regardless of a period of rainfall event and the number of events. Moreover, it is expected that

accuracy in parameter estimation is improved because each divided section at inflection points can reflect the response patterns of runoff.

In this research, a new approach for the estimation of parameters for each section by dividing a hydrograph into three parts is proposed, and it can be applied to flood forecasting for practical works. Figures 1.1 and 1.2 show a flowchart and a framework, respectively, of the research. Moreover, a conceptual diagram of the research is shown in Figure 1.3.

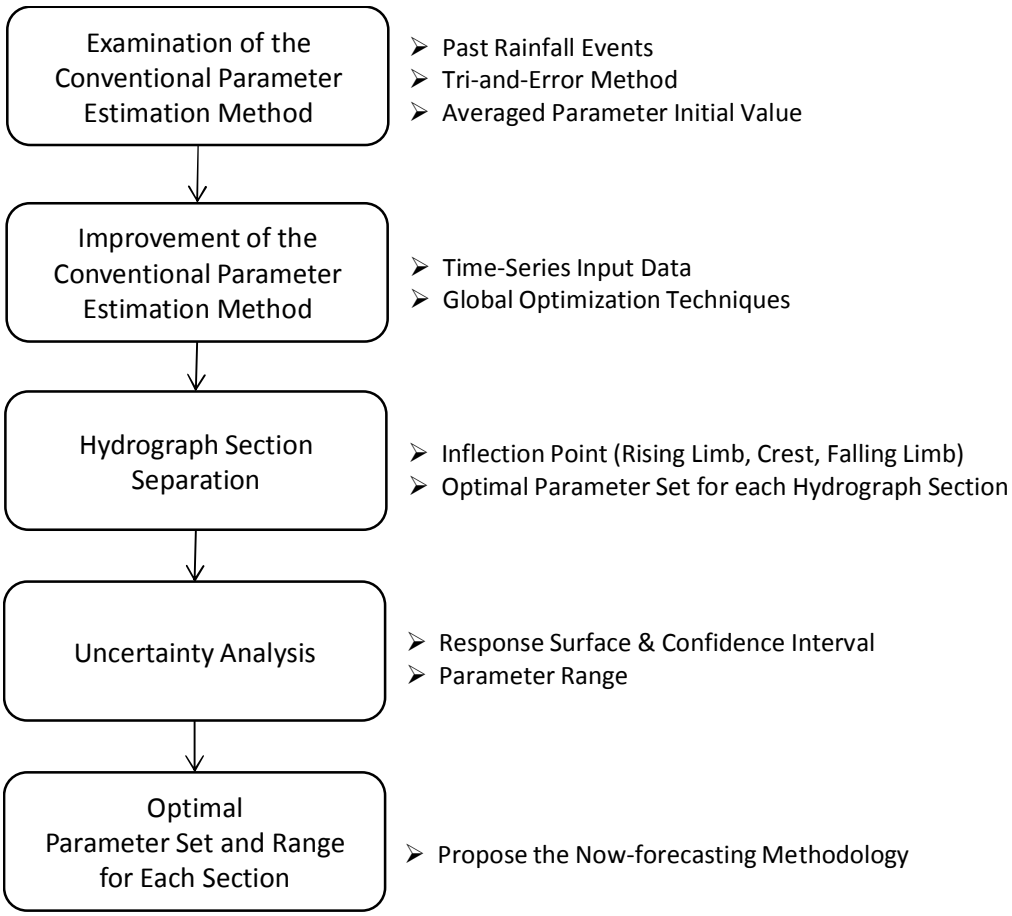

Figure 1.1 Flowchart of the research

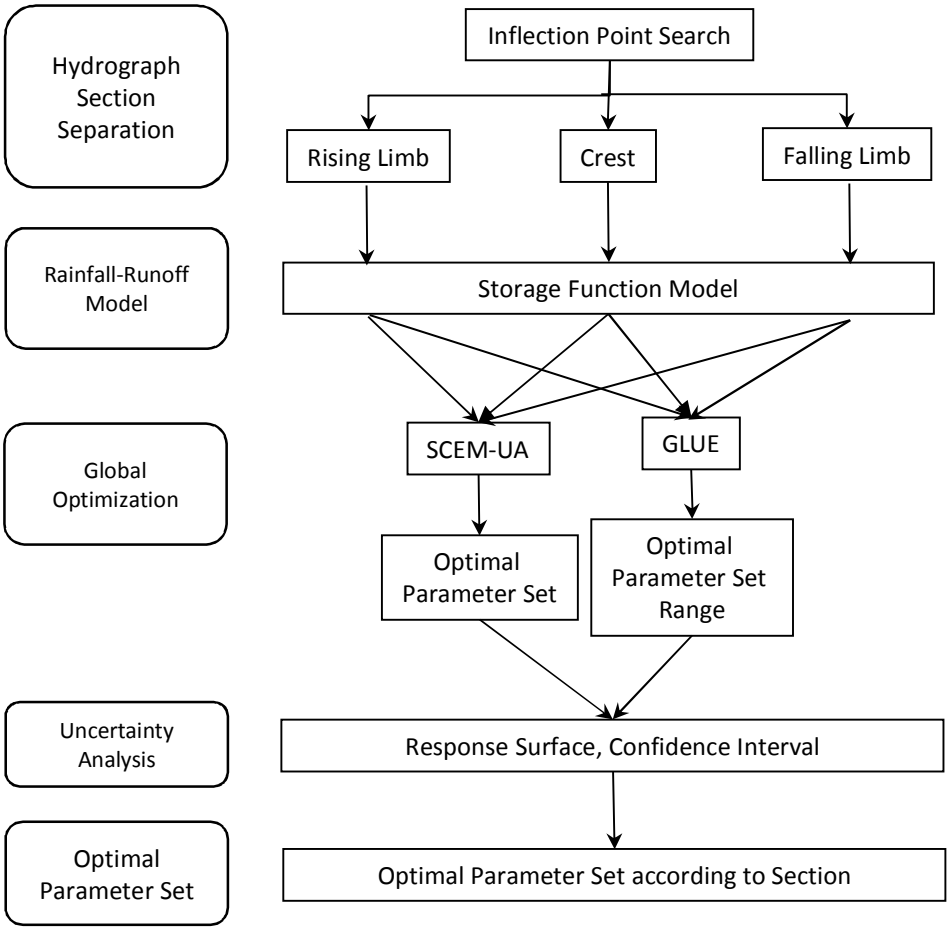

Figure 1.2 Framework of the research

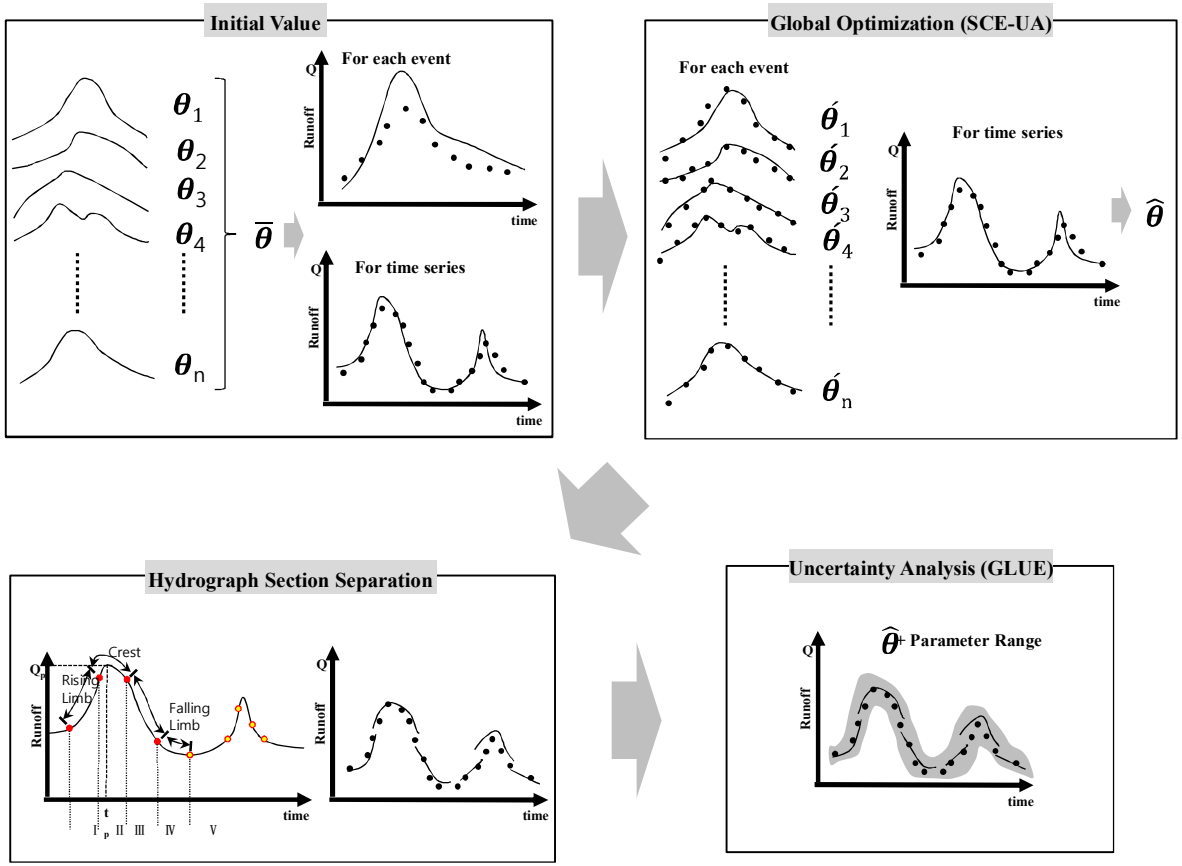

Figure 1.3 Conceptual diagram of the research

1.3 Research Organization

In Chapter 2, a research review on existing parameter estimation methodologies for the hydrologic model, uncertainty analysis methods, and hydrograph separation techniques is conducted. Chapter 3 describes the theoretical background on the storage function model, formulation of the objective function, global optimization, and the concept of HSS. Then, information on study basin and hydrological features for application is described in Chapter 4.

In earnest, existing problems in parameter estimation at field-works in Korea are determined and a methodology for improving them is proposed in Chapter 5. In Chapter 6, HSS, the application process of a proposed methodology, and its results on parameter estimation are determined and analyzed. Moreover, Chapter 7 provides a range for the optimal parameter set through uncertainty analysis in parameter estimation and discusses on how the results estimated by conducting HSS, global optimization, and uncertainty analysis can be used in real-life practical works. Finally, a summary of the research and the conclusions are described, and future study is discussed.

2. Literature Reviews

In this section, literature reviews on the formulation of the objective function, global optimization, hydrograph separation, and uncertainty analysis were conducted to help in understanding existing general procedures for parameter estimation and to determine the trend of preceding researches.

2.1 Parameter Estimation for Hydrologic Model

2.1.1 Formulation of the Objective Function

Klepper et al. (1991) composed a number of optimal parameter sets, called "acceptable parameter sets", using a single-objective function in the calibration procedure for a rainfall-runoff model. They insisted that it is more reasonable and efficient to select certain parameters from acceptable parameters sets instead of using optimized parameters based on a single-objective function. Yapo et al. (1998) pointed out the necessity of parameter calibration in rainfall-runoff models using a multi-objective function and proposed that a number of optimized parameter sets obtained using a multi-objective function are provided to model users temporally and spatially.

In addition, Gupta el al. (1998) used six objective functions to calibrate parameters in the Sacramento Soil Moisture Accounting (SAC-SMA) model and computed the Pareto solution eventually. Madsen (2000) used four objective functions and the Shuffled Complex Evolutionary (SCE) algorithm to calibrate parameters in the MIKE11 model, and computed the Pareto solution. Liong et al. (2001) calibrated parameters in the HydroWorks model using a multi-objective function that consist of the relative biases of peak discharge and discharge volume, and computed the Pareto solution. In particular, Liong et al. (2001) developed the Accelerated Convergence Genetic Algorithm (ACGA) and proposed a methodology that could improve the accuracy of the Pareto solution by integrating the ACGA and the artificial neural network theory.

In Korea, Kang et al. (2002) calibrated parameters in the TANK model automatically and found that the application that uses multi-objective function composed of the Daily Root Mean Square (DRMS) and the Nash-Sutcliffe measure showed forecast results, giving more weight to low flow than the application result that uses single-objective function. Moreover, Sung et al. (2004) applied the Simplified Version of the HYDROLOG Model (SIMHYD) model and TANK models to the

Soyanggang dam and the Yeongcheon dam basins with three objective functions and three optimization techniques, respectively, and assessed the suitability of the comparison of the Nash-Sutcliffe model efficiency coefficients as an objective function was changed.

Over the past recent years, population-based search algorithms have shown to be powerful search methods for multi-objective optimization problems and have been applied for multi-objective rainfall-runoff model calibration, especially when there are a large number of calibration parameters (Boyle et al., 2000; Madsen, 2000; Vrugt et al., 2003; Khu et al., 2005). Tang et al. (2006) comprehensively assessed the efficiency, effectiveness, reliability, and ease of use of three multi-objective evolutionary optimization algorithms (MOEAs) for hydrologic model calibration. Another comprehensive comparison between other optimization algorithms was dealt with by Wohling et al. (2008). Moreover, some researchers have applied MOEAs to develop automatic multi-objective calibration strategies for distributed hydrologic models (Madsen, 2003; Ajami et al., 2004; Muleta and Nicklow, 2005; Bekele and Nivklow, 2007).

Calibration of a distributed hydrologic model (WetSpa) has been performed through classical least squares minimization with the Parameter ESTimator (PEST) software (Doherty and Johnston, 2003; Liu and De Smedt, 2005; Bahremand et al., 2007).

Table 2.1 Summary of the research review on multi-objective function

Year	Author (s)	Literature Review
1991	Klepper et al.	Composed a number of optimal parameter sets, entitled in “acceptable parameter sets”, using a single-objective function in the calibration procedure for a rainfall-runoff model
1998	Yapo et al.	Focused on multi-objective approaches for the calibration of rainfall-runoff models
1998	Gupta et al.	Used six objective functions to calibrate parameters in the SAC-SMA model and computed the Pareto solution eventually
2000	Madsen	Used four objective functions and the SCE algorithm to calibrate parameters in the MIKE11 model and computed the Pareto solution.
2000	Boyle et al.	Used population-based search algorithms as a powerful search method for multi-objective optimization problems and applied them for multi-objective RR calibration
2001	Liong et al.	Calibrated parameters in the HydroWorks model using a multi-objective function that consists of the relative biases of peak discharge and discharge volume, and computed the Pareto solution
2002	Kang et al.	Calibrated parameters in the TANK model automatically, and found that the application that uses multi-objective function composed of the DRMS and the Nash-Sutcliffe measure showed forecast results, giving more weight to low flow than the application result that uses single-objective function

Table 2.1 Summary of the research review on multi-objective function (continued)

Year	Author(s)	Literature Review
2003	Vrugt et al.	Incorporated dominance or Pareto ranking into the SCE so that the population evolved toward the Pareto optimal set in the search space.
2004	Sung et al.	Applied the SIMHYD and TANK models to the Soyanggang dam and the Yeongcheon dam basins with three objective functions and three optimization techniques, respectively, and assessed the suitability of the comparison of Nash-Sutcliffe model efficiency coefficients as an objective function was changed
2006	Tang et al.	Assessed the efficiency, effectiveness, reliability, and ease of use of three MOEAs for hydrologic model calibration
2007	Bahremand et al.	Used the Parameter ESTimator software to calibrate a distributed hydrologic model (WetSpa) through classical least squares minimization
2008	Wohling et al.	Compared the performances of a variety of optimization algorithms

2.1.2 Global Optimization

Kang et al. (2002) used SCE-UA to calibrate estimated parameters for TANK, a daily runoff estimation model, and compared its results with those of the Downhill Simplex method to assess exploration ability for the solution. As a result, they showed that SCE-UA produced better results regardless of objective function relatively. Hwang (2003) used SCE-UA to develop a leakage detection program for a water distribution network, and Lim et al. (2004) used SCE-UA and conducted uncertainty analysis to optimize parameters. Sung et al. (2004) assessed the applicability of the SIMHYD and TANK models to the Soyanggang dam and the Yeongcheon dam basins by applying three optimization methods, such as GA, SCE-UA, and pater search multi start.

Cho et al. (2005) proposed an automatic-calibration method for a water distribution network model by integrating a hydraulic analysis module to an optimization module. In the research conducted by Cho et al. (2005), an EPANET engine was used for repeated hydraulic analysis, and SCE-UA was applied to find the optimal solution. Lee (2006) introduced an automatic-calibration method for a SWAT model in the

Bongcheoncheon basin by applying SCE-UA as an optimization methodology and by conducting Latin Hypercube One Factor at a Time (LH-OAT) sensitivity analysis. Then, Lee (2006) showed that automatically calibrated parameters of SWAT by SCE-UA depended on model performance according to the selection of calibrated data, calibrated parameters, and statistical errors.

Kwon et al. (2008) used the NWS-PC model downscaled from the National Weather Service River Forecast System (NWSRFS) to optimize parameter estimation for a rainfall-runoff model and to analyze the uncertainty. Kwon et al. (2008) applied the Bayesian Markov Chain-Monte Carlo method to estimate parameters and assess the performance of calibration, and their results were compared with the outcomes by applying SCE-UA.

Lee (2011) compared the performance of deterministic parameter estimation methodologies using univariate algorithm, Multiple Start Simple (MSX) and SCE-UA to improve parameter estimation in hydrologic models. Moreover, Chung et al. (2012) used SCE-UA to optimize parameters for the storage function model used in majority of the rivers in Korea for flood forecasting and analyzed the trends of changes on a hydrograph according to estimated parameters. Kang et al. (2012) combined Storm

Water Management Model (SWMM), a representative urban runoff analysis model, with SCE-UA to develop an automatic-calibration module for parameters and showed that simulation results using the calibrated model have improved.

Kang et al. (2014) proposed a reservoir operating model, including separate operational rules for each water level, which could be easily applied to actual dam operations. Here, SCE-UA was applied to determine the appropriate section of each water level, and a developed model was applied in Angat Dam in the Philippines. Kang and Lee (2014) applied SCE-UA to develop an automatic-calibration module for the SWMM model and determined that, by applying a developed module in the Milyang dam , the errors in peak flow decreased.

Duan et al. (1994) pointed out that SCE-UA could detect the global optimum more efficiently than MSX that parameter calibration of the SAC-SMA model. Gan and Biftu (1996) calibrated model parameters for the Sacramento Model (United States), the Nedbor-Afstomnings Model (Denmark), the Xinanjiang Model (China), and the Soil Moisture and Accounting Model (Ireland) by using SCE-UA, MSX, and Local Simplex. As a result of application, SCE-UA was the most efficient method based on the smallest number of runs. Moreover, Yapo et al. (1998) applied the SCE-UA

method to calibrate model parameters of NWSRFS-SMA. In the research by Madsen (2000), the SCE-UA method and a multi-objective function were applied to calibrate parameters of the MIKE11 model, and then, finally, the Pareto optimum was computed. Echhardt and Arnold (2001) conducted a research on the parameter automatic verification procedure by applying the SCE-UA method to a SWAT model in the Dietzholze basin, Germany, and showed relatively reliable results with calibration period, 0.7, and verification period, 0.73. Madsen (2000) used a multi-objective function and the SCE algorithm to calibrate parameters in the MIKE11 model. Van Griensven et al. (2002) also estimated parameters in a SWAT model that are related to water quality factors, such as runoff, dissolved oxygen (DO), biological oxygen demand (BOD), ammonia, and nitrate, for the Dender basin in Belgium using the SEC-UA method and sensitivity analysis.

2.2 Uncertainty Analysis on Hydrologic Model Parameter Estimation

Most fundamental uncertainties come from the conceptualization of the hydrological procedure (Wagener, 2003; Wagener and Gupta, 2005). There are many

sources of uncertainties that impact on the hydrological modeling procedure (Butts et al., 2004; Wagener and Gupta, 2005), including uncertainties caused by parameter estimation, model structure, and data uncertainty. Parameter estimation uncertainty is significantly increased when there is an inability to uniquely locate a "best" parameter set driven by the observation of system inputs and outputs (e.g., precipitation, streamflow, and temperature). Some initial uncertainties could exist in the model states at the beginning of the modeling period (Wagener and Gupta, 2005). Sources of uncertainties lead to a decrease in the predictability of the hydrological modeling system, with an increase in the amount of randomness in the system (Wagener and Gupta, 2005).

Model structure uncertainty is introduced through the conceptualization of the nature based on a hydrologist's subjective decision. Data uncertainty is caused by random and systematic errors in the measurement, sampling, or processing of data for model inputs and outputs. A common approach to model evaluation is to simulate historical behavior for which measurements are available and compare and contrast these with historical observations in search of similarities and differences (Gupta et al., 2008).

General methodologies for uncertainty analysis of a rainfall-runoff model are divided into three categories. First, Montanary and Brath (2004) presented a methodology that assumes a probability distribution to compute the optimal solution and the confidence interval. A second method is to analyze a time series of the simulation bias of a model statistically to assess the uncertainty, and this method has been applied to various researches such as statistics (Yar and Chatifiled, 1990) and hydrology (Loukas et al., 2002).

Finally, a simulation repetition method that uses resampling algorithms, such as the Monte Carlo method, has been conducted, and this methodology has evolved to the GLUE method (Beven and Binley, 1992), which validates a model and estimates reliability. Moreover, the SCEM-UA technique (Vrugt et al., 2003) combines merits of the existing SCE and Markov Chain Monte Carlo (MCMC) methods to estimate a group of optimal solutions and its confidence interval.

Kuczera (1994) explained the statistical differences of parameters between one rainfall event and another with the bias of rainfall in a target basin or the structural problem of the model, which is model simplification. Beven and Binley (1992) developed the GLUE using the Monte Carlo simulation technique for model

verification and uncertainty analysis, and then Kuczera and Parent (1998) applied both importance sampling in GLUE and Metropolis Algorithm to analyze parameter uncertainty in a hydrologic model. Haan et al. (1998) used the Monte Carlo simulation technique to analyze parameter uncertainty and pointed out that it is more important to estimate the mean and variance of input parameters rather than the probability distribution of virtual parameters.

Kavetski et al. (2002) applied a Bayesian approach to analyze the impacts of the uncertainty of rainfall inputs, the hydrologic model, and variable verification on discharge estimation. The Bayesian Total Error Analysis (BTEA) method developed by Kavetski et al. (2002) linked input uncertainty and discharge forecast uncertainty into a Bayesian method to improve model verification and the reliability of discharge forecast. Ajami et al. (2007) used various rainfall-runoff models to consider the structural uncertainty of models for runoff estimations by applying a Bayesian method. However, a method that links the uncertainties of each input data and the results of discharge forecast into a Bayesian approach shows a correlation between model structure and variables in input uncertainties, and the validation procedure of model variables is affected by input uncertainties. The results of discharge forecast influences

the input uncertainty circularly again, and this pattern causes a problem in which discharge forecast results by a model are selected depending on the inputs. To resolve this problem, the existing GLUE method, which is generally used to consider uncertainty in parameter verification of rainfall-runoff models, was extended to consider uncertainty of input data (Lee et al., 2009). The GLUE method proposed by Beven (2007) is distinguished from the Bayesian approaches proposed by Kavetski et al. (2006) and Ajami et al. (2007). The method can apply the uncertainty in model verification and that of input data independently, and use existing research results on the input data and model parameter verification. Hughes et al. (2010) analyzed uncertainty in streamflow forecasting by applying the Pitman model, a monthly hydrologic model, to Southern Africa, assuming that the uncertainty originated from parameter estimation.

Park et al. (1997) determined the applicability of genetic algorithm to the parameter estimation of storage function method for flood routing and showed that the performance of model was improved, particularly in peak discharge and time to peak. Oh (1998) analyzed how parameter uncertainties would affect model outputs and hydrological design by examining the uncertainty of model parameters to consider

uncertainties in flood estimation. The Linear Reservoir System (LRS) rainfall-runoff model was applied to Naeseongcheon, which is the first tributary of Nackdong River. The Advanced First Order Second Moment (AFOSM) method, which assesses uncertainty by analyzing the statistic characteristics of the times series of the bias, and the Mean-value First Order Second Moment (MVFOSM) method were used to develop a generalized procedure for the reliability analysis to consider the uncertainty of event-type rainfall-runoff models. In general, an event-type model is used to estimate peak flow and runoff volume.

Oh (1998) pointed out the necessity of extending uncertainty analysis by applying various methods, such as Bayesian, Latin Hypercube Simulation (LHS), Haar's Point Estimation (HPE), and Rosenblueth's Point Estimation (RPE), and suggested a future research that would focus on model parameter regionalization to estimate flood discharge in ungauged basins with regard to uncertainties. Kwon and Moon (2005) analyzed the uncertainty by generating parameters from a probability distribution using the Latin hypercube sampling method to the HEC-1 model. Kim et al. (2009) used the meta-Gaussian method developed by Montanari and Brath (2004) to compare the uncertainty analysis results between the physical-based distributed

model, VfloTM, and the lumped model, Hydrologic Engineering Center - Hydrologic Modeling System (HEC-HMS), in the Jungnangcheon basin, with a confidence interval of 95 %.

In this research, the optimal parameter set with a confidence interval of 90 % will be estimated through iterative simulations using the resampling algorithm, GLUE, for uncertainty analysis.

Table 2.2 Summary of the research review on uncertainty analysis

Year	Author(s)	Literature Review
1992	Beven and Binley	Developed GLUE, which evolved from the resampling algorithm to evaluate model performances and estimate the confidence interval
1994	Kuczera	Explained the statistical differences of parameters between one rainfall event and another with the bias of rainfall in a target basin or the structural problem of the model, which is model simplification
1997	Park et al.	Simulated floods in the past in the Daecheong dam basin using a storage function method and calibrated eight parameters for a storage function model using a Genetic Algorithm method
1998	Kuczera and Parent	Applied both importance sampling in GLUE and Metropolis Algorithm for analyzing parameter uncertainty of hydrologic model
1998	Haan et al.	Used the Monte Carlo simulation technique to analyze parameter uncertainty and pointed out that it is more important to estimate the mean and variance of input parameters rather than the probability distribution of virtual parameters
1998	Oh	Analyzed how parameter uncertainties would affect model outputs and hydrological design by analyzing the uncertainty of model parameters to consider uncertainties in flood estimation

Table 2.2 Summary of the research review on uncertainty analysis (continued)

Year	Author(s)	Literature Review
2001	Echhardt and Arnold	Conducted a research on the parameter automatic verification procedure by applying the SCE-UA method to a SWAT model in the Dietzholze basin, Germany, and showed relatively reliable results with calibration period, 0.7, and verification period, 0.73
2002	Loukas et al.	Analyzed uncertainties statistically by using the time series of simulation errors in a model
2002	Kang et al.	Estimated parameters for the TANK model using the SCE-UA and annealing-simplex methods and assessed exploration capacity according to an objective function
2002	Kavetski et al.	Applied a Bayesian approach to analyze the impacts of the uncertainty of rainfall inputs, the hydrologic model, and variable verification on discharge estimation
2002	Van Griensven et al.	Estimated parameters in a SWAT model that are related to water quality factors such as runoff, DO, BOD, ammonia, and nitrate for the Dender basin in Belgium using the SEC-UA method and sensitivity analysis
2003	Vrugt et al.	Developed SCEM-UA by combining the strengths of the SCE methodology and the MCMC technique

Table 2.2 Summary of the research review on uncertainty analysis (continued)

Year	Author(s)	Literature Review
2004	Butts et al.	Examined various factors that affect hydrological modeling, including parameter estimation, model structure, uncertainties in input data, etc.
2004	Kwon and Moon	Analyzed the uncertainty by generating parameters from a probability distribution using the Latin Hypercube Sampling method to the HEC-1 model
2004	Montanary and Brath	Assumed a probability distribution to find the optimal solution and the confidence interval
2004	Sung et al.	Assessed the application of the SIMHYD and the TANK model to the Soyanggang dam and the Yeongcheon dam basins by applying three optimization methods such as GA, SCE-UA, and pater search multi start
2005	Wagener and Gupta	Pointed out that a fundamental uncertainty in rainfall-runoff modeling came from the process that conceptualized natural hydrological phenomenon as a model
2006	Lee, D.H.	Presented the automatic calibration method to a SWAT model in the Boseongcheon basin using the LH-OAT and SCE-UA methods

Table 2.2 Summary of the research review on uncertainty analysis (continued)

Year	Author(s)	Literature Review
2007	Ajami et al.	Used various rainfall-runoff models to consider the structural uncertainty of models for runoff estimations by applying a Bayesian method
2008	Gupta et al.	Pointed out that, in general, a methodology that validated model performances was to examine the similarities and errors between simulated outputs and observations
2009	Kim et al.	Used the meta-Gaussian method to compare the uncertainty analysis results between the physical-based distributed model, VfloTM, and the lumped model, HEC-HMS, in the Jungnangcheon basin with a confidence interval of 95 %.
2010	Hughes et al.	Analyzed the uncertainty in streamflow forecasting by applying the Pitman model, a monthly hydrologic model, to Southern Africa, assuming that the uncertainty originated from parameter estimation

Lee et al. (2009) determined the impacts of rainfall input uncertainty on stream flow prediction based on the extended GLUE approach. The results showed that the extended GLUE method performed acceptably in all flow regimes, except in the underestimation of peak flows. Lee et al. (2009) pointed out that the extended GLUE approach was a potential method that could include major uncertainty in rainfall-runoff modeling. Lee and Seo (2011) conducted calibration and vilification in the flow of the Daecheong dam watershed using the SWAT-Calibration and Uncertainty Program (SWAT-CUP). In the research by Lee and Seo (2011), the Sequential Uncertainty Fitting ver.2 (SUFI-2) program and the GLUE program in SWAT-CUP were used to select the best parameters for a SWAT model.

Moreover, Joh et al. (2012) compared the performance between uncertainty analysis techniques for a SWAT model's predictability in the Chungju Dam using SUFI-2, Parameter Solution (ParaSol) and GLUE. As a result, Joh et al. (2012) showed a quantitative assessment on the uncertainty in hydrologic analysis using SWAT, and it contributed to ensuring the reliability of the simulated results by SWAT. Jang (2012) analyzed how parameter uncertainty in the rainfall-runoff mode would affect the simulated results by HEC-HMS. For this, Jang (2012) estimated model parameters

based on quantitative uncertainty analysis by applying GLUE in the upper area of the Yeongsangang basin and analyzed the distribution of simulated discharge by using estimated parameters. Jung et al. (2013) used GLUE to conduct a quantitative assessment on the uncertainty generated from roughness and rainfall by making a flood inundation map. Cho et al. (2014) applied the ISPSI-GLUE method to conduct the uncertainty analysis of Topography Model (TOPMODEL) in Texas, U.S.A. and its result was compared with the performance of a single GLUE.

Beven and Binley (1992) applied GLUE to assess the uncertainty in the most sensitive parameters related to runoff simulation and presented the confidence interval of simulated runoff by applying estimated parameters. Kuczera and Parent (1998) used both a resampling technique of GLUE and the Metropolis Algorithm to conduct parameter uncertainty analysis for a hydrologic model. Moreover, Hope et al. (2004) used GLUE to assess the uncertainty in the runoff parameters of the Hydrologic Simulation Program Fortran (HSPF) model.

Balsone et al. (2003) used the Markov Chain Monte Carlo sampling technique for the GLUE method to enhance the efficiency of uncertainty analysis and computed the improved median in prediction. Gong et al. (2011) pointed out that a deterministic

watershed model used mainly for simulating agricultural nonpoint-source pollution could not consider the uncertainty and used the GLUE method to analyze the uncertainty in parameters of the SWAT model. Moore et al. (2010) determined that GLUE provided a user with the two options of sampling. One was the Bayesian sampling using a posterior probability distribution and the other was a sampling based on the heuristic likelihood function. Cho and Olivera (2014) introduced the ISPSO-GLUE method developed by combining the Isolated-Speciation-based Particle Swarm Optimization algorithm and GLUE and showed that the ISPSO-GLUE could detect not only the global optimum but also the local optimum. It meant that this method could analyze the uncertainty in behavioral models distributed near to the local optimum.

3. Theoretical Background

In this chapter, a general classification of hydrologic models according to purpose, target object, structure, etc., is described. Moreover, a theoretical background on the storage function model that is used in the research is explained. Furthermore, SCE-UA, a global optimization methodology, and GLUE, a uncertainty analysis technique, are described briefly.

In addition, a few of the existing methods for hydrograph separation are summarized, and a theoretical background and understanding on Hydrograph Section Separation (HSS) methodology for parameter estimation which is newly proposed in the research is introduced.

3.1 Hydrologic Model

According to the temporal and spatial variability of a model or a model parameter, a hydrologic model can be classified as shown in Figure 3.1. A hydrologic model can be categorized into a distributed model and a lumped model, depending on the spatial variation of parameters.

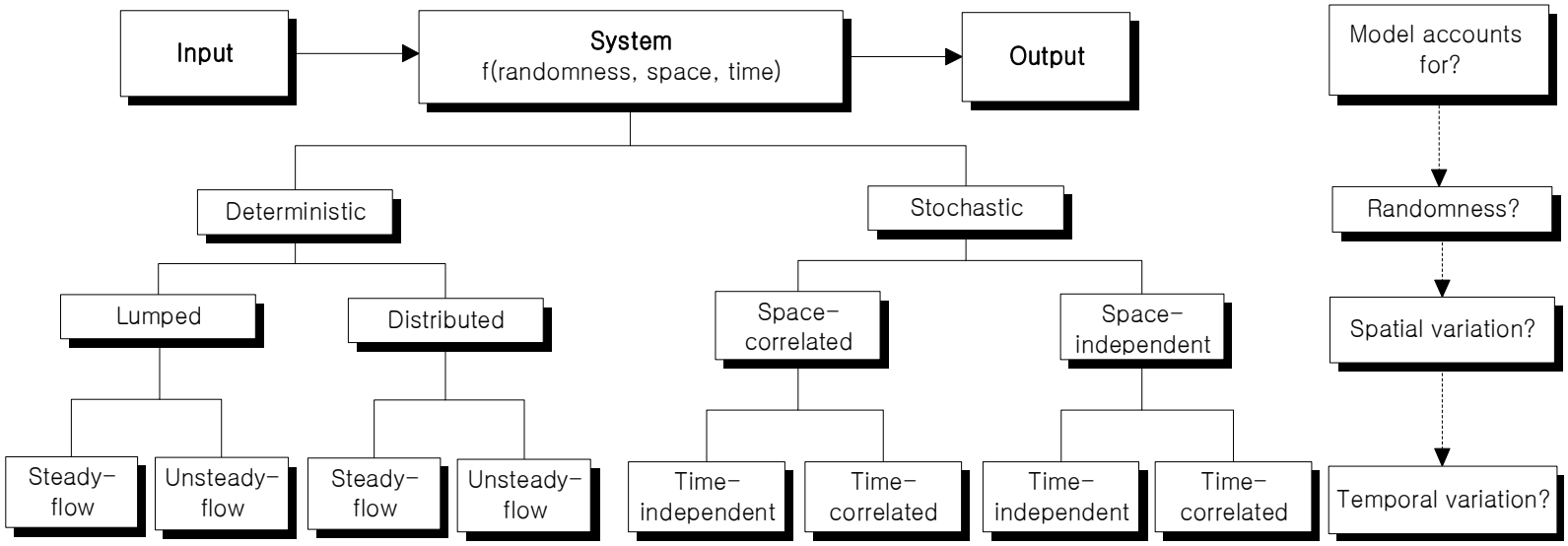

Figure 3.1 Classification of hydrologic models (Chow et al., 1998)

The lumped model computes simulation results by calculating ordinary differential equations that do not take into account spatial variation in input data, boundary conditions, and the morphological characteristics of a basin. On the other hand, the distributed model, which takes into account spatial variation computed simulation results by calculating partial differential equations as the governing equation. Although the distributed model requires complete input data, boundary conditions, and geographical information, in reality, there are many difficulties in obtaining these data. Therefore, in general, a number of models are categorized into the mixed model combining both the lumped and distributed models (refer to Table 3.1).

A rainfall-runoff model is categorized into a rural runoff model and an urban runoff model according to the characteristics of target basins. Moreover, it is categorized into an event model and a continuous model according to the impacts of prior rainfall events on a model; an event model is not affected by prior events. Taking into consideration the spatial aspect, a model is divided into a lumped model and a distributed model, with regard to the space.

Table 3.1 Rainfall-runoff model with hydrologic process (adapted from Singh, 1995)

		Rainfall-Runoff Model
Hydrological process	Lumped	HEC-1 (Hydrologic Engineering Center, 1983)
		HYMO (Williams and Hann, 1972)
		RORB (Laurenson and Mein, 1983)
		SSARR (U.S. Army Engineer, 1972)
		TANK model (Sugawara et al., 1984)
	Distributed	SHE (Abott et al., 1986)
		IHM (Morris, 1980)
		SWMM (Metcalf et al., 1971)
		NWSRFS (Hydrologic Research Laboratory, 1972)
	Mixed	Lumped + Distributed

According to the structure of a rainfall-runoff model, it is categorized into three groups: a metric, a parametric, and a mechanistic models (Wheater et al., 1993). A representative model as a metric model (called a black-box or a data-based model) is an artificial neural network. In a parametric model (called a gray-box or a conceptual model), parameter estimation is the core component. A mechanistic model (called a white box) has a physical-based structure that is able to minimize parameter estimation according to inputs, such as physical features and geographical information data.

In general, a rainfall-runoff model is used to forecast extreme events, such as floods and droughts, and analyze water balance for water resources planning and management. Recently, the accuracy of forecast and simulation with a model has been improved because of highly advanced computer technologies and the development of software programs. A distributed model based on physical theory is able to yield more accurate simulated results with spatial and temporal inputs at high-resolution. Still, however, most researches that are related to a rainfall-runoff model have been restricted to point estimation, which focuses on how the accuracy of simulation results can be improved. This is because most concerns in actual practices and projects are to

find the optimal solution rather than to quantify the uncertainty of the simulated results of a rainfall-runoff model (Brath and Rosso, 1993; Singh and Woolhiser, 2002).

Conceptual model structures are usually selected based on the modeler's perception of the relevant hydrological procedures and appropriate functional forms, which vary from person to person. There is no well-defined objective selection of an appropriate model structure. This procedure is influenced by a combination of factors, including observations about the characteristics of the catchment, available data, modeling objective, and personal preference (Wagener and Gupta, 2005).

It is necessary to calibrate and adjust model parameters until simulation results with estimated parameters can be closest in nature to the actual hydrologic system, and this can be achieved through the entire process of parameter estimation. In the conceptual model, parameter estimation is the most important step to increase the reliability of simulation results.

3.2 Storage Function Model

A rainfall-runoff model is categorized into a simplified model, such as a rational runoff method, and a complex structural model, which should treat a number of parameters as well. Typical runoff models are theHEC-1, the Hydrologic Model Computer Language (HYMO), the Streamflow Synthesis and Reservoir Regulation (SSARR), the British Road Research Laboratory Model (BRRL), the Storm Water Management Model (SWMM), and the Illinois Urban Drainage Area Simulator (ILLUDAS). Table 3.2 describes representative rainfall-runoff models by categorizing them into event-based or continuous model, and Table 4.4 describes typical models by categorizing them into lumped, distributed, or hybrid models. In this research, the storage function model that the Han River Flood Control Office is using in practical works was applied.

Table 3.2 Variety of hydrologic simulation model

Rainfall-Runoff Event Simulation Models		
1961	SFM	Storage Function Method
1972	HYMO	Hydrologic Model Computer Language
1972	USGS	USGS Rainfall-Runoff Model
1973	HEC-1	HEC-1 Flood Hydrograph Package
Continuous Sequential Simulation Models		
1958	SSARR	Streamflow Synthesis and Reservoir Regulation
1966	SWM-IV	Stanford Watershed Model-IV
1967	HSP	Hydrocomp Simulation Program (SWM version)
1969	OPSET	Self-Optimizing Hydrologic Simulation Model
1970	TWM	Texas Watershed Model (SWM version)
1972	NWSRFS	National Watershed Service River Forecast System
1972	DISPRIN	Dee Investigation Simulation Program for Regulating Networks
1972	UBCWM	University of British Columbia Watershed and Flow Model
1973	SACRAMENTO	National Water Service Sacramento Model
1974	USDAHL-74	US Department of Agriculture Hydrograph Laboratory Watershed Model
1975	IMH2-SVP	Institute of Meteorology and Hydrology of Romania Model
1980	HSPF	Hydrological Simulation Program-FORTRAN

In this research, the storage function model is selected as a hydrologic model which has been used in the practice of flood forecasting by the Han River Flood Control Office in Korea. Storage function model performs calculations on runoff in a basin as flooding.

In this research, the storage function model was selected as a hydrologic model used in practice of flood forecasting by Han River Flood Control Office in Korea. The storage function model performs calculations on runoff in a basin as flooding. The storage function model substitutes a storage function describing the relationship between flood and storage volume in a basin or a river channel to the continuity equation of flood. This allows to solve the continuity equation of flood and to estimate the volume of runoff hydrologically. In Korea, since 1997 when Han River Flood Control Office introduced the storage function to practical use for the first time, it has been used in Nakdong River, Geum River, and Yeongsan River Flood Control Offices nearly 40 years. In the basic theory of the storage function model, the storage is defined as the difference between rainfall and runoff. The runoff volume is calculated. The storage function model calculates runoff step by step in accordance with the concept that storage increases in proportion to runoff with the non-leaner relationship.

. In recent years, various runoff analysis techniques and models has been developed, but the storage function model has been consistently used in practice because of its strengths that are to consider the hydrological nonlinearity and to forecast runoff within an acceptable error range relatively.

The theoretical background on the storage function model is described as follows. Assuming that flood runoff is surface runoff that can be indicated with the Manning's formula, storage S in a basin or river channel is expressed as a power function of runoff O.

$$S = KO^p \qquad \text{(Eq. 3.1)}$$

where K and P are coefficients of a basin or river channel. Meanwhile, the continuity equation in a basin is expressed as follows.

$$\frac{1}{3.6} f r_{ave} A - O = \frac{dS}{st} \qquad \text{(Eq. 3.2)}$$

where f is the coefficient of average inflow, r_{ave} is the basin averaged rainfall per unit time (mm/hr), A is the area of a basin (km^2), O is direct runoff (m^3/s) taking into consideration lag time Tl, and S is the actual storage in a basin (m^3).

In addition, the continuity equation in a river channel is as follows.

$$\left(\sum_{j=1}^{n} f_i \, I_j\right) - O = \frac{dS}{dt} \qquad \text{(Eq. 3.3)}$$

where, f_i is the coefficient of average inflow; and I_i is the inflow from a basin or sub-basin to a channel, or is the inflow from the upstream of a river channel (m^3/s). O is runoff (m^3/s) in the downstream of a channel taking into consideration lag time Tl, and S is the actual storage in a river channel (m^3).

To calculate runoff in a basin using the storage function model, it is necessary to determine the coefficients of the storage function, K and P; the rate of primary runoff prior to saturated runoff, f_1; the saturated rainfall at the saturation point, R_{sa}; and lag time Tl, which indicates lagged time of runoff after rainfall begins.

As described above, in general, there are five parameters for the storage function method, including Tl, K, P, f_1, and R_{sa}, but the storage function in practical works can use the saturated runoff ratio (f_{sa}), rainfall multiplication ratio (α), and base flow multiplication ratio in various cases. Therefore, in practical works, a total eight parameters for the storage function are calibrated, but it is difficult to optimize all

of them at the same time. As each parameter is interconnected, at least there should be more than two parameter sets that have the optimal solution.

In applying a flood forecasting model to practical works, first, the initial value of each parameter in a basin is set up and applied. Then, a hydrograph is adjusted through the trial-and-error method by changing different parameters based on runoff from each rainfall event. As it is impossible to optimize all of eight parameters, it is likely for a user to keep one or two certain parameters to adjust other parameters. Here, it depends on the experiences of users or skillful engineers which parameter will be selected and which range parameters will be adjusted. Therefore, this study proposes an adjustable range of each parameter for every basin and tries to shorten the computation time of a hydrograph using the trial-and-error method. With these approaches, ultimately, the proposed methodology in this study presents a standardized procedure to estimate parameters for hydrograph instead of a conventional approach, depending on the experiences of engineers.

3.3 Formulation of the Objective Function

As shown in Table 3.3, the types of objective function are diverse, and in this research, the Nash-Sutcliffe model efficiency coefficient, which is used to assess the efficiency of the model simulation coefficient, and Root-Mean-Square-Error (RMSE), which is used to assess the patterns of a hydrograph that were obtained by simulating a rainfall-runoff model in comparison to observed data, were selected as the objective functions. Moreover, RE_p and RE_v were selected to assess peak flow and total discharge respectively.

The Nash–Sutcliffe model efficiency coefficient (E) is used to assess the predictive power of hydrologic models. It is defined as:

$$F_1(\boldsymbol{\theta}) = E = 1 - \frac{\sum_{i-1}^{n}\left(Q_0^i - Q_s^i\right)^2}{\sum_{i-1}^{n}\left(Q_0^i - \overline{Q_0}\right)^2} \qquad \text{(Eq. 3.4)}$$

where $\boldsymbol{\theta}$ is the model input parameter, Q_0^i is the observed discharge at time i, Q_s^i is the simulated discharge at time i, and $\overline{Q_0}$ is the average of observed discharge.

Table 3.3 Numerical criteria used in the WMO Project (Lee, 2000)

Numerical Criteria
1. Coefficient of the variation of residual of errors given by $\mathrm{Y} = \frac{\left[\frac{\sum(y_c - y_0)^2}{n}\right]^{1/2}}{\overline{y_0}}$
2. Ratio of relative error to the mean given by $\mathrm{R} = \frac{\sum(y_c - y_0)}{n\overline{y_0}}$
3. Ratio of absolute error to the mean given by $\mathrm{A} = \frac{\sum\lvert y_c - y_0\rvert}{n\overline{y_0}}$
4. Arithmetic mean given by $\mathrm{D} = \frac{\sum y_{0,c}}{n}$
5. Phasing coefficient (PH) for the monthly peak flows are given by the number of times that the simulated peak is shifted in time from the corresponding observed peak by at least one day
6. Coefficient of persistence (PE) given by $\frac{\sum_{i=1}^{k} \mathrm{B}_i^2}{\mathrm{V}}$

In the above equation:

$y_0 =$ observed discharge

$y_c =$ computed discharge

$n =$ total number of observations

$\overline{y_0} = \frac{\sum y_0}{n}$

$k =$ number of positive and negative runs

$\mathrm{V} = \sum_{i=1}^{n}(y_0 - y_c)^2$ for n items

$\mathrm{B} =$ the individual areas for each segment

Nash–Sutcliffe model efficiency coefficients can range from ∞ to 1. An efficiency of 1 (E = 1) corresponds to a perfect match of modeled discharge to the observed data.

An efficiency of 0 (E = 0) indicates that the model predictions are as accurate as the mean of the observed data, whereas an efficiency less than zero (E < 0) occurs when the observed mean is a better predictor than the model or, in other words, when the residual variance (described by the numerator in the expression above), is larger than the data variance (described by the denominator). Essentially, the closer the model efficiency is to 1, the more accurate the model is.

Noted that the Nash–Sutcliffe efficiency (NSE) can also be used to quantitatively describe the accuracy of model outputs other than discharge. This method can be used to describe the predictive accuracy of other models as long as there are observed data to compare the model results with.

Root Mean Square Error (RMSE) is defined mathematically as:

$$F_2(\boldsymbol{\theta}) = RMSE = \sqrt{\frac{\sum_{i-1}^{n}(Q_0^i - Q_s^i)^2}{n-1}} \qquad \text{(Eq. 3.5)}$$

where $\boldsymbol{\theta}$ is the model input parameter, Q_0^i is the observed discharge at time i, and Q_s^i is the simulated discharge at time i. n is the number of observations.

RMSE is a measure of the "average" error, weighted according to the square of the error. It answers the question, "What is the average magnitude of the forecast errors?", but does not indicate the direction of the errors. RMSE is influenced more strongly by large than by small errors because it is a squared quantity. Its range is from 0 to ∞, with 0 being a perfect score.

RMSE is a quadratic scoring rule that measures the average magnitude of the error. The equation for RMSE is given in both of the references. Expressing the formula in words, the difference between forecast and corresponding observed values are each R-squared and then averaged over the sample. Finally, the square root of the average is taken. As errors are squared before they are averaged, RMSE gives a relatively high weight to large errors. This means that RMSE is most useful when large errors are particularly undesirable.

RE_p (relative error of peak) is a measure that compares observed and simulated peak discharge.

$$F_3(\boldsymbol{\theta}) = RE_p = \frac{\left|Q_{sim,peak} - Q_{obs,peak}\right|}{Q_{obs,peak}} \quad \text{(Eq. 3.6)}$$

where $\boldsymbol{\theta}$ is the model input parameter, $Q_{obs,peak}$ is the observed peak discharge, and $Q_{sim,peak}$ is the simulated peak discharge.

RE_v (relative error of volume) is a measure that compares observed and simulated total volume.

$$F_4(\boldsymbol{\theta}) = RE_v = \frac{\left|Q_{sim,volume} - Q_{obs,volume}\right|}{Q_{obs,volume}} \quad \text{(Eq. 3.7)}$$

where $\boldsymbol{\theta}$ is the model input parameter, $Q_{obs,volume}$ is the observed discharge volume and $Q_{sim,volume}$ is the simulated discharge volume.

Parameter estimation is conducted in each segment obtained through HSS according to the objective function. In the rising limb and falling limb, the multi-objective function, including the NES, RMSE, and RE_v is applied because of considering RE_v, which is more important than RE_p as it estimates the hydrograph time-series pattern. In addition, in the crest, objective functions, such as NSE, RMSE, RE_v, and RE_p are applied to estimated parameters.

As estimating parameters by using HSS described in the next section in detail, the objective function for each section is constructed as follows. NSE and RE_v are selected as the objective function for a rising limb and a falling limb. Also, RMSE and RE_p are used for a crest to estimate parameters. NSE defined as the mean error in hydrologic model simulation is applied to all sections in accordance with HSS. RE_v is to used assess the accuracy of the simulated total volume for all sections. In addition, RE_p is used to estimate parameters for simulating a crest.

3.4 Global Optimization

An error surface for optimizing the parameters of a flood forecasting model may vary in complexes, so it is easily expected that there may be a number of local solutions. Thus, it is reasonable to apply a global optimization method that computes the optimal solution by detecting the entire surface of planar errors. Global optimization methodology uses a certain optimization technique to evolve the solutions and as a result the population of solutions ultimately converges to the optimal solution (Chung et al., 2012).

Optimization is a problem that frequently appears in system engineering and is often indicated as a mathematical planning problem. Global optimization techniques can be classified into deterministic and stochastic approaches. Algorithms based on the deterministic approach have a finite number of repeated calculations to converge to the global optimum point, which provides a finite number of allowable errors. Thus, when it reaches a certain point, ultimately, a solution is obtained, and the solution is guaranteed to be globally optimal. As the amount of calculation rapidly increases according to the increase in the size of the problem, deterministic algorithms are likely to be applied to a small scale of the problem.

On the other hand, algorithms based on the stochastic approach let the probability in reaching the global optimum solution approach "1" infinitely through iterative calculation. In other words, stochastic algorithms cannot guarantee global optimality; instead, they can be applied to a relatively large problem. In addition, their strength is that the intermediate result is, at least, a local minimum point so useful results can be obtained within a reasonable time duration. If the time allowed, the calculation can be conducted continuously to increase the possibility of obtaining a better optimal solution (Choi, 2004).

One of the most commonly used method based on stochastic global optimization is GA. GA, which was proposed by Holland (1975), is a methodology that detects the global optimum through a process that consists of random selection, cross-over, and mutation by imitating Darwin's evolution theory. GA is based on the hypothesis that the best solution can be found in the domain that contains a number of good solutions relatively. As the original GA shows the chromosome with the binary value, the algorithm is suitable not only for combined optimization, but also for function optimization without constraints (Choi, 2004). In fact, GA has been applied to a variety of hydrological research since the late 1990s, and its performance has also been proven in various ways.

In addition, Simulate Annealing (SA), which was devised by Kirkpatrick et al. (1983), is a method that derived the idea of the quenching process of metals. According to change in temperature, a randomly selected parameter is converted slowly. As a result, if the converted parameter has a much better solution, it can be taken. Otherwise, by comparing $\varepsilon^{\frac{\Delta E}{T}}$ to a random number (an equivalent random number between 0 and 1), when the random number is less a solution is updated; otherwise, a solution is not updated. Here, E is the difference in energy between the

existing parameter and the new parameter. T is the temperature, and the value is reduced according to a decrease in T. It means that the probability in updating a solution is reduced. Therefore, at first, the probability of movement is high because the temperature is high and the optimal solution is far away. However, as the temperature is lower, that is, increasingly closer to the optimal solution, it is necessary to adjust the probability in movement to a lower level. The SA method has an advantage that the solution close to the global optimum can be found; but it takes quite a long time in terms of calculation. In line with this, there are many efforts to shorten the calculation time by using a parallel processing model, such as the Bolzmann machine.

There are a number of methods proposed as a global optimization methodology; in this research, SCE-UA, having a fast convergence speed to detect the optimal solution, was used for parameter estimation.

SCE method, a global optimization technique, has been reputed as an efficient and well-performed method in automation calibration (Sorooshian et al., 1993; Gan and Biftu, 1996; Kuczera, 1997; Madsen, 2000). SCE-UA is a method that finds the optimal solution by adding the concept of complex shuffling to GA, Simplex exploration, and Controlled Random Search (CRS)). The purpose of SCE-UA is to

detect the optimal parameter set in a space of potential parameters. In other words, SCE-UA is a method that finds the solution over the course of evolution in the population of parameters continuously by blocking the progression of any parameters that have a small probability in a space of parameters. Thus, SCE-UA is a reliable method for finding the global optimized minimum in a parameter space (Kwon et al., 2008).

The major features of SCE-UA indicated by Duan et al. (1994) can be described as follows: (a) a combination of deterministic and probabilistic optimization approaches, (b) systematic evolution of a complex that consists of points for detecting the global optimum, (c) competitive evolution, and (d) complex shuffling. The concepts of (a) to (c) have been successfully proven in a number of previous studies, and the concept of (d) was introduced by Duan et al. (1992) (Kang et al., 2014).

In the procedure of SCE-UA, first, an initial population is formed from a space of appropriate parameters through random sampling. A space of appropriate parameters is defined as the minimum value of parameters to the maximum, and an initial population from random sampling is divided into p complexes. A complex consists of $2p+1$ objects, and each formed complex evolves by using the simplex algorithm

independently. Then, a complex is periodically shuffled to create a new complex for sharing new information in the exploration procedure. Simulations are repeated until the convergence conditions are satisfied, and finally, the optimal solution is found in the entire space of parameters.

Competitive evolution and complex shuffling as majors feature of SCE-UA enable complexes to be reproduced, and they have information that has to be delivered by the population to the next generation. This can prevent the degradation of information on the detection space through the course of evolution, and it allows SCE-UA to effectively detect the global optimum effectively in a wide range of problems (Kim et al, 2009).

To apply SCE-UA, the number of complexes, the number of objects, the number of objects in sub-complexes, and the number of evolving steps admitted in each complex should be defined primarily. Duan et al. (1994) revealed that the number of complexes is the most important variable in applying SCE-UA. As the number of complexes (p) increases, the probability of finding the optimal solution increases; however, because the number of simulations increases in proportion to the number of complexes, a

longer calculation time is required. Kuczera (1997) recommended that the number of complexes is defined following the dimension of estimated parameters (see Figure 3.2).

Until now, SCE-UA is still widely applied to estimate optimized parameters for a hydrologic model, and analyze and resolve problems that are related to optimality in a water sector.

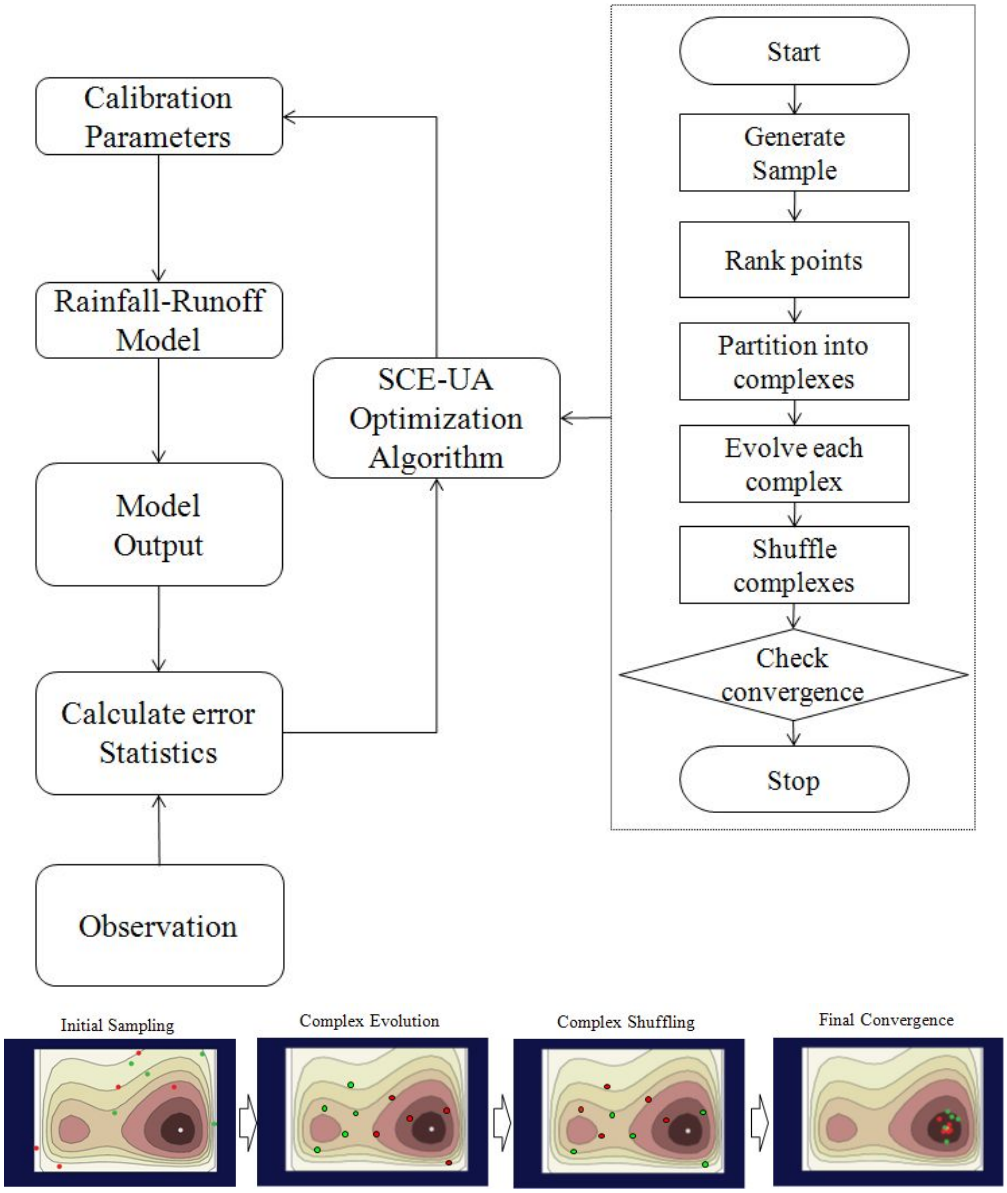

Figure 3.2 Framework of the automatic calibration with the SCE-UA method

(Han River Flood Control Office, MOLIT, 2011)

3.5 Uncertainty Analysis

The GLUE methodology was proposed by Beven and Binley (1992) to analyze the uncertainties in parameter estimation. The concept of GLUE was originally derived from the Monte Carlo simulation technique using TOPMODEL (Beven and Kirkby, 1979). George Hornberger conducted sensitivity analysis on model parameters by using the Monte Carlo simulation technique with Bob Spear and Peter Young, his colleagues. GLUE was developed based on Hornberger-Spear-Young (HSY) global sensitivity analysis method (Hornberger and Spear, 1981; Spear et al., 1994). The GLUE methodology offers a user the option to choose between purely Bayesian sampling of the posterior parameter probability distribution and sampling based on heuristic likelihood functions (Moore et al, 2010).

The most fundamental uncertainty occurs in the process of conceptualizing the hydrological phenomenon in nature (Wagener, 2003; Wagener and Gupta, 2005). Various factors, such as parameter estimation, model structure, uncertainties in data, etc., affect the simulation process of a hydrologic model. (Butts et al., 2004; Wagener and Gupta, 2005).

In 1992, Beven and Binley introduced the GLUE method to consider the structural uncertainties of rainfall-runoff models. The GLUE method was initially developed based on the improvement of the limitation of existing hydrological simulation methods, which could not reproduce identically the complicated hydrological actions themselves in natural basins using numerical techniques. Moreover, the GLUE method was developed to consider the following several understandings: (i) similar forecast results of the optimal streamflow can be obtained by simulating various models; and (ii) in fact each model performs equally, and an acceptable model and its parameters exist more than once. With regard to these facts, assuming that the equal-finality of hydrologic models was caused by uncertainties in the model structure and parameters, the GLUE method was applied to present a streamflow forecast that takes into consideration the uncertainties in hydrologic models. More detailed information on the GLUE method is described in Figure 3.3 as follows.

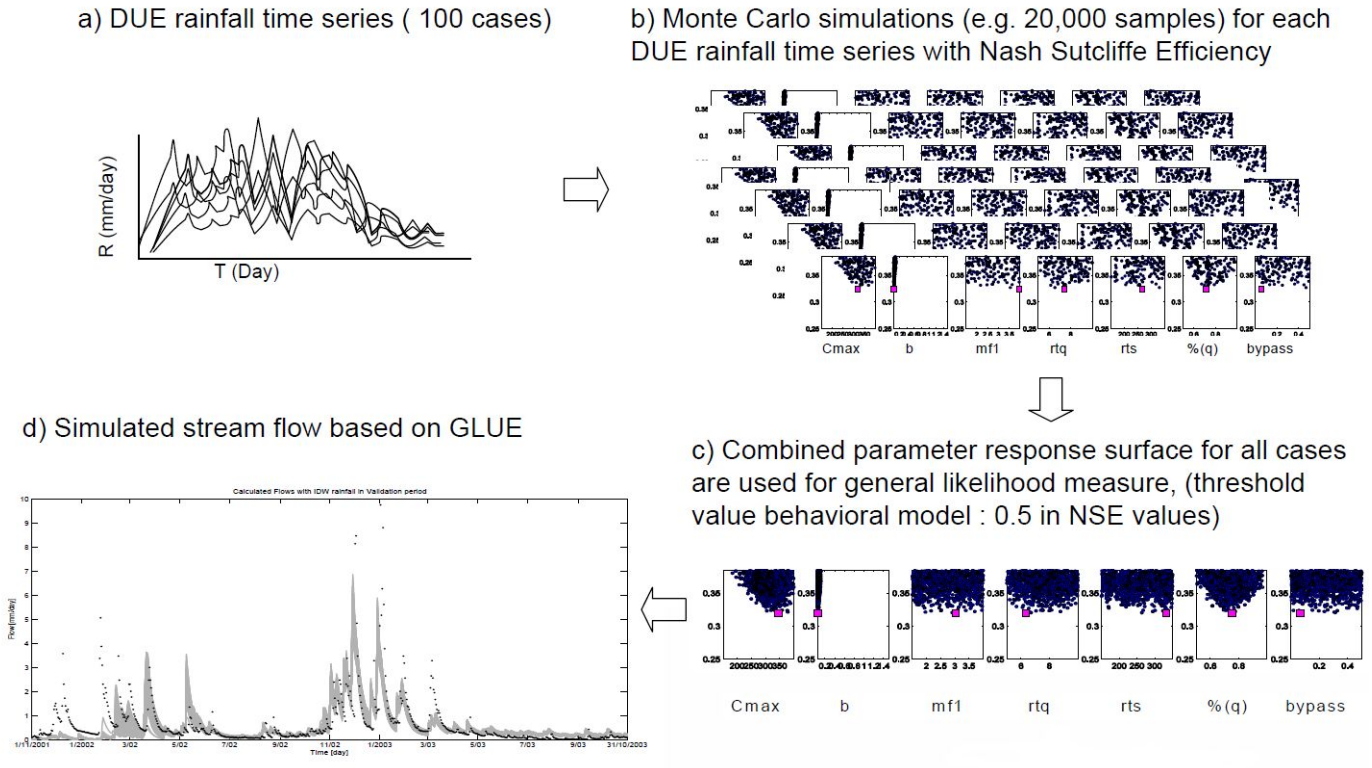

Figure 3.3 Framework of the automatic calibration with the GLUE method (adapted from Lee et al., (2009))

(a) First, a generalized likelihood measure to determine the model performance is defined. Here the likelihood is not necessarily the statistical definition. Instead, it can be defined as an objective function that can determine the model performance with a value between 0 and 1 (Cho et al., 2014). According to the objectives, various likelihood measures can be used, but NSE is usually applied (Beven and Freer, 2001) (refer to the formulation of NSE in the previous subsection [*3.3 Formulation of Objective Function]*).

(b) To find optimal parameters for a given model, a number of parameter sets are extracted randomly. As there is no accurate advance information on the application of a given model to a basin, a uniform distribution is usually used to extract parameter sets.

(c) Each parameter set is divided into behavioral and non-behavioral sets according to the threshold of the selected likelihood function. In general, the subjective judgment by a model user intervenes with the selection of the threshold of model in terms of model performance and objectives.

(d) The weight of a likelihood function is calculated using a formulation as in Eq. 3.8, and it is applied to outstanding parameter sets out of behavioral sets, showing better performance.

$$W_i = \frac{L(Q_i)}{\sum_{k=1}^{N} L(\theta_k)} \quad \text{(Eq. 3.8)}$$

where N is the number of behavioral sets.

(e) Streamflow forecast using the GLUE method is assessed according to a cumulative quantile of simulated streamflow using weighted model parameters. Commonly, the 90^{th} quantile, excluding 5 % from each tail, is used to assess forecast results and shows the reliability of a streamflow forecast.

3.6 Hydrograph Section Separation

There are traditional methods for hydrograph separation such as the groundwater depletion curve method, straight line method, N-day method, and modified N-day method and in general these methods horizontally divide the total runoff on a hydrograph into base and direct flow. A hydrograph is a schematic graph that show the temporal distribution of the total discharge caused by an independent rainfall event at any cross-section of river. When the rain starts, initial loss is caused by blocking, infiltration, etc., and then runoff starts increasing, drawing the rise of the curve called rising limb. Finally, it leads to the peak flow. Once runoff reaches the peak flow, it is gradually reduced as a falling limb until the next rainfall event occurs. In general, the shape of the rising limb on a hydrograph is dependent on the characteristics of rainfall, and an inflection point is interpreted as the time in which direct runoff from a watershed ends. The falling limb on a hydrograph represents discharge change over time after an inflection point, and here, retention volume in a basin shall be deemed to be discharged into the river

The shape of the falling limb is deemed to be almost independent to the characteristics of rainfall and is rather dependent to the soil layer of the underground or the features of aquifers. There are various relational formula to explain the characteristics of the falling limb, but the most typical relationship is shown in Eq. 3.9 as follows.

$$Q_t = Q_0 K_r^t = Q_0 e^{-\alpha t} \quad \text{(Eq. 3.9)}$$

where Q_0 is the discharge at the falling limb, Q_t is the discharge after time t from Q_0, K_r is the regression constant, and α is the coefficient of soil and aquifer characteristics ($\alpha = \ln K$) (Yoon, 2009).

The major factors that influence a hydrograph can be divided into topographical and meteorological factors. Topographical factors are the size and the shape of the basin area, distribution of river channels, the slope of the channel and the surface etc. Moreover, meteorological factors are rainfall intensity and duration, spatial and temporal distributions of rainfall, the direction of the movement of rainfall, etc. (Seonwoo, 2010). A hydrograph shows the temporal variation of discharge at the exit of a basin caused by any rainfall and discharge at a time, which is the sum of surface

runoff, interflow, base flow, and rainfall that directly falls on a channel. In other words, a hydrograph is a sum of the existing discharge in a river before rainfall and the new discharge caused by a certain rainfall. Thus, to analyze the relationship between a certain rainfall and the resulting runoff, the new discharge caused by a certain rainfall should be separated from the total discharge.

In general, hydrograph separation is defined as the separation of direct runoff and t base flow from a hydrograph and base flow primarily means the outflow of groundwater. In fact, the basis for the distinction between direct runoff and base flow in a river basin in practical works is unclear. In addition, each concept of direct runoff and base flow has a relative randomness so the separation of a hydrograph and its analysis are also arbitrary. Nevertheless, it is important to properly separate direct runoff and base flow for a hydrograph to predict runoff discharge at any point of a river as rainfall occurs. So as to separate direct runoff and base flow exactly, a variety of data on hydrogeological information such as the exact range of a watershed, the soil features of underground aquifers, percolation capacity, and water flow capacity, aer necessary.

In reality, however, there has not been a clarified way to identify these hydrogeological characteristics analytically, so a few simplified methods have been used. At present, there are several methods for hydrograph separation such as, the groundwater depletion curve method, straight line method, N-day method, and modified N-day method . These methods may be applied according to the random selection of the hydrologists.

(1) Groundwater Depletion Curve Method

This method overlaps the falling limbs of hydrographs to obtain a representative depletion curve of the basin. This approach can be applied when the past hydrographs are available. The steps on creating a groundwater depletion curve is as follows. First, continuous discharge records of the past few years need to be illustrated and only their recession curves are selected. The selected recession curves are listed on in ascending order from right to left, and a rough tangent is drawn at the lowest value of the regression curve. Then, a computed tangent is transferred and drawn at the arithmetic axis this is a groundwater depletion curve that represents a hydrograph. Finally, the recession curve obtained above is superimposed to the falling limb of an actual

hydrograph to find the point in which the separation of the curve starts, and direct runoff and base flow can be separated by connecting the point to the origin of the rise on the curve.

(2) Straight Line Method

The straight line method draws a horizontal line from the start of the rising limb. First, it needs to identify when direct runoff begins. This method is based on the assumption that the temporal change of base flow rate is not large in a short time when rainfall is continuous. Although its rationale is somewhat inadequate, the straight line method is widely used in practice because of its convenience and simplicity.

(3) N-day Method

First, this method selects a point that corresponds to the falling limb after N days from the occurrence of peak flow. Then, this point is connected to the origin of the rise in which direct runoff begins and, finally, direct runoff and base flow can be separated. Here the number of days (N) is computed by using Eq. 3.10 as follows.

$$\mathrm{N} = 0.827\, A^{0.2} \qquad (\mathrm{Eq.}\ 3.10)$$

where N is the number of days, and A is the size of a basin (km^2).

(4) Modified N-day Method

The speed of rise of groundwater elevation is slower than that of surface runoff so the recession curve right before the beginning of a certain rainfall is reduced for a while even if rainfall is continuous. The modified N-day method assumes the base flow rate to maintain the tendency of attaching to the peak time. In addition, it analyzes base flow and direct runoff directly to the line that connects the point of the falling limb after N days from the peak flow using a straight line.

(5) Variable Slope Method

In this method, the base flow part of the curve before the rising limb of a hydrograph is extended. Similarly, the base flow curve of the falling limb is also extended inwards to intersect the ordinate that joins the point of the inflection point of the falling curve. A perpendicular line is drawn at this junction, and the two extended lines are joined.

Unlike the existing hydrograph separation methods described earlier, HSS, a methodology that, vertically divides a hydrograph into three sections, such as rising limb, crest, and falling limb, was newly proposed and applied in this. The key purpose of this method is reflect runoff characteristics for each section as estimating parameters. Thus, the HSS method is distinct from the conventional hydrograph separation that separates direct runoff and base flow in the longitudinal direction.

To apply the proposed method, primarily, an inflection point in which the direction of a curve changes on a hydrograph should be found (refer to Figure 3.4). Mathematically the definition of inflection point is a point in which the value of its derivative is zero (0) and the sign of the derivative value before and after the point changes (refer to Eq. 3.11 and see Figure 3.5).

$$\frac{\partial^2 Q}{\partial t^2} < 0 \rightarrow \frac{\partial^2 Q}{\partial t^2} > 0 \quad \text{or} \quad \frac{\partial^2 Q}{\partial t^2} > 0 \rightarrow \frac{\partial^2 Q}{\partial t^2} < 0\,, \quad \text{and} \quad \frac{\partial^2 Q}{\partial t^2} = 0 \quad \text{(Eq. 3.11)}$$

So as to help in better understanding the figure, an inflection point is obtained on a hydrograph using 30-min-interval runoff data in accordance with the mathematical definition.

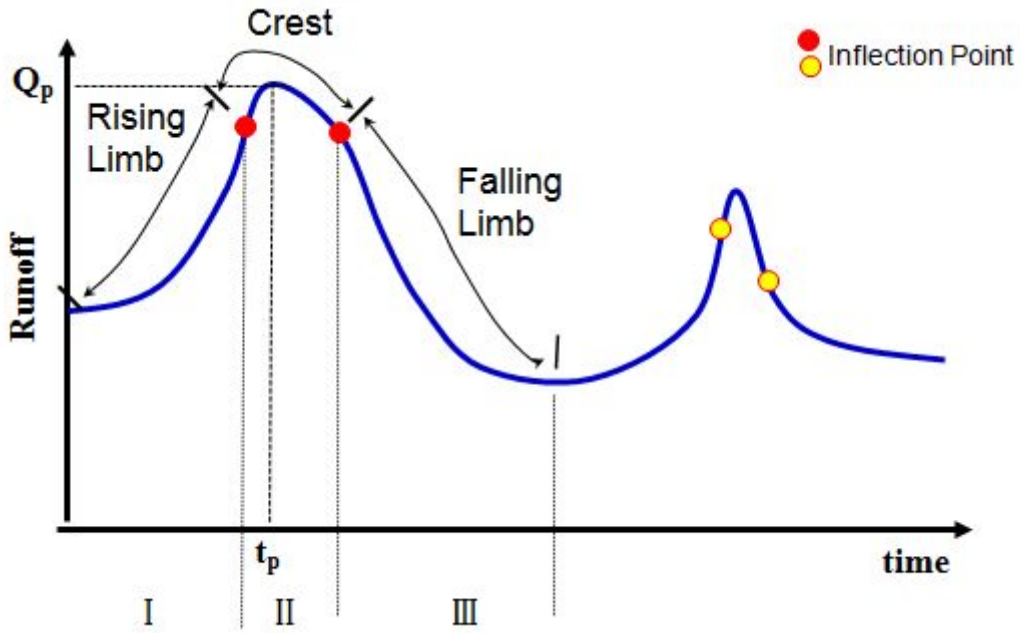

Figure 3.4 Conceptual diagram of hydrograph section separation

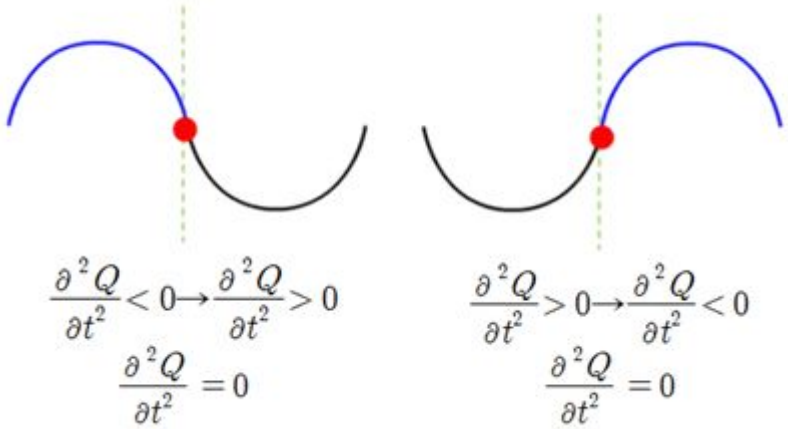

Figure 3.5 Definition of inflection point

First, a hydrograph is second-order differentiated, and then the average rate of change in 30-min-interval data is calculated. Here, the calculated value is differentiated to find the inflection point. However, if the fluctuation of runoff data is severe, it is not possible to simply find an inflection point using a second-order differential value. In this case, another method that can be applied is as follows. First, a polynomial equation can be estimated by conducting polynomial fitting according to a linear or nonlinear regression analysis based on runoff data. Finally the inflection point can be found by conducting second-order differential on the calculated polynomial equation.

However, this method cannot work when the degree of estimated polynomial is too high or if there are no points with zero (0) value even after conducting second-order differential. In this case, in advance, the moving average of 30-min-interval runoff data is computed to reduce the fluctuation of the original data, and then second-order differential is conducted to find an inflection point. Alternatively, a cumulative discharge curve can be computed to reduce data fluctuation instead of the moving average.

4. Study Area and Its Hydrological Characteristics

In the previous chapters, there are reviews on the trends of existing researches on parameter estimation in hydrologic models and determination of problems in existing parameter estimation methods. Moreover, to improve those problems, a new methodology for separating a hydrograph is proposed.

In this section, before the actual application of the proposed method, the information on study area and its hydrological characteristics are reviewed, and the storage function model as a hydrologic model applied in this research is analyzed for a better understanding of the method.

4.1 Study Area

In the research, the study area is the Jeongseon basin which is one of the sub-basins in the Han River basin. The Jeongseon basin has the point for flood forecasting and, there are no infrastructures blocking or controlling discharge, such as dams and reservoirs in the upstream. Figure 4.1 shows the schematic diagram of 30 sub-basins in the Han River basin, including the Jeongseon basin, as well as the location of the water level

gauging station in the Jeongseon basin, the schematic runoff flow, and an aeronautic chart. The gauged data in the Jeongseon station is summarized in Table 4.1.

The Jeongseon basin is located at 128°30′~128°59′ east longitude and 37°09′~37°35′ north latitude. The basin located at the upper area of South Han River is contiguous with several cities and provinces - Gangneung-si in the north, Pyeongchang-gun in the northwest, Yeongwol-gun in the south, and Donghae-si, Samcheock-si and Taebaek-si in the east. In the basin, there are 10 streams, including Odaecheon, Seokhyangcheon, Jijangcheon, and Gojicheon. More than 85 % of the basin is forest, and the alpine region is widely distributed in the basin. Annually, the maximum temperature is 23.7°C in July, and the minimum is –3.83°C in January. The Jeongseon basin shows the characteristics of the continental climate because the basin is located in a mountainous inland. The distribution of average temperature is similar to the central inland region of South Korea and the annual mean precipitation is 1,124 mm. In summer, the localized heavy rainfall may appear as the southwest monsoon that passes over the Taebaek Mountain (MOCT and K-water, 2004).

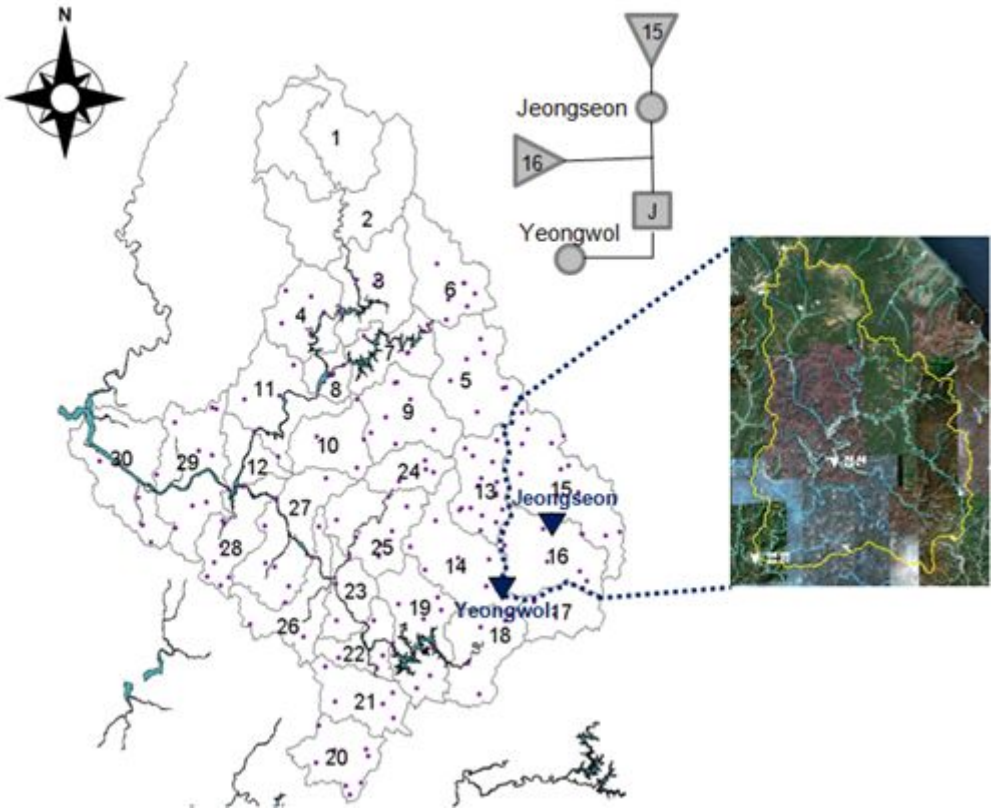

Figure 4.1 Han River sub-basins (Han River Flood Control Office, MOLIT, 2011)

Table 4.1 Characteristics of the case study area (Han River Flood Control Office, MOLIT, 2011)

Name of Stage Station	Code of Station	Altitude	Longitude	Management Organization	Area (㎢)
Jeongseon	1001655	37-22-42	128-39-26	MOLIT	1,688.41

The area of the basin is 1688.41 km^2 and in terms of morphological features, the river in the basin has curved channels both up-stream and down-stream. Both the left and right banks have been well maintained, and the river bed is composed of pebbles that are relatively coarse particles. The Jeongseon gauging station is located at the outlet of the basin.

When selecting a study basin for parameter estimation, a basin in which the water used is frequently changed and the discharge volume is fluctuated because of artificial hydraulic structures (dam, reservoir, retention, etc.) is not suitable. Instead, it is more appropriate to select a basin located at the most upstream area, which is less affected by man-made activities. To ensure the applicability of the proposed methodology in this research, it may require selecting a variety of basin for application. However, regardless whether a basin is an urban area or an area with a variety of hydraulic structures, what should be considered in changing a target basin might be the number of parameters to be estimated. Except for this, it is determined that there would not be significant changes in any conditions that affect simulation results. Any change in the number of parameters influence the total time for parameter estimation and it can bring out a problem in the prediction time for flood forecasting. However these concerns in

the time for parameter estimation or flood prediction can be resolved by upgrading a hardware, such as a computer. Ultimately, it is determined that a variety of basins as study areas do not significantly affect the feasibility and applicability of the proposed methodology in this research.

4.2 Hydrologic Characteristics

At downstream from the Jeongseon Gauging Station, there is the Yeongwol Gauging Station. The Yeongwol Station for flood forecasting is located at the most upstream area of the Han River main stream. Both the Jeongseon and the Yeongwol Stations have kept qualified hydrological data on water stage, stage-discharge relationship curve, etc. The Jeongseon Gauging Station started gauging under a jurisdiction by the Ministry of Construction and Transport (MOCT), Korea since 1918.

In this research, the data on rainfall and water level for parameter estimation were the most recent records from the 2000s to consider the current trends and patterns of rainfall. In addition, the data on 30-min-interval area average rainfall and discharge from 2004 to 2011, qualified by the Quality Control System of Hydrologic Data

operated by the Han River Flood Control Office (HRFCO) of MOLIT were used in this research. The rainfall events for parameter estimation were separated from the rainfall data from 2004 to 2011. The separation technique of rainfall events is used from the outputs of the research on "Improvement of Flood Forecasting Framework Using a Stochastic Approach (Han River Flood Control Office, MOLIT, 2011)". To define the minimum inter-event time of the absence of rainfall, the Inter-Event Time Definition (IETD) concept was used.

Applying the methodology used in "Improvement of Han River Watershed Runoff Program (Han River Flood Control Office, MOCT, 1991)" and Huff (1967), a rainfall event is separated from historical data based on the criteria that is no rainfall lasts more than six hours. Since the minimum value of rainfall gauging is 0.1 mm, a case that the areal average rainfall is estimated to be less than 0.1 mm is treated as no rainfall.

As the minimum value of observed rainfall is 0.1 mm, less than 0.1 mm of area average rainfall was considered as "no-rain". The criteria for selecting rainfall events were the amount of precipitation and the duration of rainfall. According to these two factors, 1-hr cumulative rainfall, 24-hr cumulative rainfall, total rainfall, the minimum duration, and the maximum duration were set. According to Huff (1967), total rainfall,

the minimum rainfall, and the maximum rainfall were set at more than 25.4 mm, more than 3 hr, and more than 48 hr respectively. In cases of hourly discharge and daily discharge, the standard that has been applied in HRFCO for the preparation phage in flood forecasting was applied. Hourly and daily discharge were set to greater than 30 and greater than 80 mm, respectively.

Using the criteria determined above, the rainfall events for 7 years from April 2004 to August 2011 in the Jeongseon basin were separated. As a result of separating rainfall events, a total of 18 events were selected. Table 4.2 summarizes the selected rainfall events in this research. Most of the selected events occurred in a flood season between July and September, but a few events (No. 1, 6, 13, and 14) occurred in April and May. As shown in (a) ~ (r) of Table 4.2, the peak flow in event No. 1, 3, 4, 5, 6, 8, 13, and 14 is less than 500 m^3/s and event No. 2, 11, 12, 15, 17, and 18 show 1,000 ~ 2,000 m^3/s of peak flow. Even the peak flow of event No. 7, 10, and 16 is more than 2,000 m^3/s. In addition, event No. 7, 10, and 11 needed more attention with regard to estimating parameters because they were complex rainfall events.

In terms of rainfall duration, it was identified that a variety of events were selected. The maximum duration of rainfall was 175.5 hours (about 2 days) and the minimum

was 47.5 hours (about 7.3 days). Also, there were some events where peak flow occurred quickly after rainfall started such as event no.1, 3, and 4. On the other hand, there were some cases where peak flow occurred a little late such as event no. 14 and 18. The runoff rate for each rainfall event was calculated as the proportion of total runoff to total rainfall. As a principle, it was considered to examine the proportion of direct runoff to effective rainfall. However, in the way that the uncertainty would increase as dividing effective runoff and base flow and the analysis in this research was focusing on rainfall characteristics in a single sub-basin, it was determined that the runoff rate calculated with the proportion of total runoff to total rainfall was quite acceptable.

Consequently, although a single sub-basin is selected as a study area in this research, it can be determined that the diversity of rainfall is considerably reflected in parameter estimation with a variety of rainfall events in terms of rainfall duration, peak flow occurrence time, time-series pattern, runoff rate, and single/complex event etc.

Table 4.2 Selected rainfall events in the Jeongseon sub-basin

No.	Rainfall Event Start Time	Rainfall Event End Time	Rainfall Event Duration (hr)	Total Rainfall (mm)	Runoff (mm)	Runoff Rate (%)
1	2004-04-26 14:30	2004-04-30 21:00	103	72.58	39.00	53.74
2	2004-07-07 06:00	2004-07-10 06:00	72.5	60.29	47.01	77.98
3	2005-07-01 00:30	2005-07-02 23:30	47.5	76.86	48.74	63.41
4	2005-07-11 06:00	2005-07-13 18:00	60.5	62.25	71.59	115.01
5	2005-09-21 05:30	2005-09-24 05:30	72.5	58.9	79.11	134.31
6	2006-05-06 02:00	2006-05-08 02:00	48.5	61.53	20.98	34.10
7	2007-09-14 14:00	2007-09-21 21:00	175.5	187.64	168.91	90.02
8	2008-08-22 07:30	2008-08-25 07:30	72.5	66.87	36.44	54.49
9	2009-07-09 03:00	2009-07-11 20:00	65.5	133.62	104.97	78.56
10	2009-07-11 21:00	2009-07-17 19:00	142.5	249.98	231.51	92.61
11	2009-07-17 19:30	2009-07-20 19:30	72.5	86.96	90.53	104.10
12	2010-09-21 08:00	2010-09-23 13:00	53.5	79.71	82.79	103.86
13	2011-04-30 01:00	2011-05-02 13:00	60.5	74.83	69.04	92.26
14	2011-05-09 14:00	2011-05-13 14:00	96.5	82.54	56.94	68.98
15	2011-06-29 12:00	2011-07-02 00:30	61	69.28	51.05	73.68
16	2011-07-03 04:00	2011-07-05 04:00	48.5	117.22	116.93	99.75
17	2011-07-26 18:00	2011-07-30 04:00	82.5	79.37	54.38	68.52
18	2011-08-16 17:30	2011-08-19 17:30	72.5	80.78	54.83	67.87

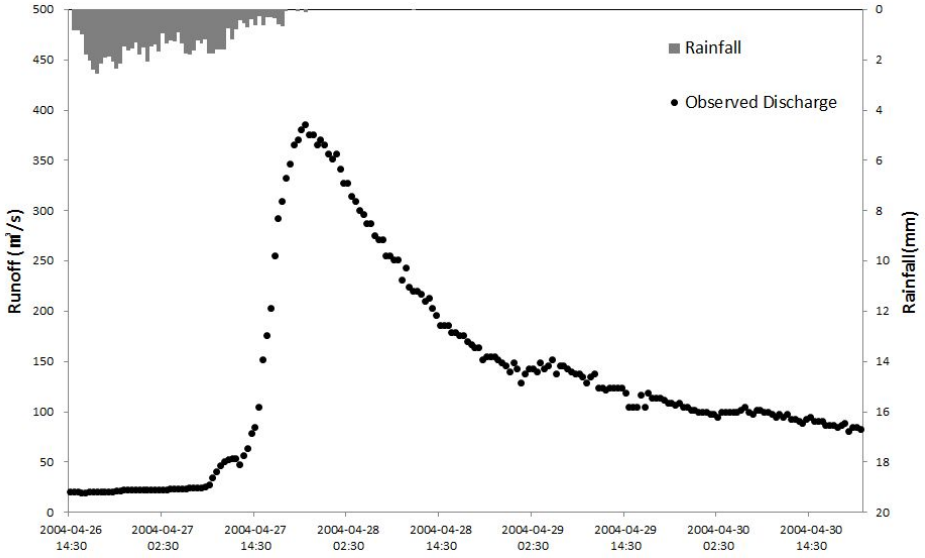

(a) Rainfall event No. 1

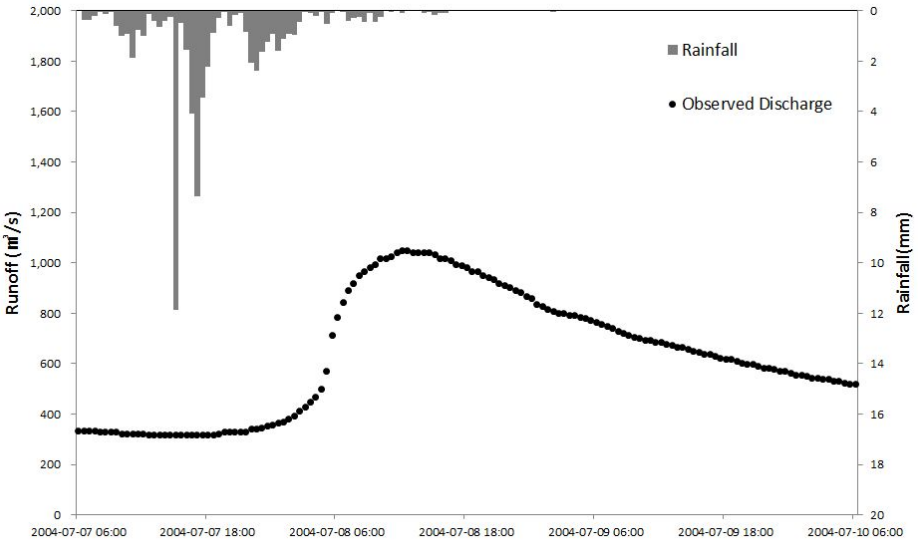

(b) Rainfall event No. 2

Figure 4.2 Rainfall-Runoff Data

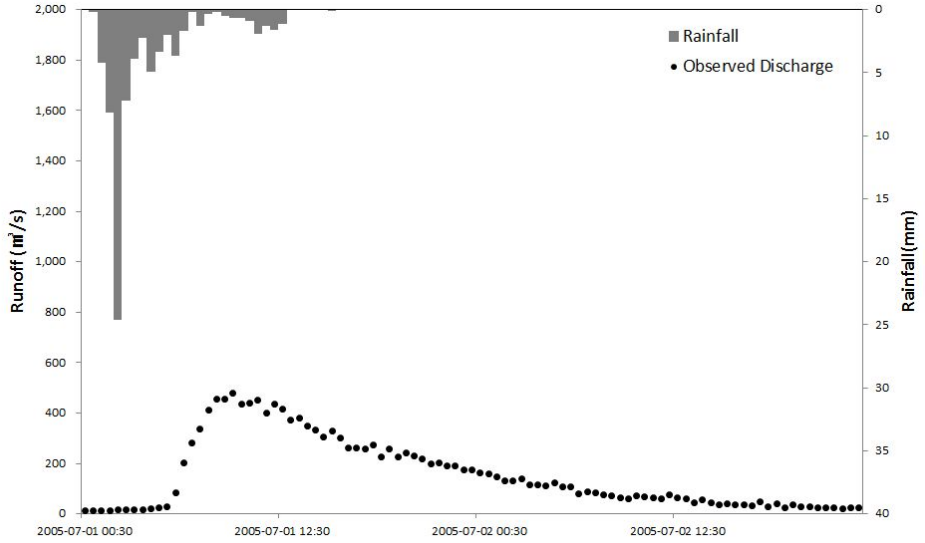

(c) Rainfall event No. 3

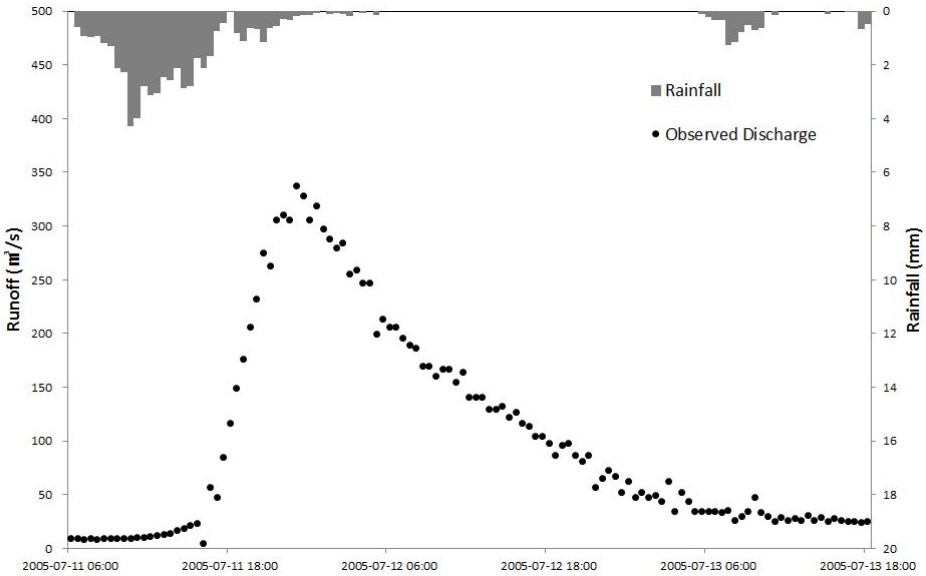

(d) Rainfall event No. 4

Figure 4.2 Rainfall-Runoff Data (continued)

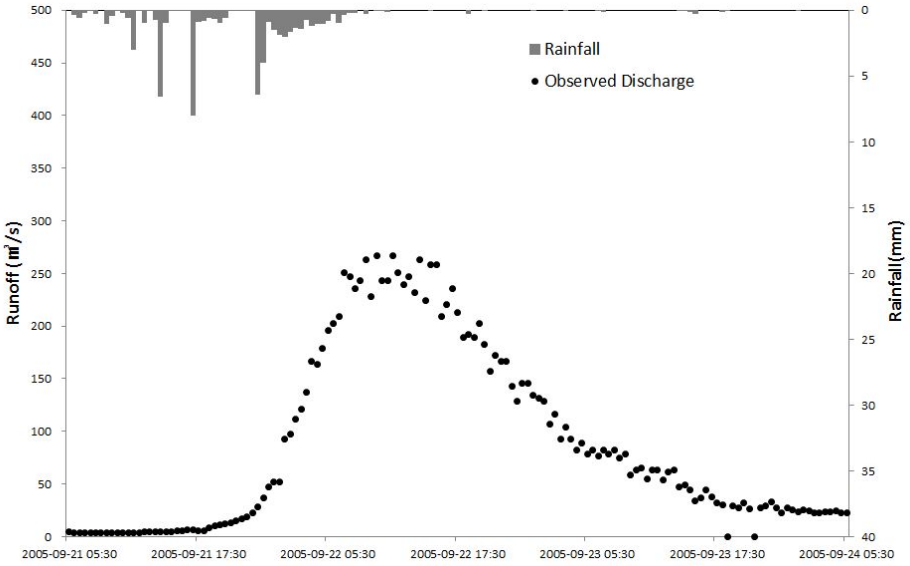

(e) Rainfall event No. 5

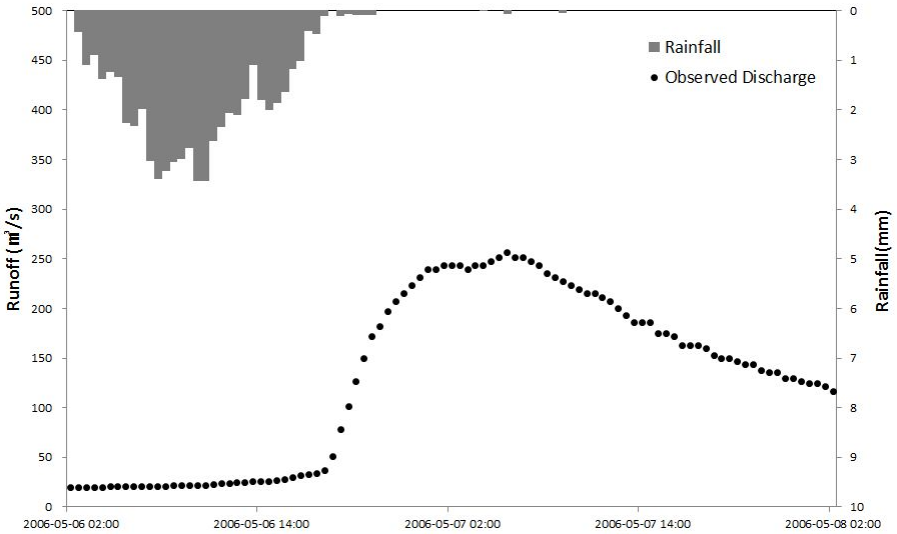

(f) Rainfall event No. 6

Figure 4.2 Rainfall-Runoff Data (continued)

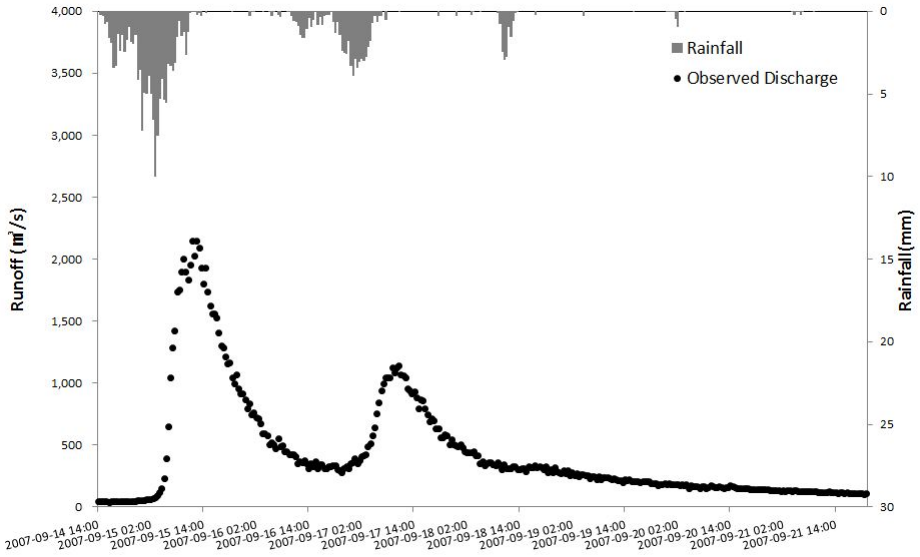

(g) Rainfall event No. 7

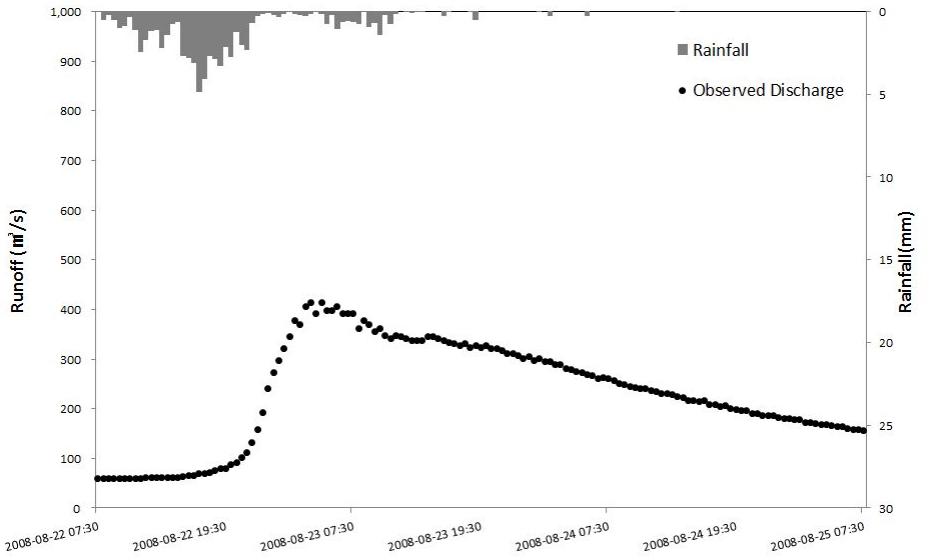

(h) Rainfall event No. 8

Figure 4.2 Rainfall-Runoff Data (continued)

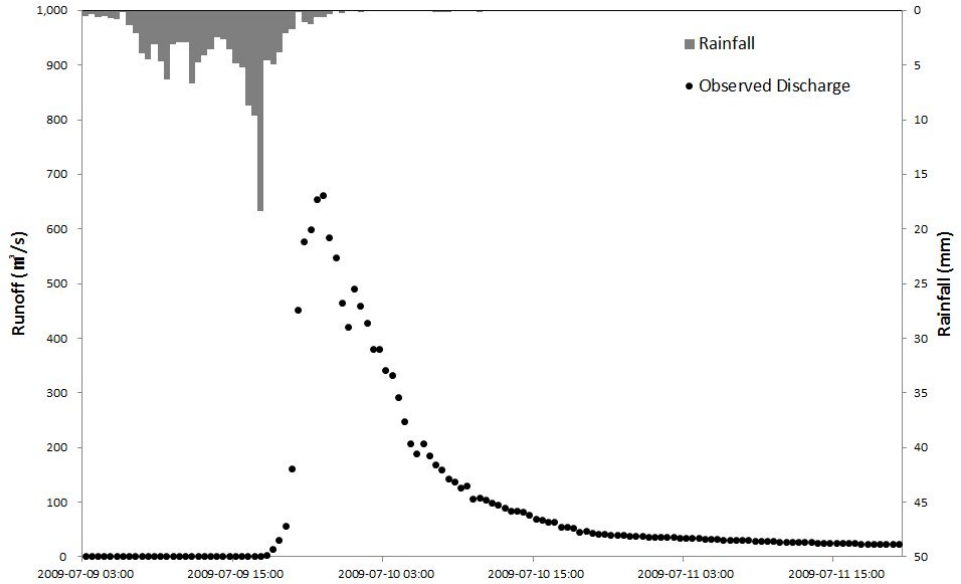

(i) Rainfall event No. 9

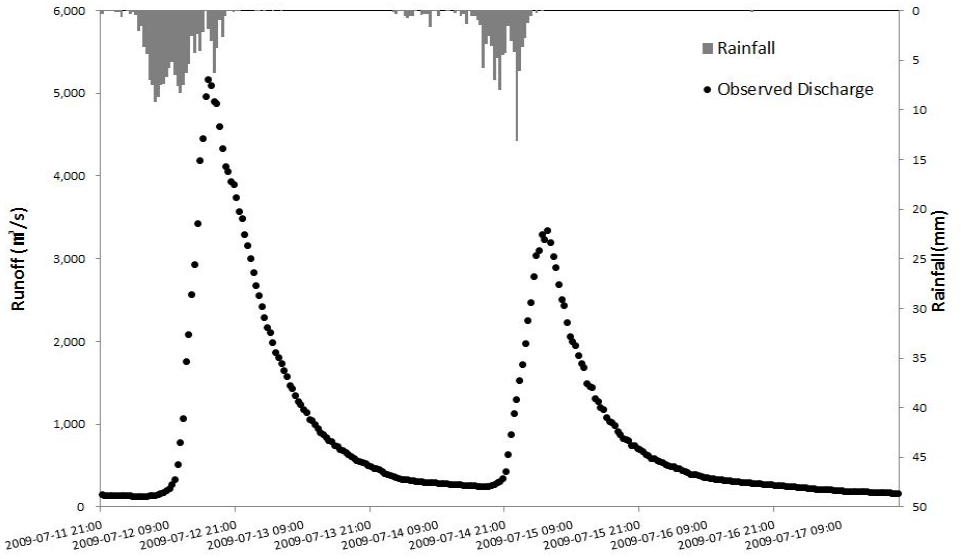

(j) Rainfall event No. 10

Figure 4.2 Rainfall-Runoff Data (continued)

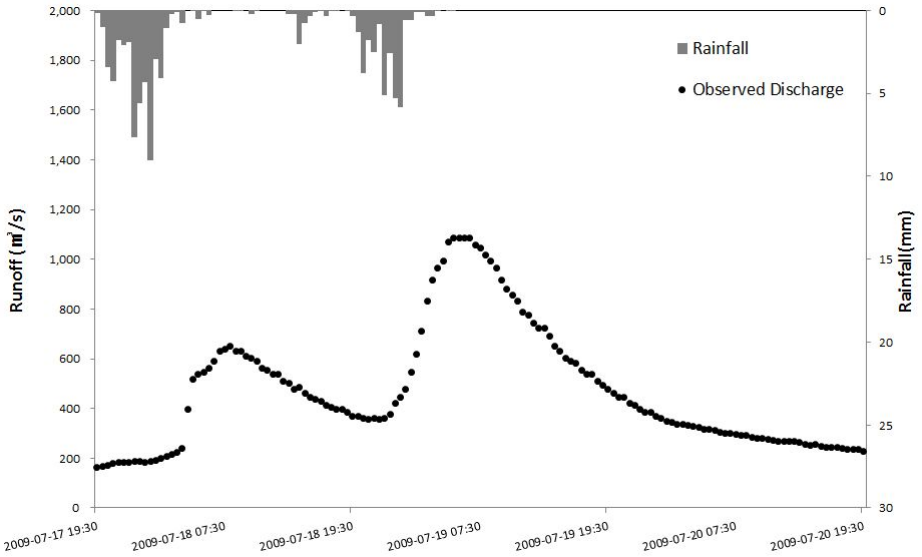

(k) Rainfall event No. 11

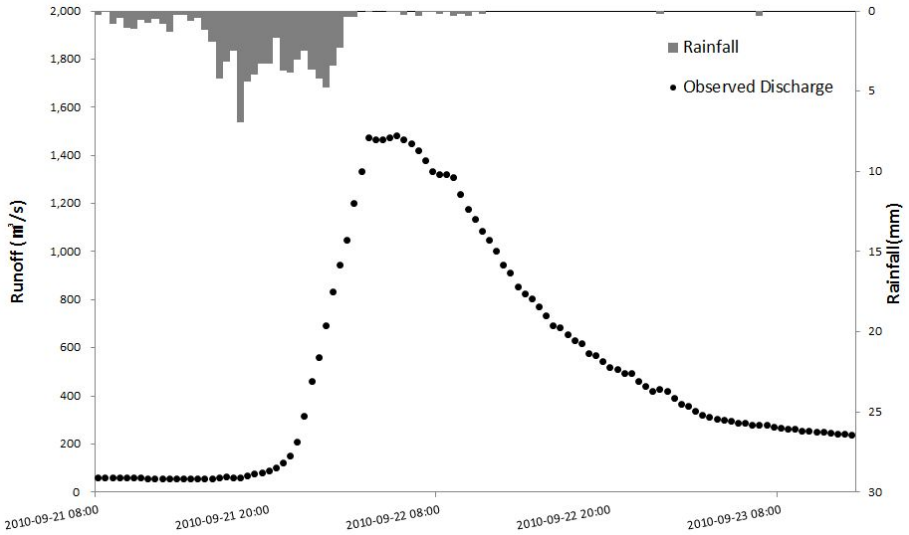

(l) Rainfall event No. 12

Figure 4.2 Rainfall-Runoff Data (continued)

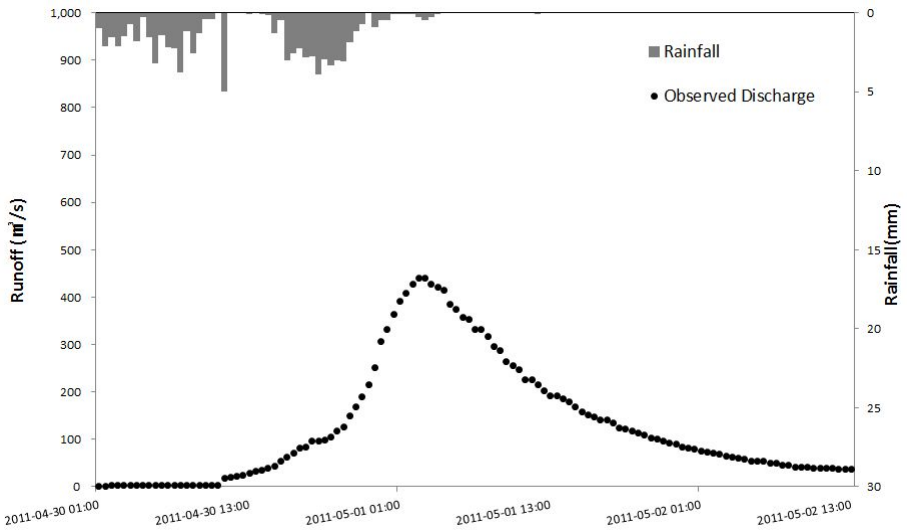

(m) Rainfall event No. 13

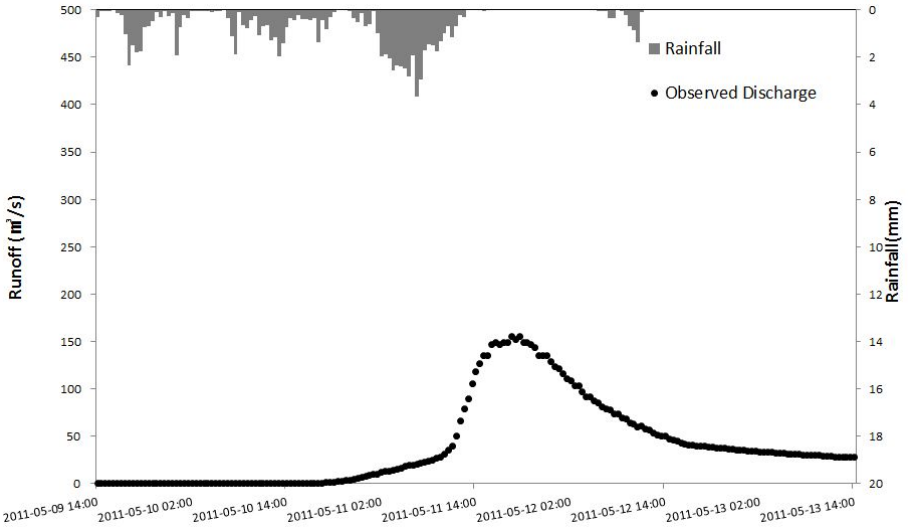

(n) Rainfall event No. 14

Figure 4.2 Rainfall-Runoff Data (continued)

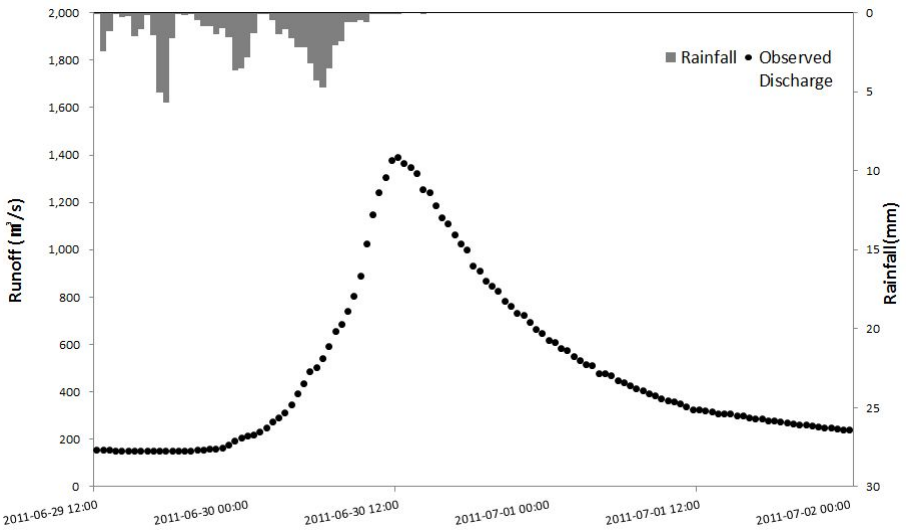

(o) Rainfall event No. 15

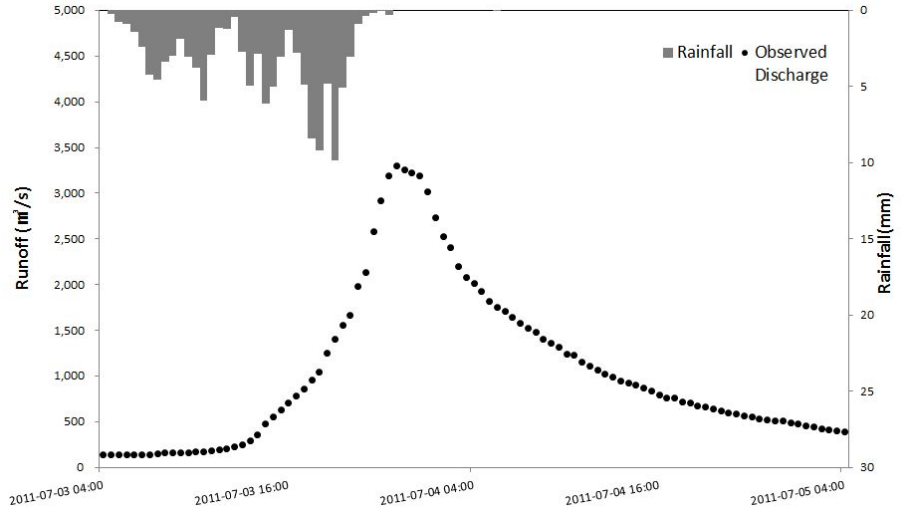

(p) Rainfall event No. 16

Figure 4.2 Rainfall-Runoff Data (continued)

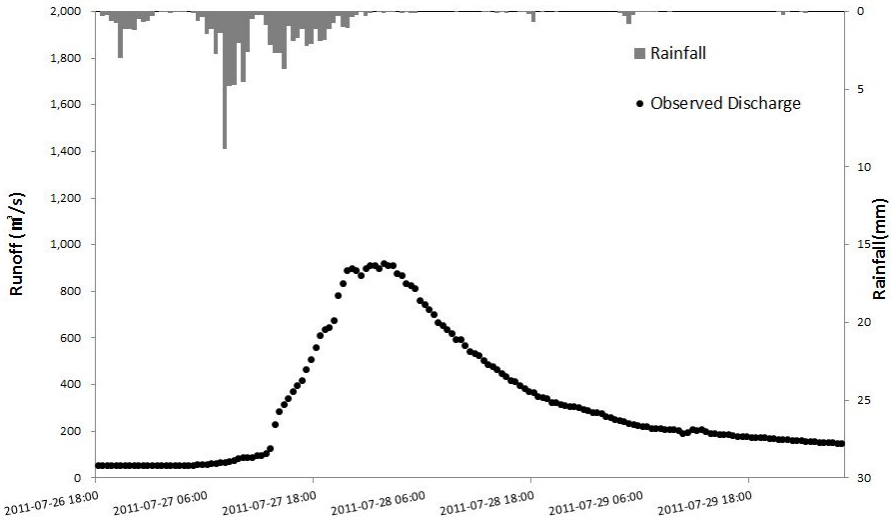

(q) Rainfall event No. 17

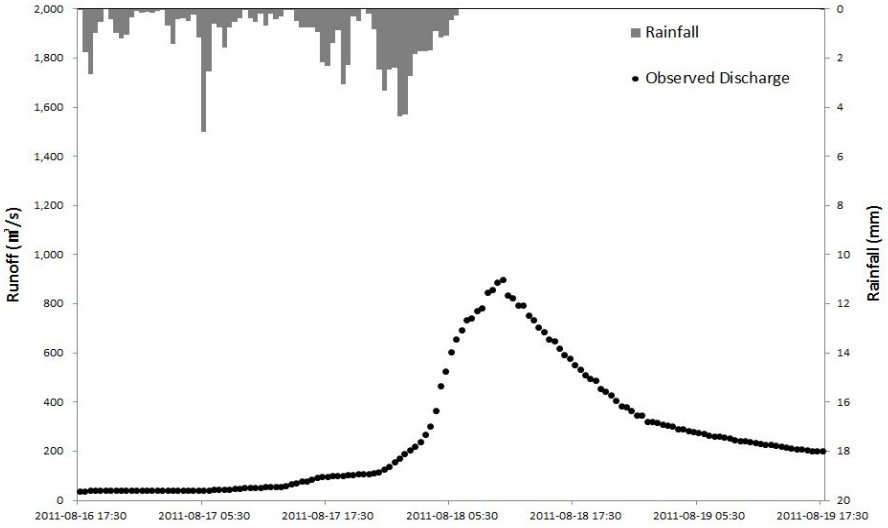

(r) Rainfall event No. 18

Figure 4.2 Rainfall-Runoff Data (continued)

5. Existing Parameter Estimation Used in Practice and Its Improvement

In Korea, the existing problems in parameter estimation for flood forecasting using a storage function model in the field were examined. To improve examined problems, as estimating parameters, a global optimization method was applied and time-series data on rainfall and discharge were used instead of even-based data. Then the results of parameter estimation were analyzed and compared with the existing methodology. As a result of comparison, it was determined that the improved methodology in this research estimated parameters more efficiently than the conventional method. Nevertheless, a concern that will remains was that the uncertainty existed in parameter estimation. To reduce the uncertainty, the HSS method proposed in the research was applied to estimate parameters for each separated section. Finally, real-time flood forecasting methodology in the field through the application of the proposed method and procedure in this research was suggested.

The hydrologic data used for parameter estimation were historical records from April 2004 to December 2001. Among them, the data for April 2004 - December 2005

were used as the warming-up data set, and the data for January 2006 - December 2009 were used for calibration. Moreover, the data for January 2010 - December 2011 were used for the verification of estimated parameters.

5.1 Sensitivity Analysis

For parameter estimation, sensitivity analysis, which diagnoses the most sensible parameter to a hydrologic model, should be conducted by priority. The factors that affect the outputs of the storage function model applied in this research are model constant K and P; the first flow rate, f1, which indicates the flow rate before saturated runoff; saturated rainfall, R_{sa} at the saturation point; and the lag time of a basin, T1, which indicates the lag condition of runoff from rainfall. In addition, there are including three additional parameters that enable the storage function model to be applied to various rainfall events: saturated flow rate (f_{sa}), rainfall magnification (α), and groundwater level regression curve (gwlrc). That is, a total of eight parameters for storage function were used to conduct sensitivity analysis.

To analyze the impacts of changes in each model parameter on runoff simulation results, the optimal parameters estimated by applying SCE-UA was set as the reference value. Then, To compare the simulated runoff to the reference value, the value was changed by $\pm 10\%$ in steps. The comparison results were converted to the change rate of peak flow and total runoff. The results of sensitivity analysis are shown in Figures 5.1 and 5.2. It was found that both peak flow and total runoff were the most affected by the storage function constants K and P. Moreover, first flow rate, f1; the lag time of a basin, T1; and saturated rainfall, R_{sa}, gave slightly greater impacts on total runoff. Therefore, the model was configured using the above mentioned five parameters (K, P, f1, T1, and R_{sa}). In addition, the occurrence time of peak flow according to changes in each parameter was analyzed. As a result, it was found that parameter change hardly affected the occurrence time of peak flow.

Changes of runoff pattern in accordance with the change of each parameter are as follows. When storage function constants K and P; the lag time of a basin, T1; and saturated rainfall, R_{sa}, increase, peak flow and total runoff show a tendency to decrease. In contrast, as first flow rate, f1, increase, the increase in both peak flow and total runoff is identified. It is determined that fist flow rate gives the greatest impact on total

runoff until runoff in the storage function reaches saturation. This affects the pattern of drastic runoff. In addition, it is found that changes in rainfall magnification (α) and groundwater level recession curve (gwlrc) are relatively insensitive.

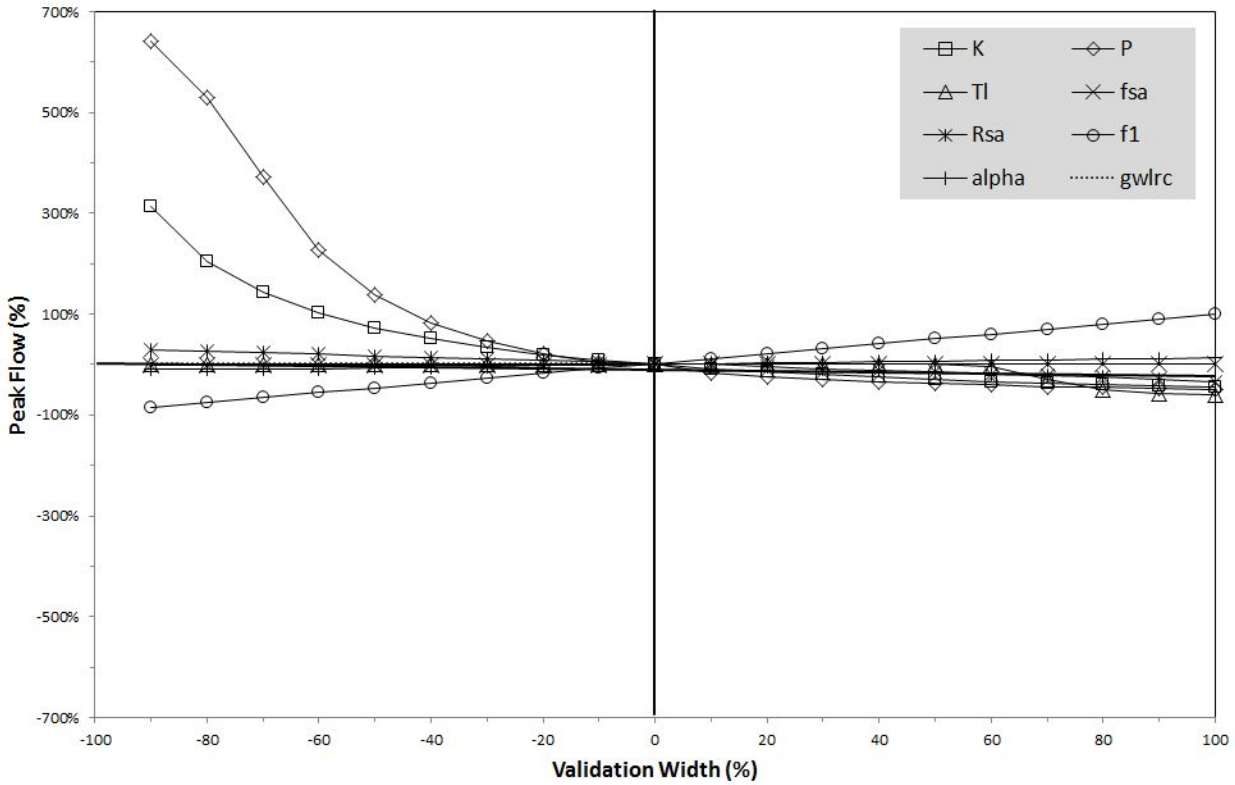

Figure 5.1 Sensitivity analysis in peak flow

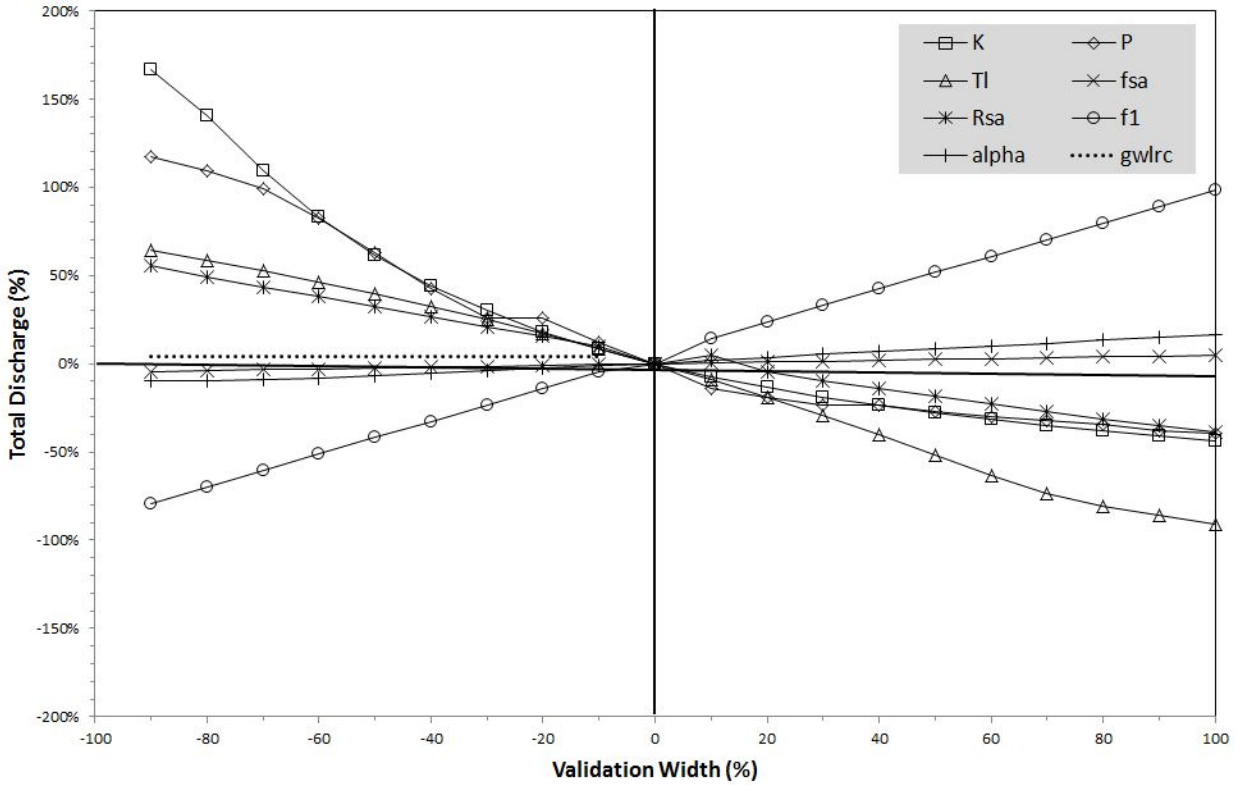

Figure 5.2 Sensitivity analysis in total discharge

5.2 Problem Diagnosis of the Existing Parameter Estimation in Practical Use

Han River Flood Control Office (HRFCO), which is in charge of flood forecasting in Korea, has simulated runoff by using a storage function and by conducting the trial-and-error method based on the predetermined parameter initial values for each sub-basin. Here the parameter initial value is the mean value of predetermined parameter estimates using trial-and-error method based on a single historical rainfall event. Identifying the accurate period of the data is impossible because of the limitation of its availability, but it is determined that historical rainfall events that are applied to estimate the initial values of parameters are high-water level data during a flood season (July - September in Korea). By applying estimated parameters based on the historical events with high-water level, reliability in runoff forecasting, including a peak flow of less than 1,000 m^3/s in the Jeongseon basin, is determined to be low. The existing parameter estimation method used in practical works is likely to bring about a local optimum for flood forecasting because a parameter is estimated based on a single rainfall-event.

Using the initial value of the parameter set above the Jeongseon basin, runoff simulation was conducted for 18 individual rainfall events during April 2004 - December 2011, and then their results are summarized in Table 5.1 and Figure 5.3. They show large differences in both NSE and RMSE. In addition, the NSE model simulation with a time-series data for a calibration period (January 2006 - December 2009) and a verification period (January 2010 - December 2011), respectively, were not good. It is examined that these results seem to have been caused by the limitations of the trial-and-error method used for parameter estimation and the simulation approach that uses the mean value of each estimated parameter based on a single historical rainfall event. One thing that needs further attention is the NSE (a value of 0.668) computed by applying a time- series data that cover the entire period of available data, which is significantly improved compared to the mean value of NSE (a value of -1.965) computed by applying each of the 18 events individually.

Table 5.1 Simulation results by the initial value of parameters estimated by the existing methodology in practical use

	K	P	Tl	fl	R_{sa}		NSE	RMSE	RE_p	RE_v
Initial Value (for each events)	34.987	0.458	2.84	0.503	83.6	Average	-1.965	336.371	0.586	0.295
						Standard Deviation	6.000	315.103	0.580	0.420
						Minimum	-17.566	146.787	0.063	0.001
						Median	0.537	247.781	0.421	0.119
						Maximum	0.611	1161.27	1.596	1.307
						Coefficient of Variation	-3.054	0.937	0.990	1.424
Initial Value (for time-series) estimation period	34.987	0.458	2.84	0.503	83.6		0.668	52.474	0.199	0.106
Initial Value (for time-series) verification period							0.622	51.499	0.116	0.205

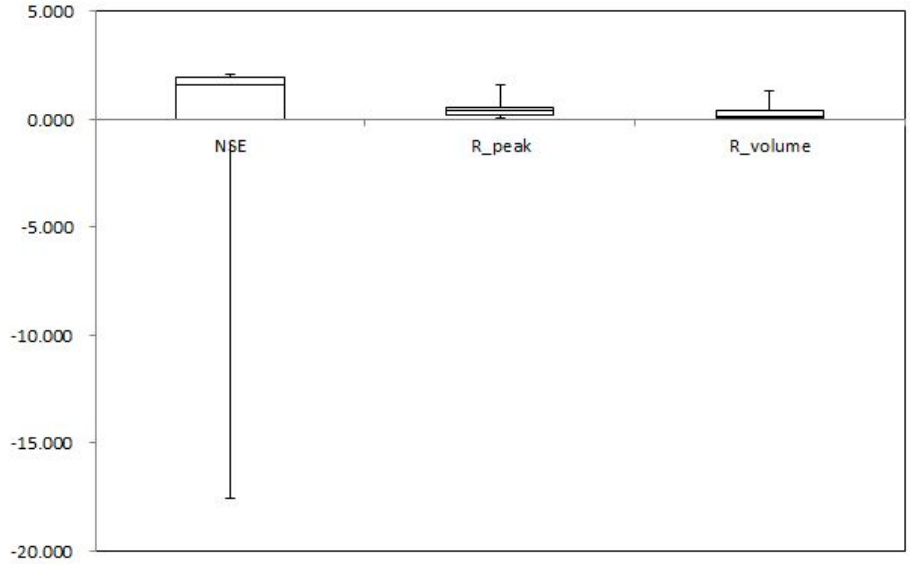

(a) NSE, RE_p and RE_v

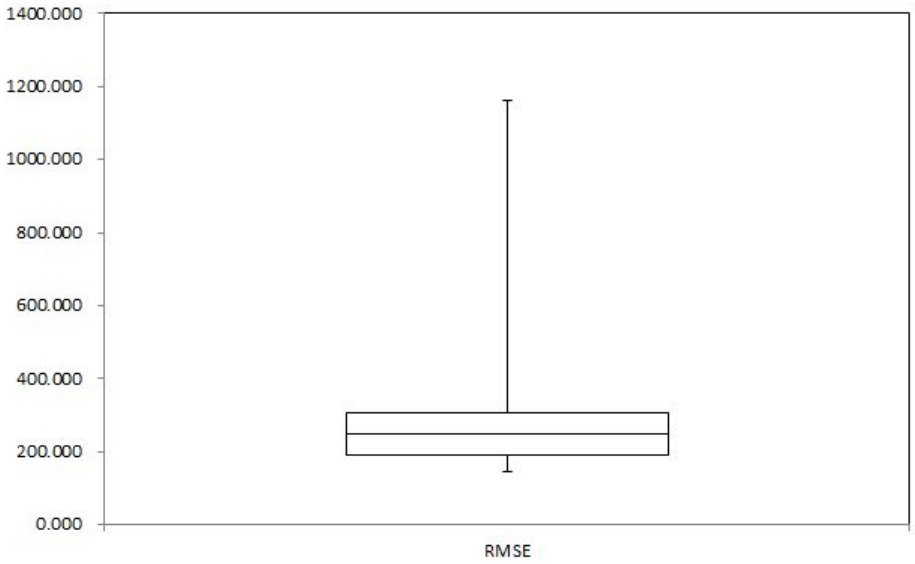

(b) RMSE

Figure 5.3 Box-and-Whisker plot of the objective function by simulating with the initial value of parameter for each event

5.3 Improvement of the Existing Parameter Estimation in Practice Use

A problem that was determined in the existing parameter estimation for flood forecasting used in practice is that initial values of the parameter for each event are estimated using the trial-and-error method and then their mean value is applied for flood forecasting. The limitation of the trial-and-error method can bring out a local optimum. Moreover, the approach that use only the mean value of parameters that depend only on historical data cannot consider the non-stationarity of future rainfall events, and it causes the lower efficiency of model simulation for flood forecasting in the future. Therefore it is more appropriate to apply a global optimization approach that provides the optimal parameter set that satisfies the multi-objective function. In addition, it is more preferable to apply a time-series data for the whole period available to conduct continuous simulation instead of applying a single rainfall event to estimate parameter. This can contribute to the improvement in the efficiency of model simulation for future rainfall events.

In this research, as a global optimization, SCE-UA that features a high speed of convergence and provides an optimal parameter set was applied to estimate

parameters. To examine the range of rainfall events for parameter estimation, SCE-UA was applied to estimate parameters for a single event of a total of 18 events and for the entire period with a time-series data. Then, the results were analyzed and summarized in Table 5.2 and Figure 5.4. As results of reviewing the objective functions NSE, RMSE, RE_p, and RE_v, the mean value of NSE (a value of 0.659) that conducted parameter estimation through the application of a global optimization SCE-UA for each event was improved compared to that of NSE (a value of -1.965) that applied the trial-and-error method. In addition, the mean value of NES (a value of 0.725) that applied SCE-UA for time-series data was improved compared to that of NSE (a value of 0.659) that applied SCE-UA for each event. Figures 5.5 and 5.6 as well as Table 5.3 show the results of calibration and verification using parameter initial value through trial-and-error method and applying SCE-UA, respectively. The simulation results using parameter initial value were overestimated compared to the observations. On the other hand, the results applying a global optimization SCE-UA were slightly underestimated compared to the observations. The parameter estimation results by applying SCE-UA based on each of the events was compared

to the results based on a time-series data. As a result, the verification period when SCE-UA was applied with a time-series showed better results.

Table 5.2 Results of simulation by estimated parameter with SCE-UA

Parameter		K	P	Tl	F1	R_{sa}	NSE	RMSE
SCE-UA (for each events)	Average	27.53	0.66	6.63	0.62	28.77	0.689	154.446
	Standard Deviation	9.65	0.12	2.68	0.26	26.61	0.806	101.516
	Minimum	17.05	0.39	3.49	0.01	0.14	-2.483	29.143
	Median	24.97	0.67	6.36	0.70	23.47	0.946	121.343
	Maximum	48.82	0.87	13.55	0.94	76.51	0.994	319.241
	Coefficient of Variation	0.40	0.45	0.43	0.50	0.95	1.223	0.657
SCE-UA (for time-series)		23.70	0.75	4.60	0.35	167	0.725	47.790

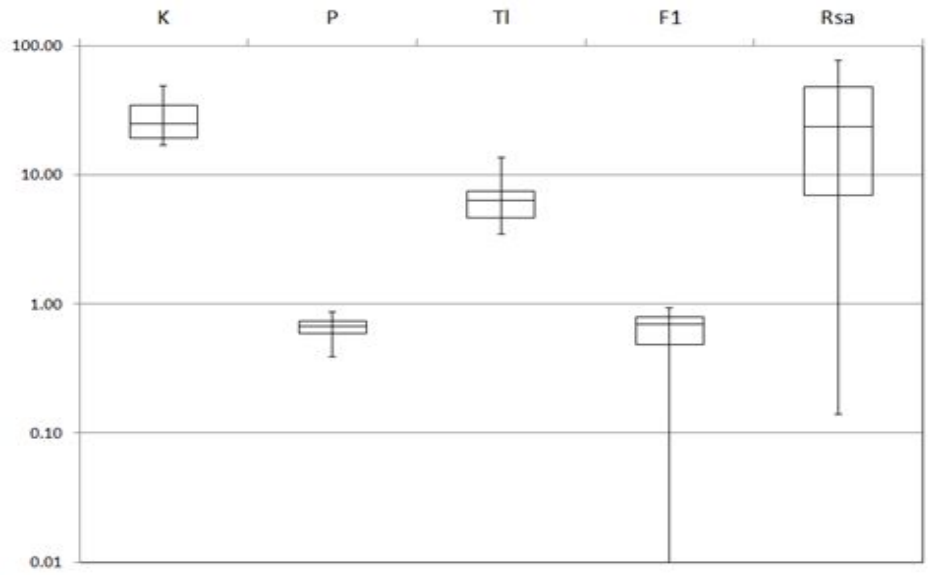

(a) K, P, Tl, F1, and R_{sa}

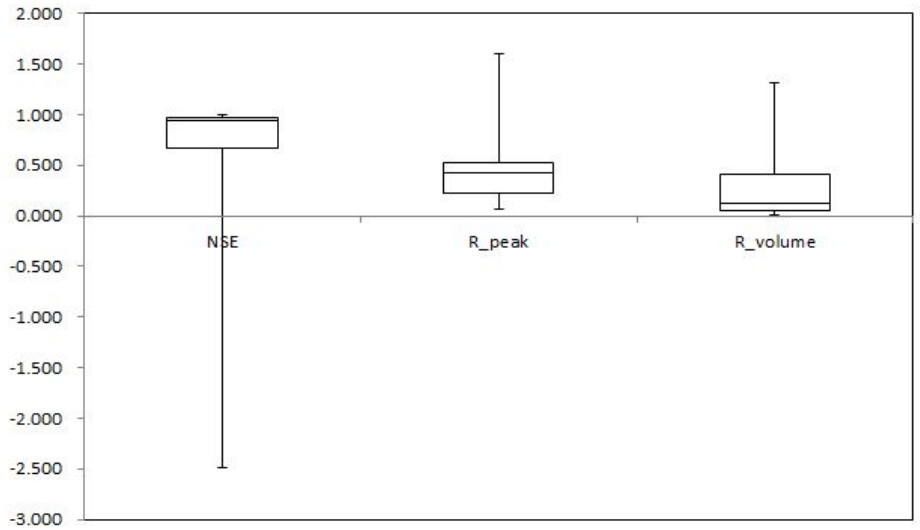

(b) NSE, RE_p, and RE_v

Figure 5.4 Box-and-Whisker plot of estimated parameters by SCE-UA

for each event

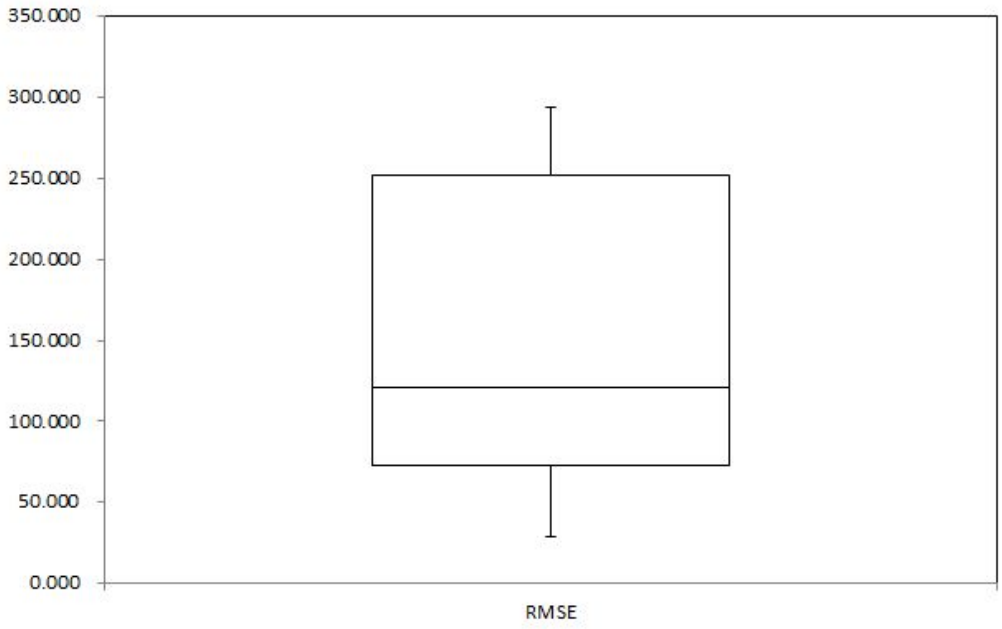

(c) RMSE

Figure 5.4 Box-and-Whisker plot of estimated parameters by SCE-UA

for each event (continued)

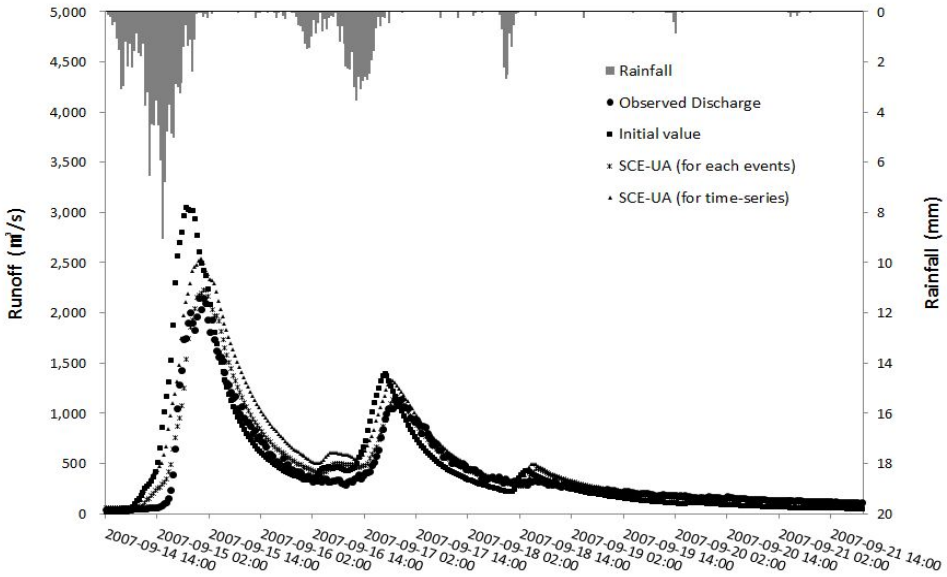

(a) 2007/09/14 14:00-09/21 21:00

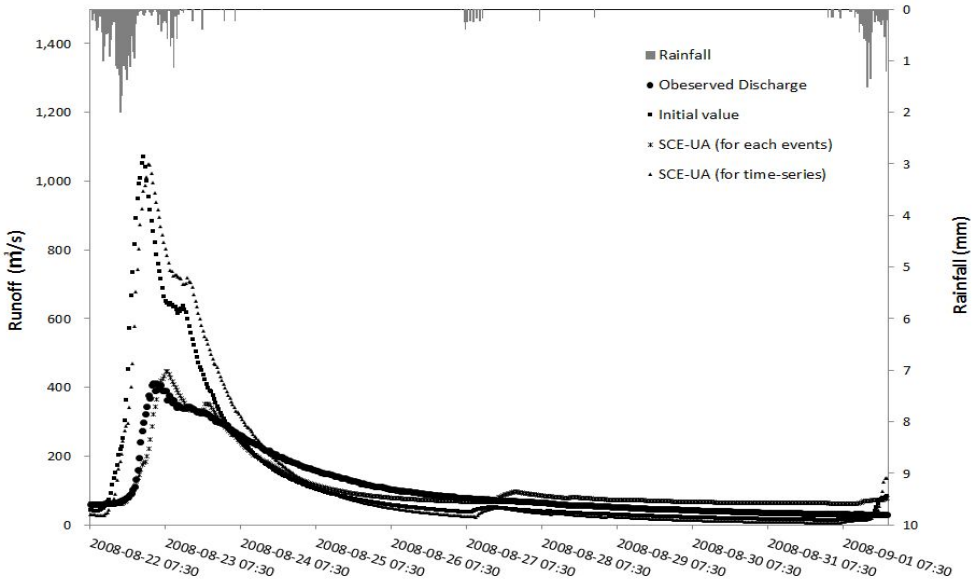

(b) 2008/08/22 07:30-09/01 21:30

Figure 5.5 Comparison of the parameter estimation by initial value and SCE-UA

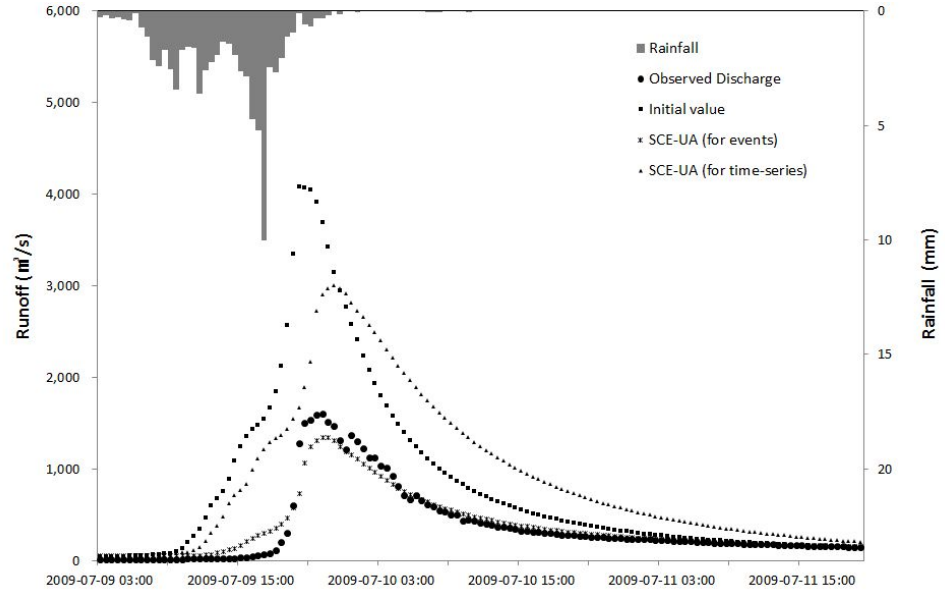

(c) 2009/07/09 03:00-07/11 20:00

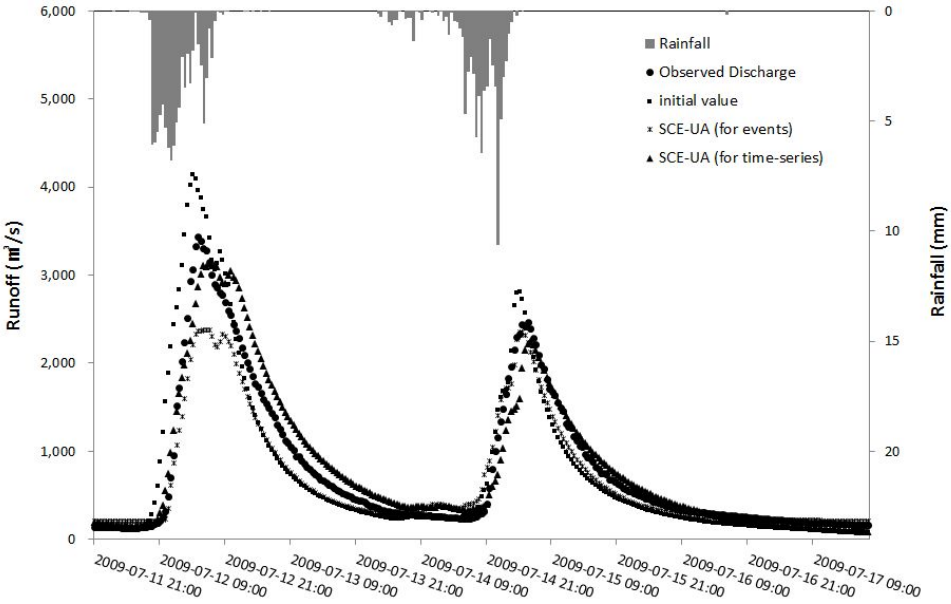

(d) 2009/07/11 21:00-07/17 19:00

Figure 5.5 Comparison of the parameter estimation by initial value and SCE-UA

(continued)

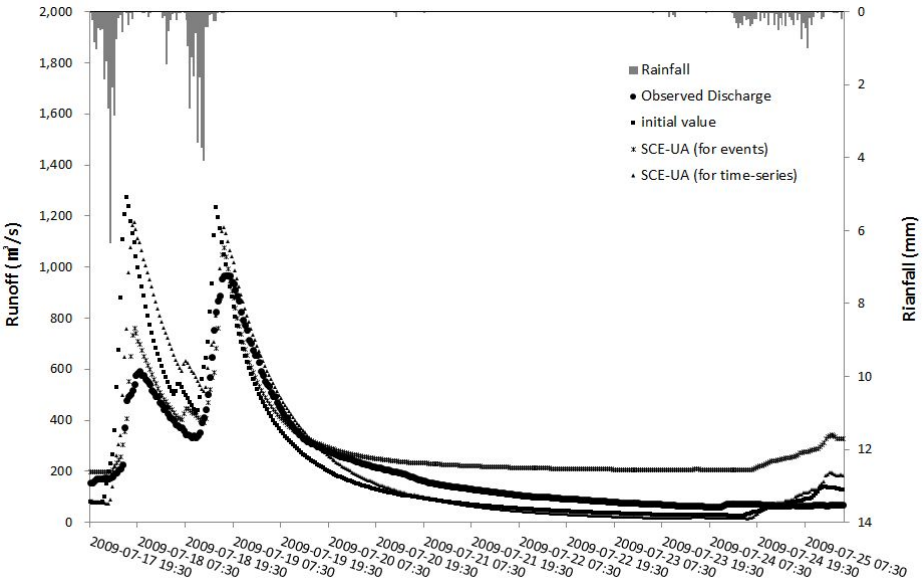

(e) 2009/07/17 19:30-07/25 17:00

Figure 5.5 Comparison of the parameter estimation by initial value and SCE-UA

(continued)

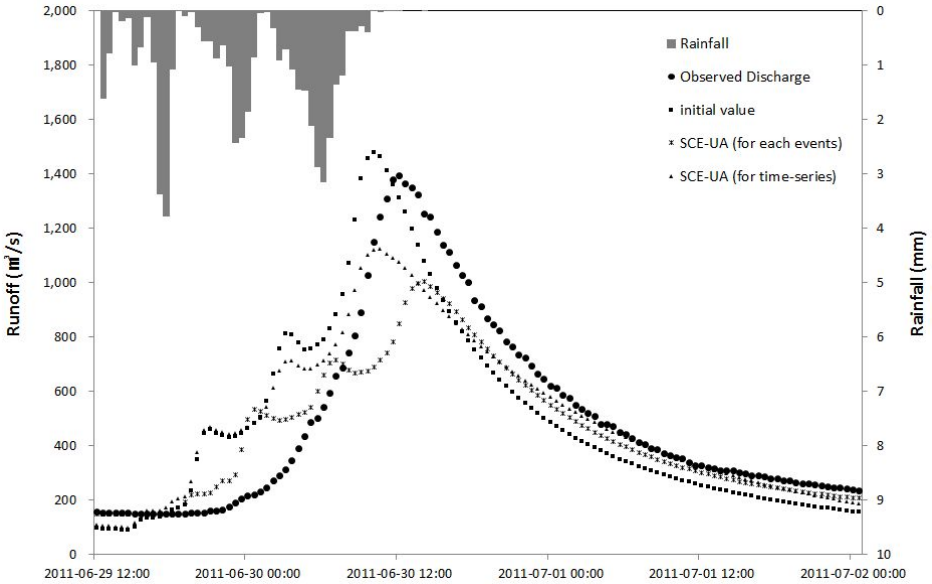

(a) 2011/06/29 12:00- 07/02 00:30

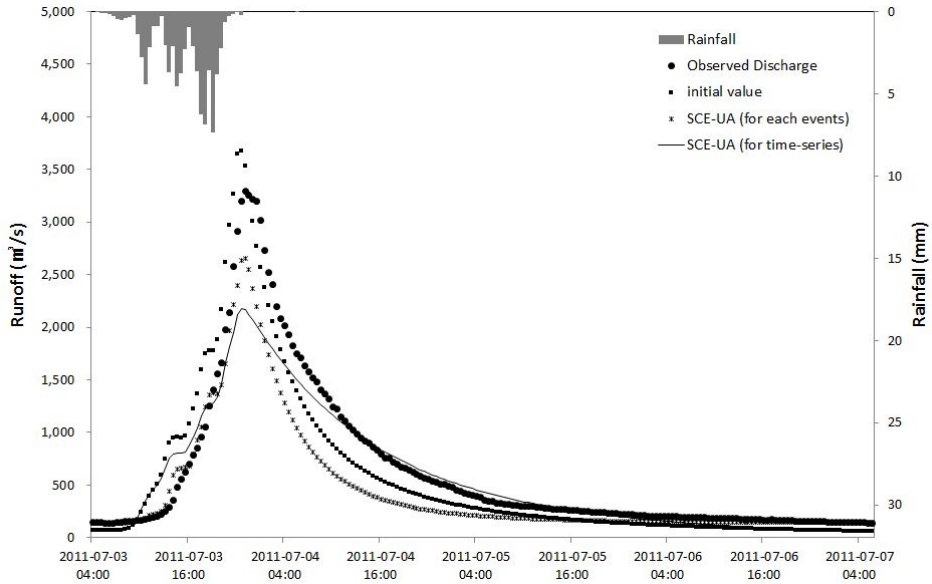

(b) 2011/07/03 04:00-07/07 05:30

Figure 5.6 Comparison of the parameter verification by initial value and SCE-UA

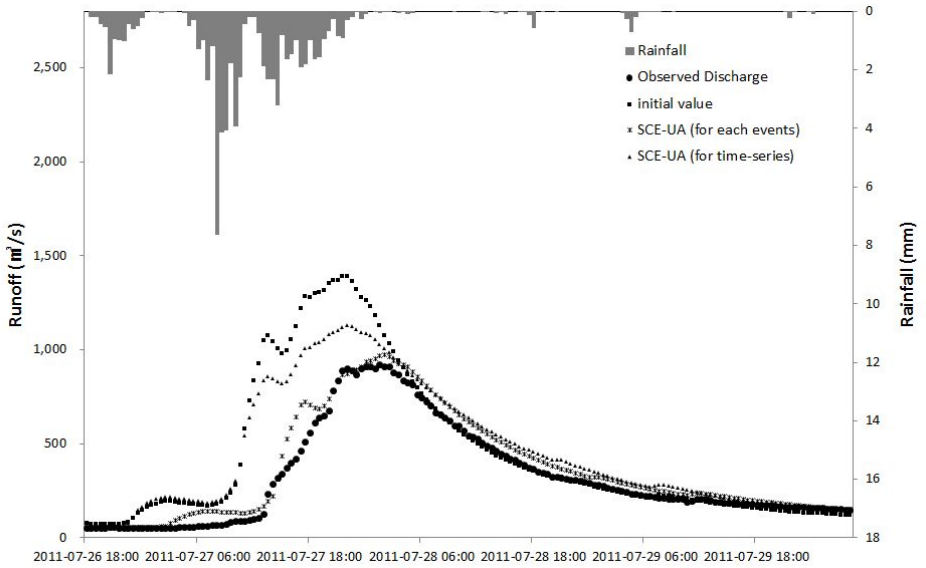

(c) 2011/07/26 18:00-07/30 04:00

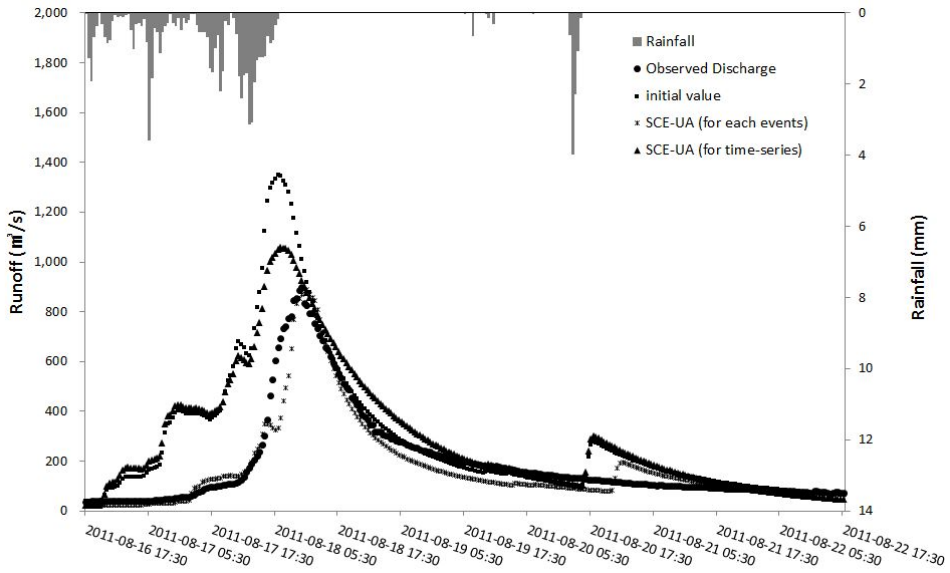

(d) 2011/08/16 17:30-08/22 17:30

Figure 5.6 Comparison of the parameter verification by initial value and SCE-UA

(continued)

Table 5.3 Runoff rate for each event

No.		Observed Discharge	Initial Value	SCE-UA	
				for each event	for time-series
Runoff Rate (%)	7	90.02	111.00	98.19	102.20
	8	54.49	80.05	70.74	83.60
	9	78.56	132.03	80.91	143.00
	10	92.61	112.92	96.76	109.22
	11	104.10	103.98	102.92	111.67
	15	73.68	74.43	66.59	74.49
	16	99.75	105.38	94.95	14.05
	17	68.52	90.22	73.61	90.09
	18	67.87	103.61	61.54	105.10

6. Parameter Estimation Using Hydrograph Section Separation

6.1 Methodology and Application of HSS

In fact, although SCE-UA was applied to a time-series data for the whole period available to estimate parameters, there are a number of cases that could not simulate the rising and falling limbs of a hydrograph sufficiently. In contrast, the time-series pattern of a hydrograph was well simulated, but at the same time, peak flow was not simulated properly. Therefore, the necessity of a more efficient methodology that satisfies both the time-series pattern of a hydrograph and the objective function coincidentally was raised. For this reason, HSS, which separates a hydrograph into three sections according to the inflection point, was newly proposed and applied to estimate a more appropriate parameter for each section. In general, the concept and theory of hydrograph separation has been applied to separate base flow from the total volume, but there has been no example of applying it for parameter estimation.

6.1.1 Inflection Point Detection

According to the theoretical background on HSS defined in Chapter 3, first, the inflection point should be estimated mathematically, and then, each section of a hydrograph, such as the rising limb, crest, and falling limb, can be separated based on the inflection point. However, it is difficult to find a suitable inflection point that satisfies the theoretical definition when there is a second-order derivative of 30-min-interval runoff data. This is because there are sections that show a frequent increase or decrease in runoff as shown in Figure 6.1.

The parabolic fitting method can be considered in finding the inflection point from runoff data. The first step is to find the optimal polynomial and function that excellently fits to runoff data, and then the second order differential value can be computed to obtain the inflection point. However, because of the diversity of rainfall the order of fitting available polynomials can be variously calculated as the fourth, sixth, or seventh order. As a second derivative of such a high-order polynomial is not a value of "0", it is still impossible to obtain the inflection point.

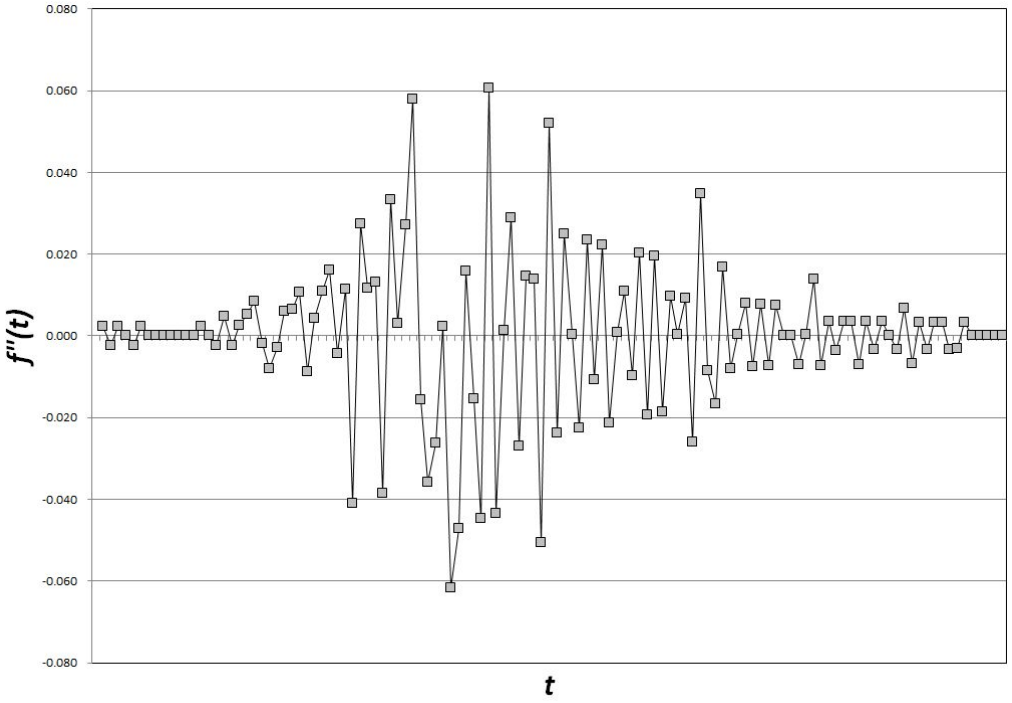

Figure 6.1 Second derivative values of the observed discharge

(2011/06/29 12:00-07/02 00:30)

The method described above is a case of applying the parabolic fitting from the 30-min interval data source of runoff. Since the second order differential value of 30 min-interval runoff data increases or decreases frequently, it can consider to find the inflection point from 30-min interval cumulative runoff data. As shown in Figure 6.2, the variation of the second order differential value of cumulative runoff decreases but only one inflection point can be detected. This is because the cumulative runoff curve with a shape of 'S' cannot find the inflection point in the falling limb of hydrograph. In addition, the most proper polynomial equation can be found through the parabolic fitting to the cumulative runoff curve, but a degree of polynomial is high and there are some cases that a second order differential value cannot be found like 30-min interval original runoff data (refer to Figure 6.3). In regard to these aspects comprehensively, it is determined that detecting the inflection point by using the cumulative runoff curve is not appropriate.

Therefore, it needs to make a hydrograph smother by adjusting the increase or decrease in 30-min-interval runoff data when comparing with the original data. For this, the moving average method was applied. As shown in Figure 6.4, 1 , 2, 3, and 4 hr moving average, respectively, were calculated. Like Figure 6.5 - 6.8, the second-

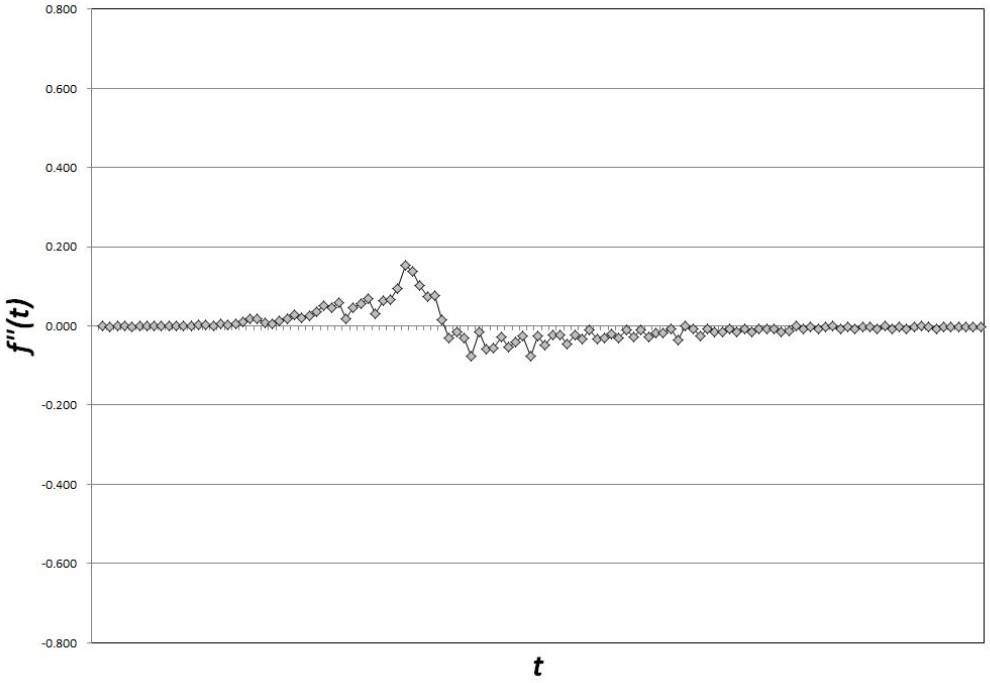

Figure 6.2 Second derivative values of the accumulated observed discharge

(2011/06/29 12:00-07/02 00:30)

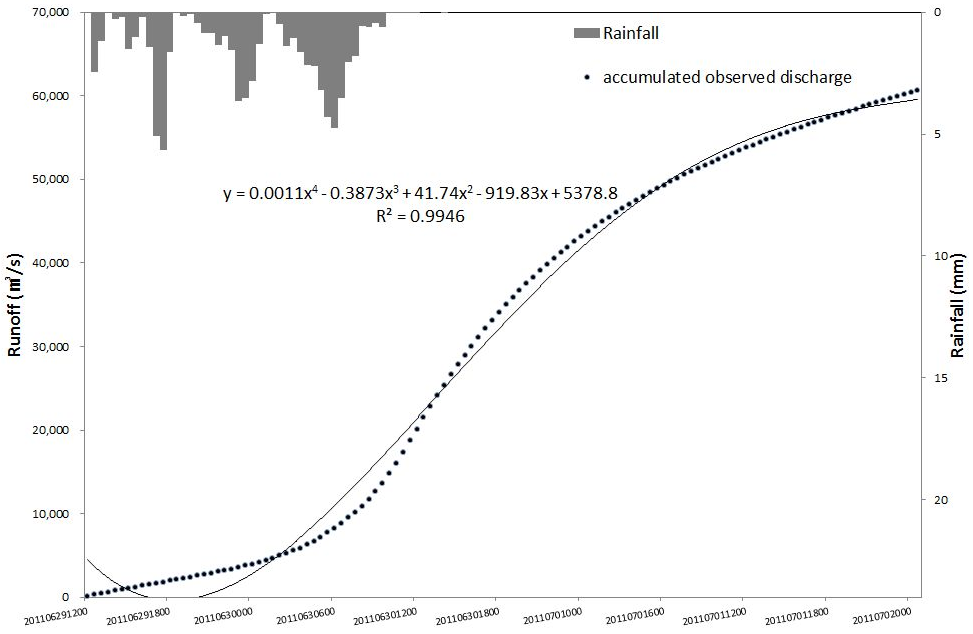

Figure 6.3 Curve fitting of the accumulated observed discharge

(2011/06/29 12:00-07/02 00:30)

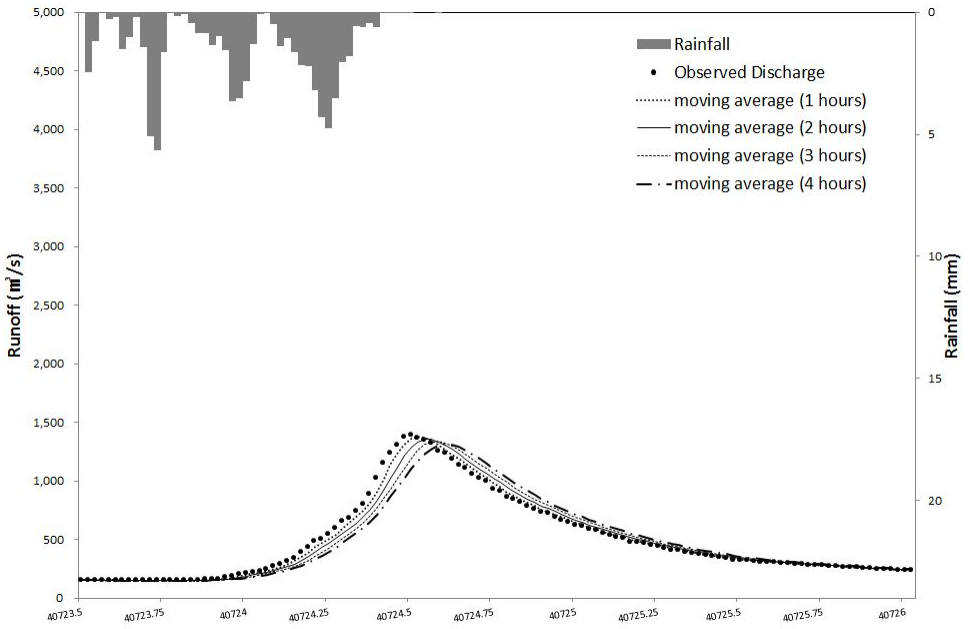

Figure 6.4 Moving average method of the observed discharge

(2011/06/29 12:00-07/02 00:30)

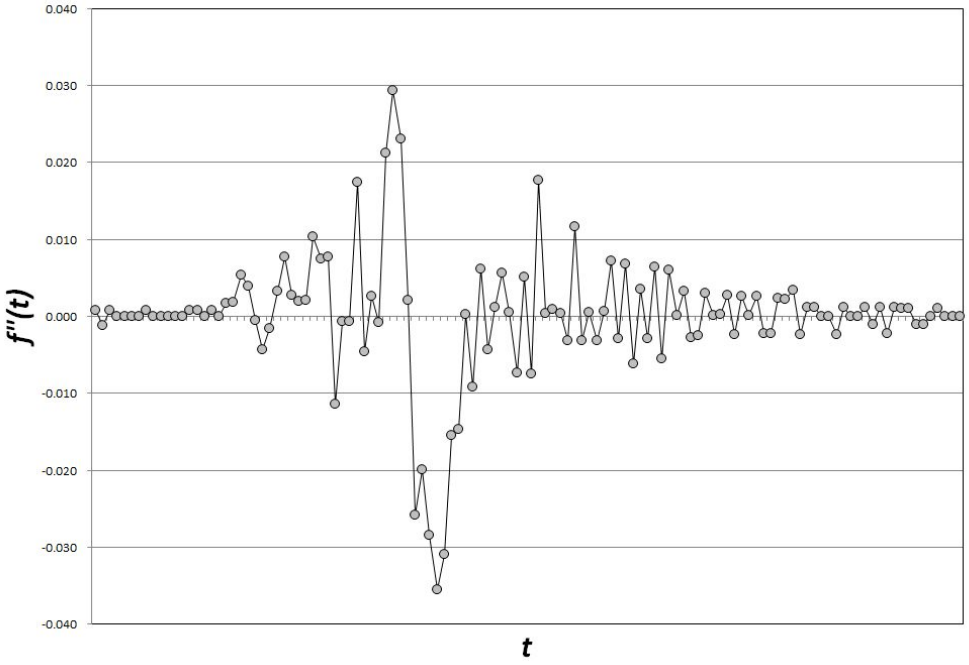

Figure 6.5 Second derivative values of 1-hr moving average discharge

(2011/06/29 12:00-07/02 00:30)

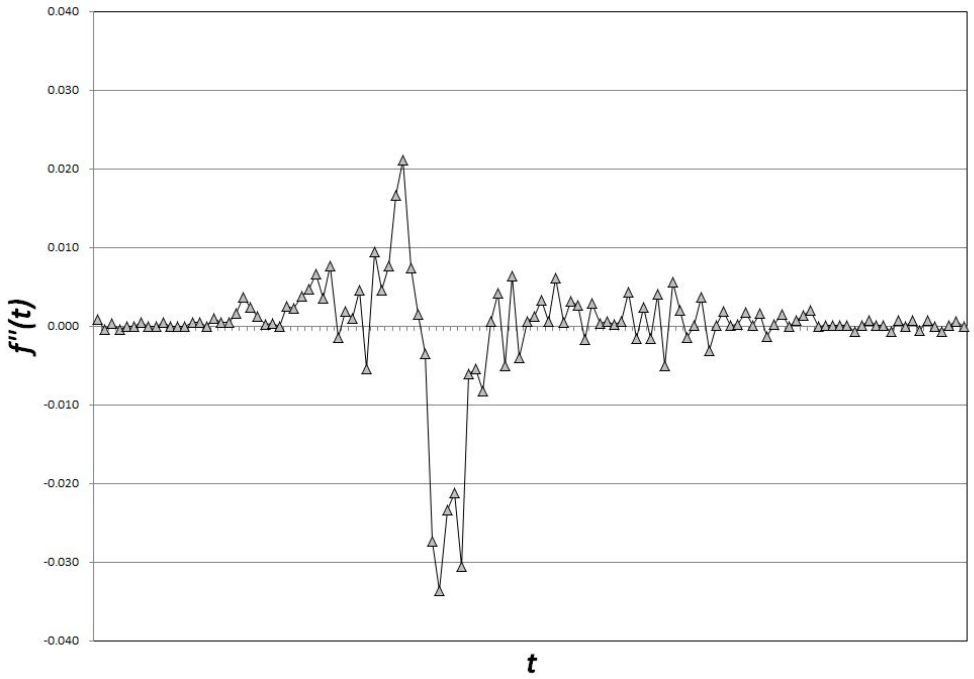

Figure 6.6 Second derivative values of 2-hr moving average discharge

(2011/06/29 12:00-07/02 00:30)

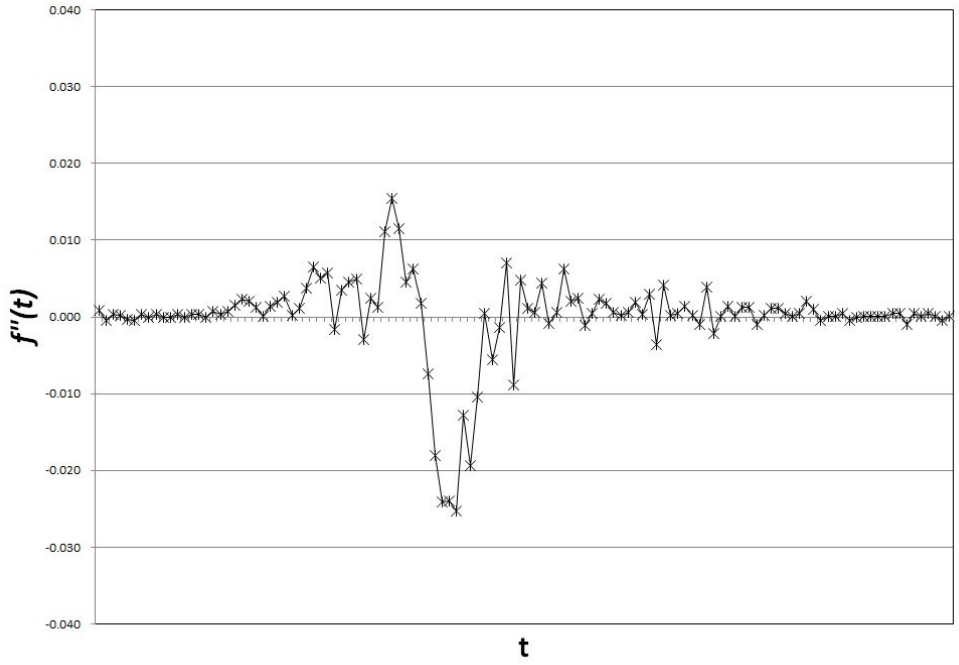

Figure 6.7 Second derivative values of 3-hr moving average discharge

(2011/06/29 12:00-07/02 00:30)

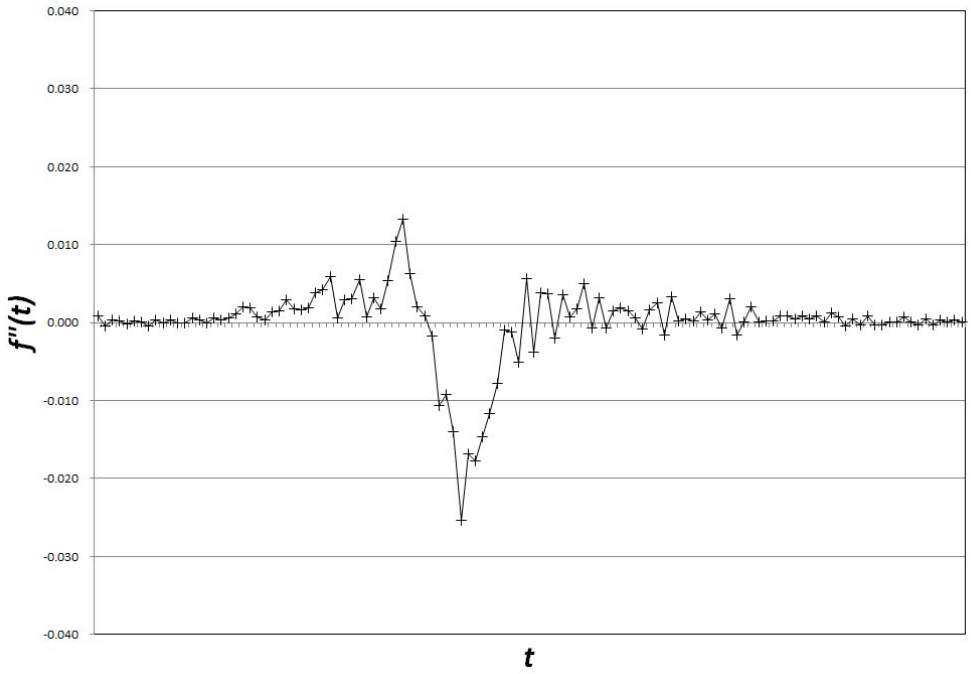

Figure 6.8 Second derivative values of 4-hr moving average discharge

(2011/06/29 12:00-07/02 00:30)

order differential value of each moving average based on 30-min-interval runoff data was computed. By examining the second-order differential value, it was found that peak flow is the minimum of the second-order differential value, and as the time interval for moving average was increased, the number of points at “0” value by the second-order differential was decreased. However, it is improper to find a point with only two differential values by increasing the time interval of the moving average infinitely because those graphs would be largely different from a hydrograph produced based on the original runoff data.

First the graph was visualized using the second order differential values of moving-averaged runoff data. Then, considering the peak flow occurrence point with the lowest value of second order differential as the basis, the zero (0) value point first occurring on the left side was defined as the inflection point of rising limb. Likewise, the zero (0) value point first occurring on the right side from the peak flow occurrence was assumed as the inflection point of falling limb. Table 6.1 and Figure 6.9 shows the summary in the occurrence time of inflection point. Even in the case of more than 3 hours moving averaged data, there was no change in the occurrence time of inflection

Table 6.1 Inflection point occurrence time according to moving average

	Inflection Point 1 (Rising Limb)	Peak Flow	Inflection Point 2 (Falling Limb)
1-hr Moving Average	2011/06/30 09:30	2011/06/30 11:30	2011/06/30 14:30
2-hr Moving Average	2011/06/30 10:00	2011/06/30 11:30	2011/06/30 15:00
3-hr Moving Average	2011/06/30 10:30	2011/06/30 13:00	2011/06/30 16:30
4-hr Moving Average	2011/06/30 10:30	2011/06/30 13:00	2011/06/30 17:30

	Sum of sets		Intersection	
	Inflection Point 1 (Rising Limb)	Inflection Point 2 (Falling Limb)	Inflection Point 2 (Falling Limb)	Inflection Point 2 (Falling Limb)
1 hr	2011/06/30 09:30	2011/06/30 11:30	2011/06/30 09:30	2011/06/30 11:30
1 ~ 2 hr	2011/06/30 09:30	2011/06/30 15:00	2011/06/30 10:00	2011/06/30 14:30
1 ~ 3 hr	2011/06/30 09:30	2011/06/30 16:30	2011/06/30 10:00	2011/06/30 14:30
1 ~ 4 hr	2011/06/30 09:30	2011/06/30 17:30	2011/06/30 10:00	2011/06/30 14:30

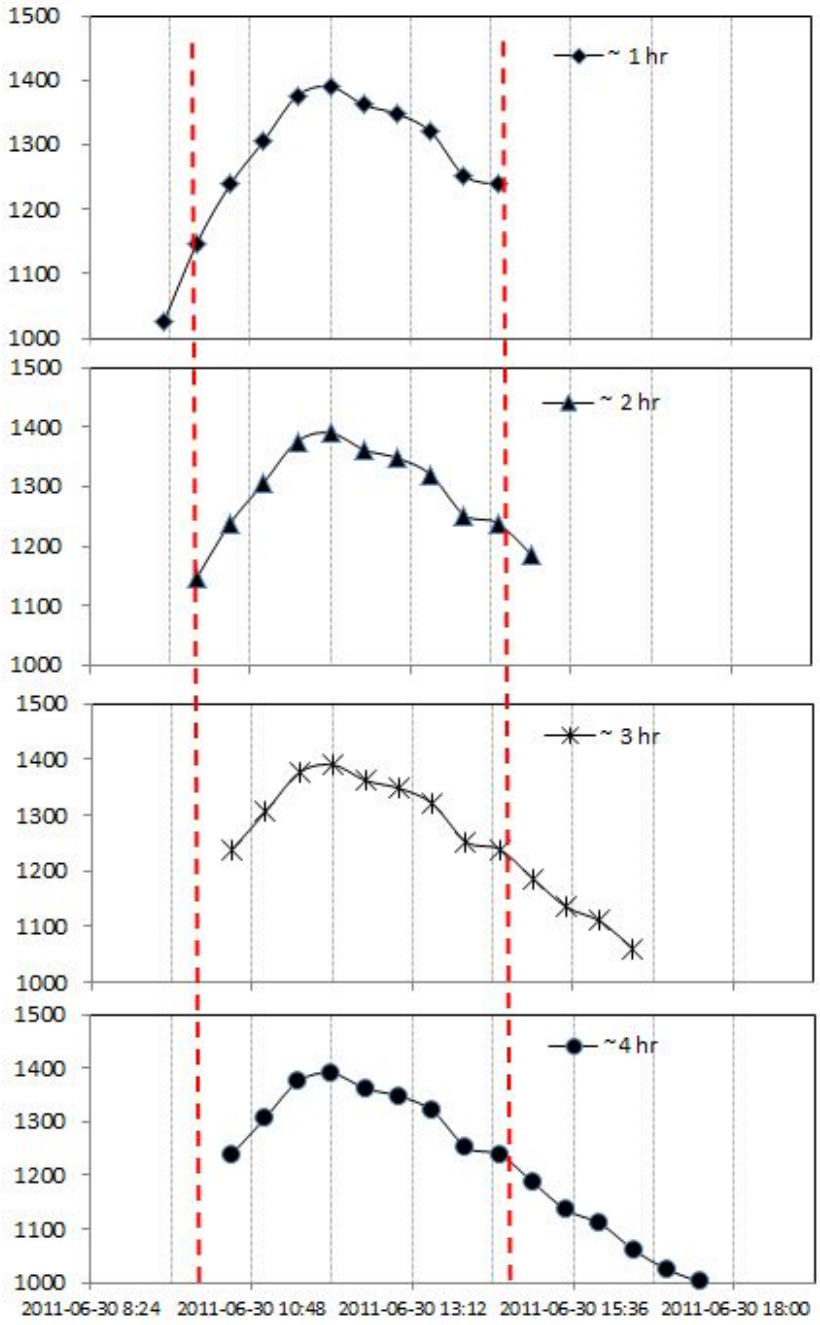

Figure 6.9 Search for the inflection point by the intersection of second derivatives value interval

point in common. Thus, in order to detect the inflection point, first the 2-hour moving averaged runoff data was calculated and then the second order differential values of which were computed to find its lowest bound. According to the lowest value, the occurrence time of each point first appealing on the left or the right was identified. Last the intersection of occurrence time could be the occurrence time.

According to the above procedure, the inflection point for the event no.15 (starting at 12:00 on 29 June 2011 and ending at 00:30 on 2 July 2011) could be found as shown in Figure 6.10. Also, the same procedure was applied to the event no.16 (starting at 04:00 on 3 July 2011 and ending at 05:30 on 7 July 2011) (refer to Figure 6.11 to Figure 6.17) and then its inflection point could be detected as shown in Table 6.2 and Figure 6.18.

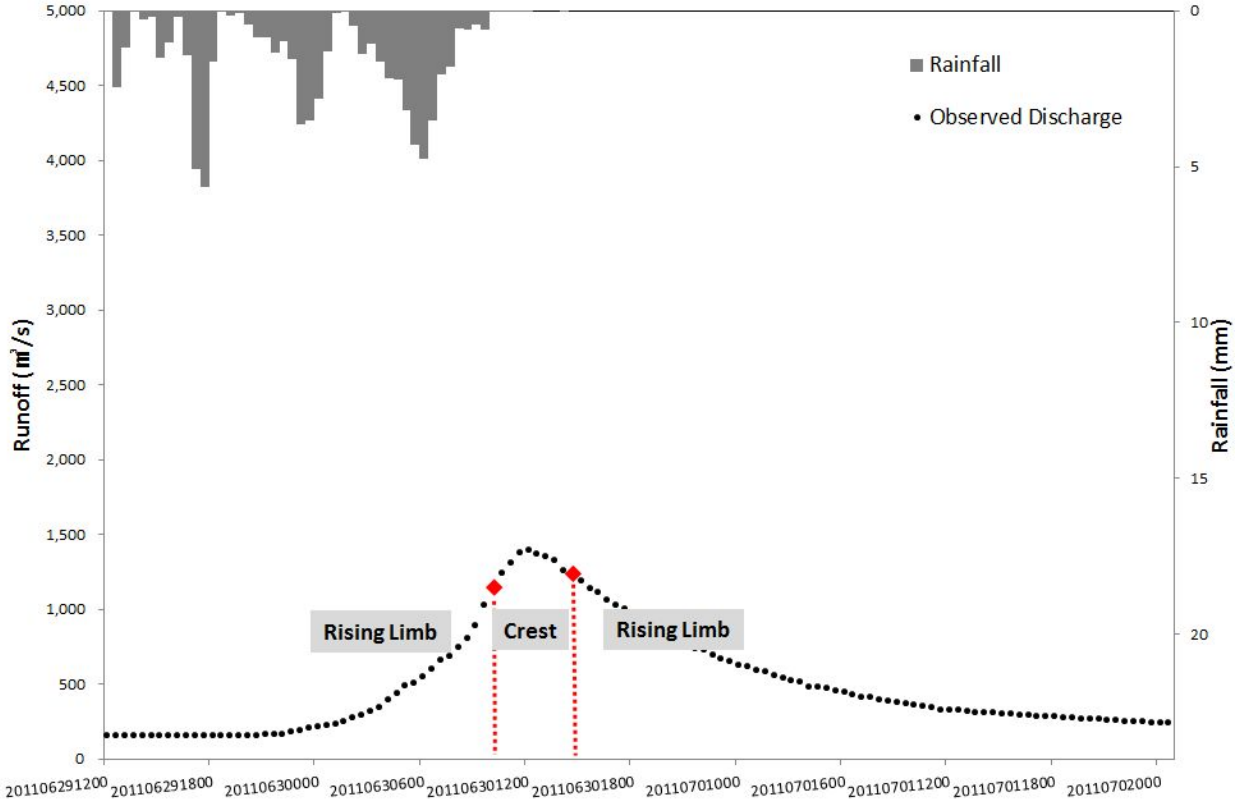

Figure 6.10 Hydrograph section separation using moving average (2011/06/29 12:00-07/02 00:30)

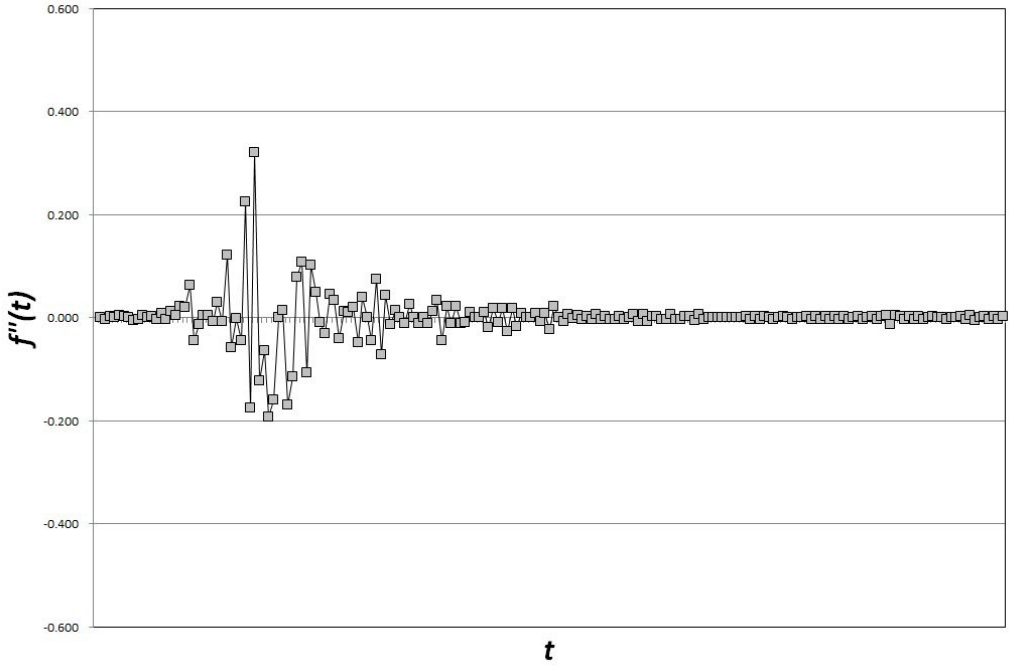

Figure 6.11 Second derivative values of the observed discharge

(2011/07/03 04:00-07/07 05:30)

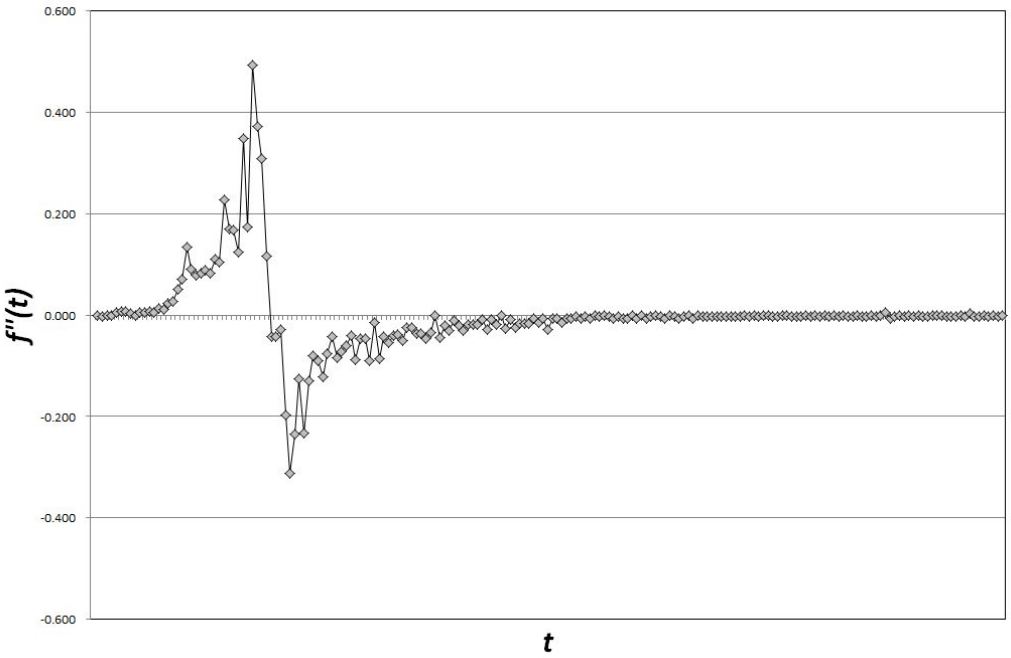

Figure 6.12 Second derivative values of the accumulated observed discharge

(2011/07/03 04:00-07/07 05:30)

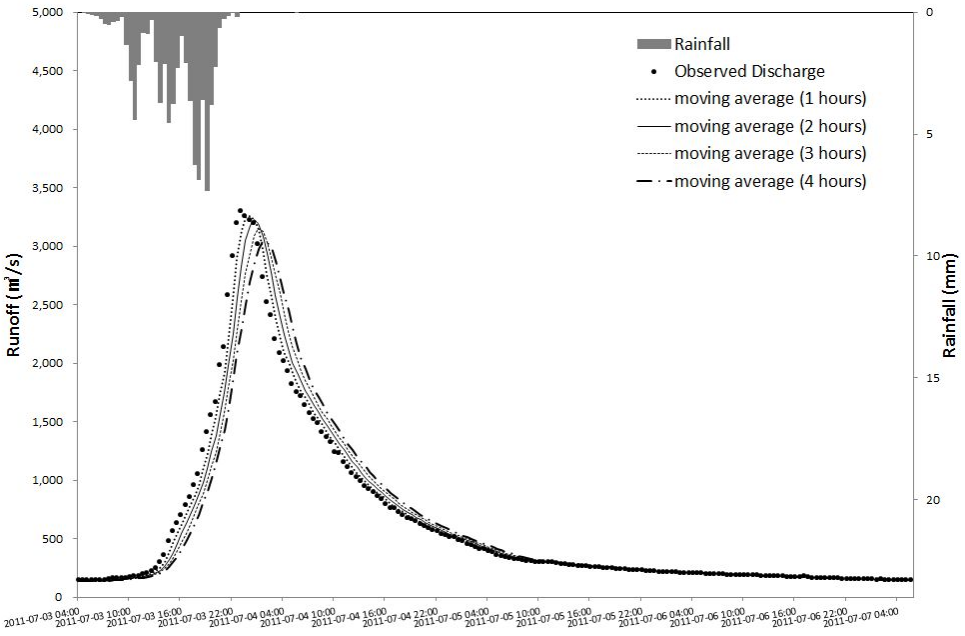

Figure 6.13 Moving average method of the observed discharge

(2011/07/03 04:00-07/07 05:30)

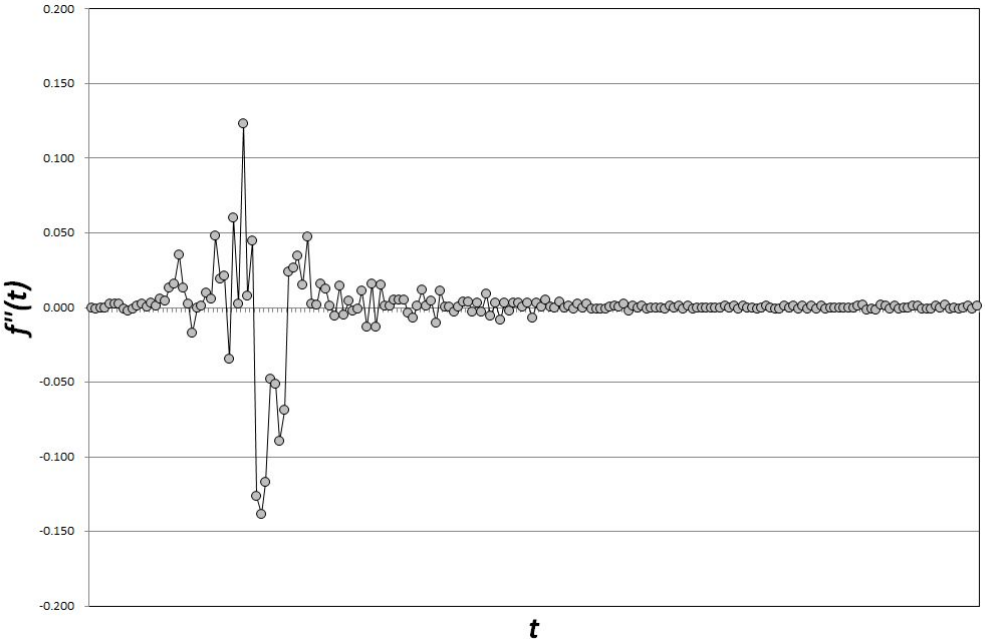

Figure 6.14 Second derivative values of 1-hr moving average discharge

(2011/07/03 04:00-07/07 05:30)

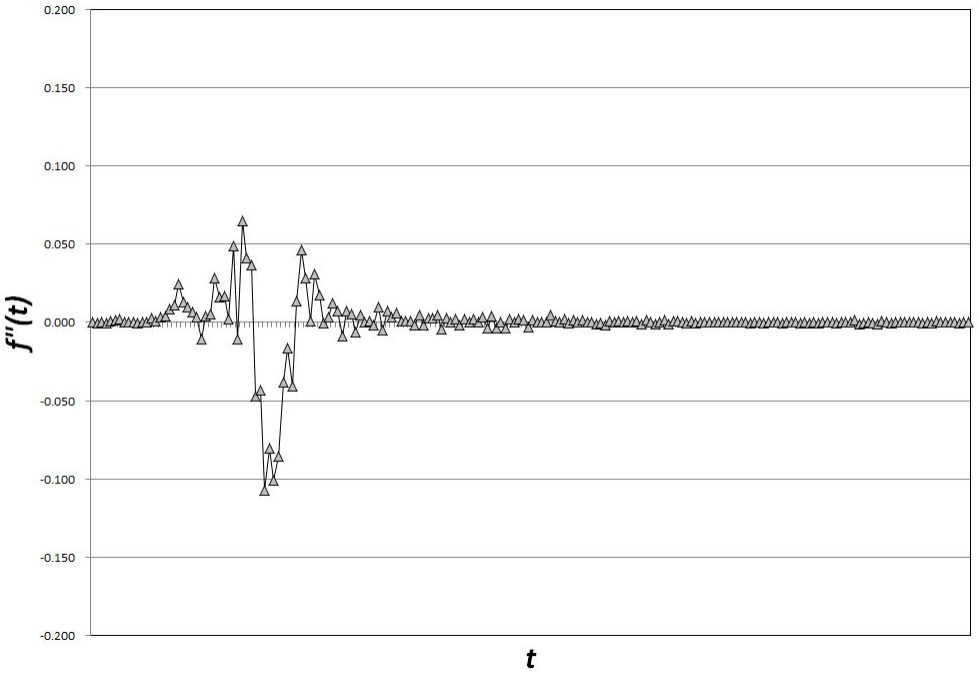

Figure 6.15 Second derivative values of 2-hr moving average discharge

(2011/07/03 04:00-07/07 05:30)

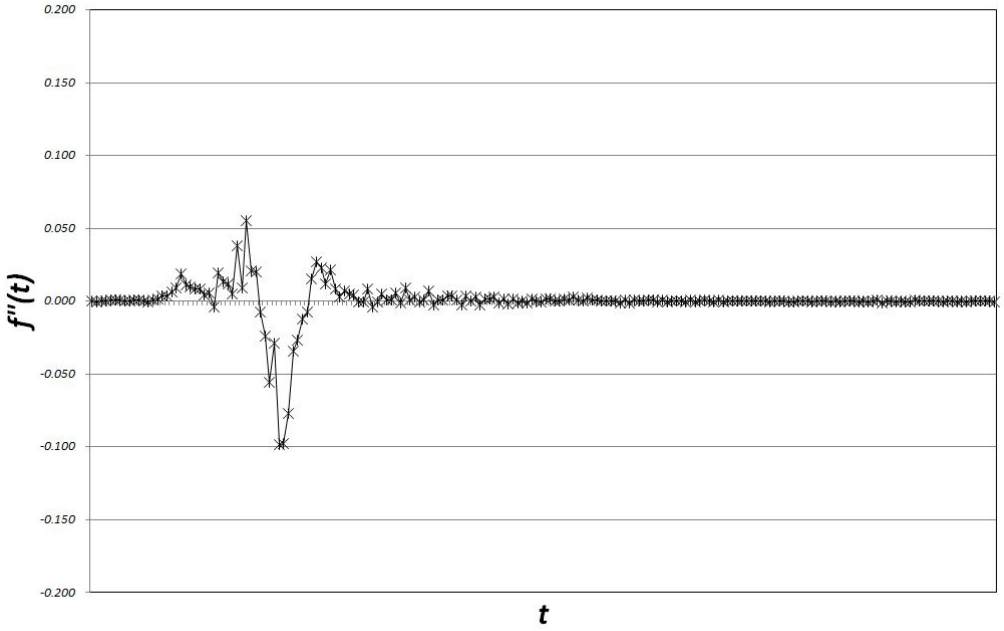

Figure 6.16 Second derivative values of 3-hr moving average discharge

(2011/07/03 04:00-07/07 05:30)

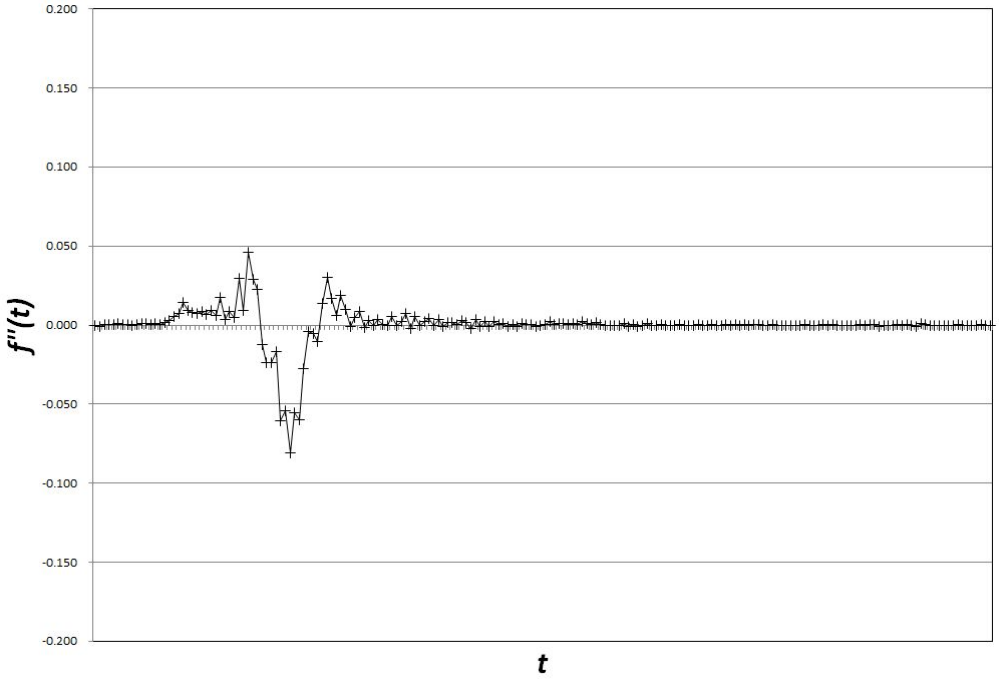

Figure 6.17 Second derivative values of 4-hr moving average discharge

(2011/07/03 04:00-07/07 05:30)

Table 6.2 Inflection point occurrence time according to moving average(2011/07/03 04:00-07/07 05:30)

	Inflection Point 1 (Rising Limb)	Peak Flow	Inflection Point 2 (Falling Limb)
1-hr Moving Average	2011/07/03 21:30	2011/07/03 22:30	2011/07/04 01:30
2-hr Moving Average	2011/07/03 21:00	2011/07/03 23:00	2011/07/04 02:30
3-hr Moving Average	2011/07/03 21:30	2011/07/04 00:00	2011/07/04 03:30
4-hr Moving Average	2011/07/03 21:30	2011/07/04 01:00	2011/07/04 04:30

	Sum of sets		Intersection	
	Inflection point 1 (Rising Limb)	Inflection point 2 (Falling Limb)	Inflection point 2 (Falling Limb)	Inflection point 2 (Falling Limb)
1 hr	2011/07/03 21:00	2011/07/04 01:30	2011/07/03 21:30	2011/07/04 01:30
1 ~ 2 hr	2011/07/03 21:00	2011/07/04 02:30	2011/07/03 21:00	2011/07/04 01:30
1 ~ 3 hr	2011/07/03 21:00	2011/07/04 03:30	2011/07/03 21:00	2011/07/04 01:30
1 ~ 4 hr	2011/07/03 21:00	2011/07/04 04:30	2011/07/03 21:00	2011/07/04 01:30

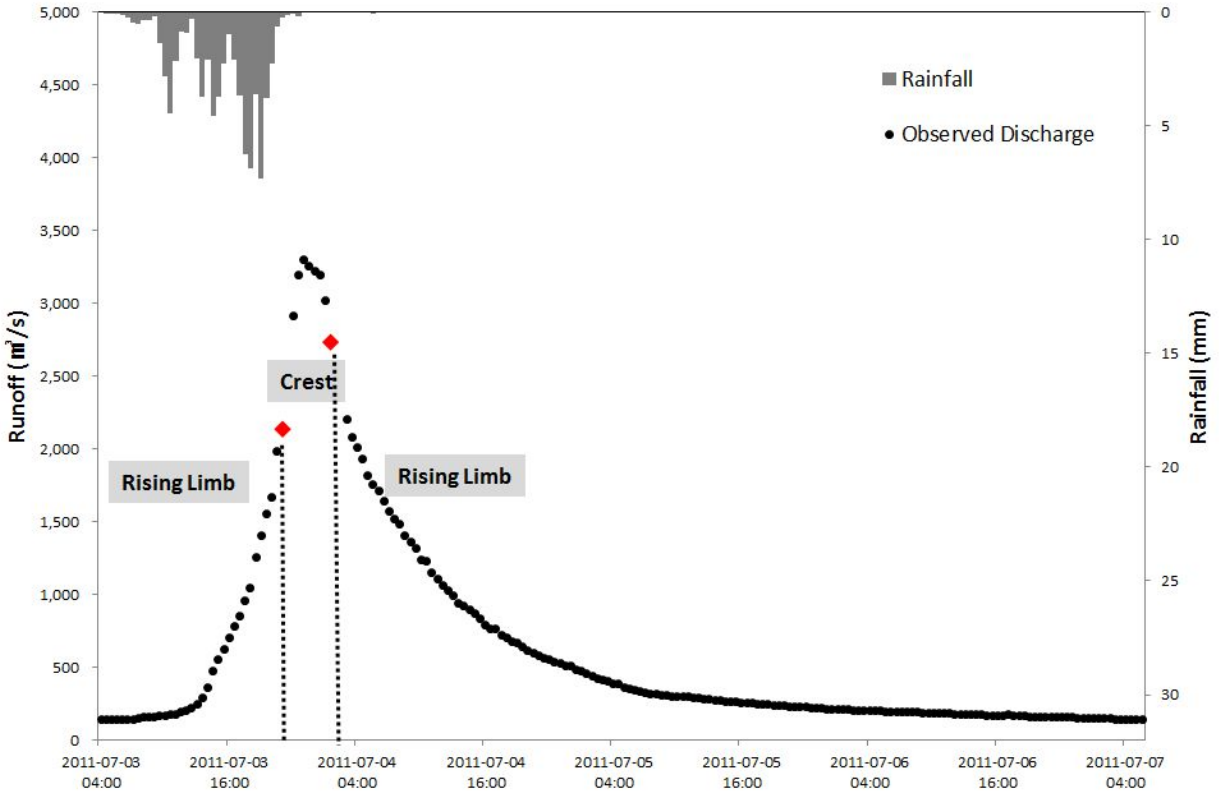

Figure 6.18 Hydrograph section separation using moving average (2011/07/03 04:00-07/07 05:30)

The results of obtaining the inflection point using the moving average method for the 18 rainfall events in this research are summarized in Table 6.3. As shown in Figure 6.19, the occurrence of inflection point at a falling limb takes a longer time than the occurrence at a rising limb when the occurrence time of peak flow is regarded as the reference point. This tendency, in general, can be found in most of hydrographs. This supports the form of hydrograph that is not likely to be perfectly bell-shaped. Instead, a rising limb is increasing sharply, but a falling limb is decreasing gradually with a long tail. According to a review on existing literature and researches, it is determined that there has not been a certain rule for defining the occurrence time of inflection point so far. In case of the Jeongseon basin, the inflection point at the beginning of the rising limb appears before the maximum 9.5 hr or the minimum 1.5 hr on the basis of the peak flow occurrence. In addition, the inflection point at the beginning of the falling limb appears after the maximum 20 hr or the minimum 2 hr based on peak flow.

Table 6.4 and Figure 6.20 shows the comparison in the inflection points (a) estimated from the overlapping range using the moving average method and (b) estimated by applying the accumulated discharge curve method, respectively.

Table 6.3 Inflection point of selected rainfall events by moving average method

No.	Inflection Point 1 (Rising Limb)	Difference from Peak Time to Point 1	Peak Time	Difference from Peak Time to Point 2	Inflection Point 2 (Falling Limb)
1	2004/04/27 17:00	3:30	2004-04-27 20:30	9:30	2004/04/28 06:00
2	2004/07/08 02:00	9:30	2004-07-08 11:30	8:00	2004/07/08 19:30
3	2005/07/01 07:00	2:30	2005-07-01 9:30	17:00	2005/07/02 02:30
4	2005/07/11 19:00	4:00	2005-07-11 23:00	17:30	2005/07/12 16:30
5	2005/09/22 04:00	6:00	2005-09-22 10:00	20:00	2005/09/23 06:00
6	2006/05/06 21:30	8:00	2006-05-07 5:30	12:30	2006/05/07 18:00
7	2007/09/15 07:30	4:00	2007-09-15 11:30	5:30	2007/09/15 17:00
	2007/09/17 05:00	4:00	2007-09-17 9:00	9:30	2007/09/17 18:30
8	2008/08/23 00:00	3:00	2008-08-23 3:00	16:30	2008/08/23 19:30
9	2009/07/09 20:00	1:30	2009-07-09 21:30	5:00	2009/07/10 02:30
10	2009/07/12 14:00	2:00	2009-07-12 16:00	5:00	2009/07/12 21:00
	2009/07/15 01:00	2:30	2009-07-15 3:30	5:00	2009/07/15 08:30
11	2009/07/18 04:30	3:30	2009-07-18 8:00	5:30	2009/07/18 13:30
	2009/07/19 02:30	2:30	2009-07-19 5:00	6:30	2009/07/19 11:30
12	2010/09/22 01:30	1:30	2010-09-22 3:00	11:30	2010/09/22 14:30
13	2011/04/30 23:00	3:00	2011-05-01 2:00	11:00	2011/05/01 13:00
14	2011/05/11 12:30	5:30	2011-05-11 18:00	12:30	2011/05/12 06:30
15	2011/06/30 10:00	1:30	2011-06-30 11:30	3:00	2011/06/30 14:30
16	2011/07/03 21:00	2:00	2011-07-03 23:00	2:30	2011/07/04 01:30
17	2011/07/27 19:00	6:30	2011-07-28 1:30	6:00	2011/07/28 07:30
18	2011/08/18 05:00	5:00	2011-08-18 10:00	6:00	2011/08/18 16:00

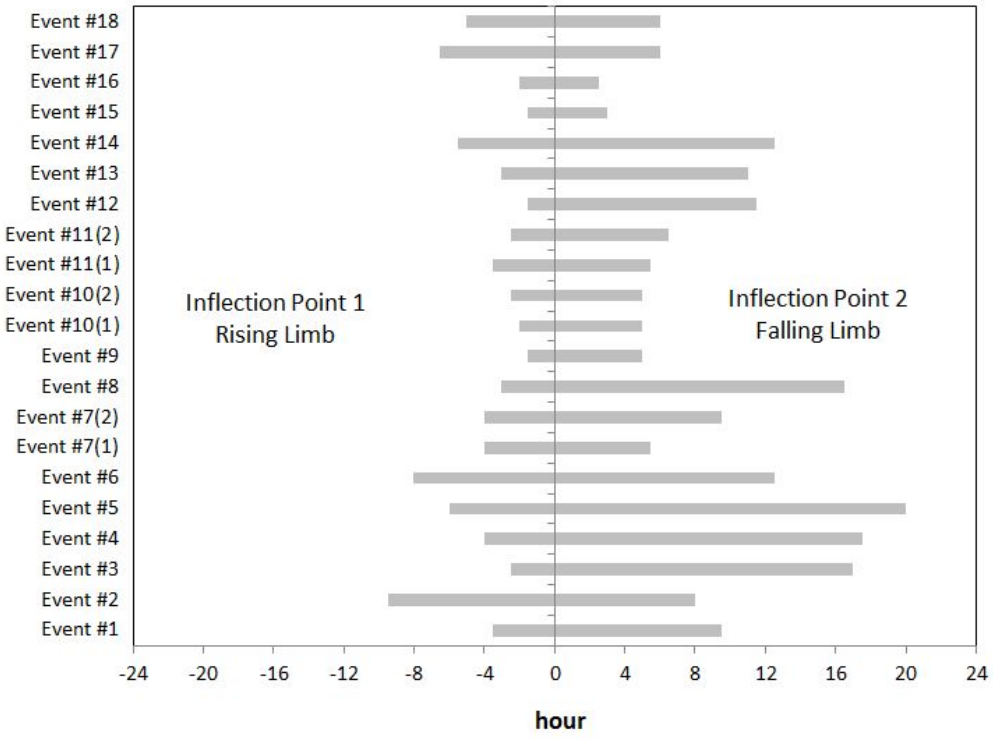

Figure 6.19 Duration of the inflection point from peak time

Table 6.4 Inflection point of selected rainfall events by an accumulated discharge curve

No.	By Accumulated Discharge Curve Inflection Point 1 (Rising Limb)	Difference from Moving Average Method to Accumulated Discharge Curve	By Moving Average Method Inflection Point 1 (Rising Limb)
1	2004-04-27 16:00	- 1:00	2004/04/27 17:00
2	2004-07-08 1:30	- 0:30	2004/07/08 02:00
3	2005-07-01 8:30	+ 1:30	2005/07/01 07:00
4	2005-07-11 18:30	- 0:30	2005/07/11 19:00
5	2005-09-22 5:00	+ 1:00	2005/09/22 04:00
6	2006-05-06 21:00	- 0:30	2006/05/06 21:30
7	2007-09-15 6:00	- 1:30	2007/09/15 07:30
	2007-09-17 6:30	+ 1:30	2007/09/17 05:00
8	2008-08-22 23:00	- 1:00	2008/08/23 00:00
9	2009-07-09 20:00	+ 0:00	2009/07/09 20:00
10	2009-07-12 14:30	+ 0:30	2009/07/12 14:00
	2009-07-15 0:30	- 0:30	2009/07/15 01:00
11	2009-07-18 4:00	- 0:30	2009/07/18 04:30
	2009-07-19 3:00	+ 0:30	2009/07/19 02:30
12	2010-09-22 3:00	+ 1:30	2010/09/22 01:30
13	2011-04-30 23:30	+ 0:30	2011/04/30 23:00
14	2011-05-11 14:30	+ 2:00	2011/05/11 12:30
15	2011-06-30 9:00	- 1:00	2011/06/30 10:00
16	2011-07-03 22:30	+ 1:30	2011/07/03 21:00
17	2011-07-27 19:30	+ 0:30	2011/07/27 19:00
18	2011-08-18 5:30	+ 0:30	2011/08/18 05:00

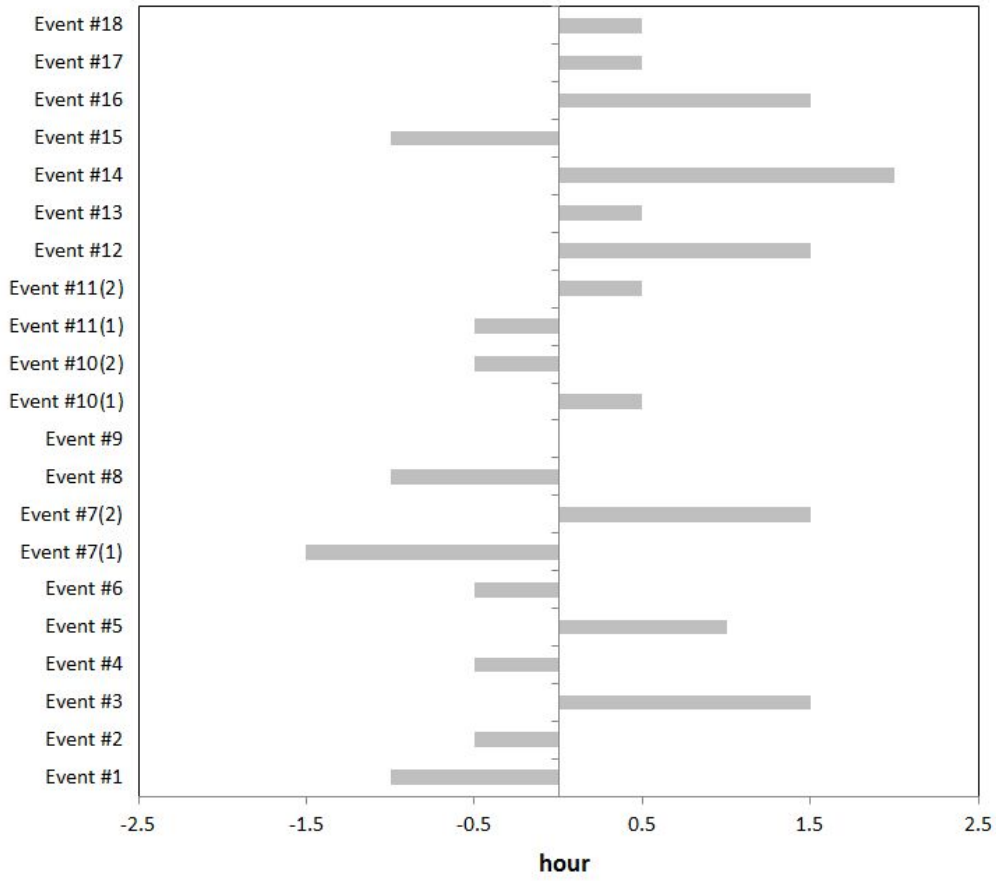

Figure 6.20 Duration of inflection point with an accumulated discharge curve from the inflection point by a moving average method

To obtain the overlapping range applicable to both 30-min-interval raw data and 2-hr moving average results, the first 2-hr moving average with the raw data was conducted, and each value of the second-order differential was computed. Then, it was found that two inflection points that occurred as the first on the left and right, respectively, based on the peak flow occurrence and the distance between these two points was the range that contains the first inflection point that occurred on the left and that on the right was the range. As a result of comparison, it was difficult to find a certain rule implied in each method and difference in advantage of the performance. However, it was examined that only one inflection point could be found at the beginning of the rising limb when the accumulated discharge curve was applied. Moreover, the inflection point obtained by the accumulated discharge curve appeared faster or slower than the inflection point estimated through the moving average within 2 hr. After a comprehensive review on these two methods, it was concluded that it is more proper to apply the moving average method to estimate the inflection point rather than the accumulated discharge curve method.

The moving average method was applicable even to complex rainfall event No.7, 10, and 11. In case of a complex rainfall event, there were two peak flows. However,

there was no problem in estimating the inflection point by applying the moving average method, and like other events, each inflection point before and after the occurrence of a peak flow was estimated. In addition, the total volume of peak flow in applied events varies from 500 m^3 to 2,000 m^3, and the duration of rainfall events also varies from 47.5 hr (about 2 days) to 175.5 hr (about 7.3 days). It was considered to ensure a variety of rainfall events for application in terms of the total volume, runoff discharge, and duration. Moreover, the efficiency and effectiveness of obtaining the inflection point using the moving average method were identified through the application of various time-series rainfall data and rainfall events with different-scaled runoff rate.

The mathematical definition of an inflection point is a point that changes the bending radius of the curve and the physical description of an inflection point at the rising limb is the starting point of the crest on a hydrograph. Moreover, mathematically, an inflection point at the falling limb is defined as the starting point of base flow right after the end of direct runoff. The purpose of a proposed HSS method is to estimate the most proper parameter by reflecting the runoff characteristics for each separated section of a hydrograph through a comprehensive consideration of both the

mathematical and physical definitions of an inflection point. However, the obtained inflection point using the moving average method suggested in this research somehow needs to have further examination with regard to its consistency with the mathematical and physical definitions.

The inflection point estimation method suggested in this research can be compared with an existing methodology such as the N-day method, which separates base flow from a hydrograph. In this research, the inflection point was used to separate a hydrograph vertically to obtain three sections that reflect the distinctive runoff property of each other. However, it might be possible to utilize the inflection point estimation method proposed here to divide base flow from direct runoff horizontally.

By applying N-day method to the study area in this research, the calculated N is 3.66 days (about 4 days). It means that base flow can be divided from a hydrograph on the basis of 4 days later from the occurrence of peak flow. However, this analysis shows a difference of two more days from the results by considering the inflection point estimation method. Therefore, if only a falling limb after a peak flow is considered, the total volume of base flow computed by the proposed inflection point estimation method can be much greater than that calculated using the N-day method.

The limitation of the N-day method is that an empirical formula considers only the area of a basin and simply divides base flow and direct runoff by inferring the start point of base flow depending on the formula. On the other hand, the inflection point detection method proposed in this research is based on mathematical and physical backgrounds. In the chapter on further study, the expansion of applicability would be discussed and determined.

6.1.2 Parameter Estimation Results Using HSS

To attenuate the increase in 30-min-interval flow data, 2-hr moving average was conducted, and the second-order differential value for each data was computed. Calculated values were illustrated, and the location of the first inflection point that appears on the left and right based on the peak flow occurrence was detected. Then, a hydrograph was divided into a rising limb, crest, and falling limb according to the inflection point for parameter estimation in each section.

The results of applying SCE-UA with time-series data is compared to those applying HSS with time-series data as summarized in Table 6.5. By applying the HSS method, the value of NSE was improved, showing 0.799, 0,765 and 0.788 for each section. It means that reliability is also improved. One event from each calibration and verification period, respectively, was selected to determine the efficiency of HSS for each rainfall event. Figure 6.21 and Table 6.6 show the analysis results of parameter estimation by applying SCE-UA and HSS, respectively, to an event that occurs in July 2009. The NSE computed through HSS is 0.765, and the value is significantly improved from the NSE (-2.785) that did not apply HSS.

Table 6.5 Efficiency of the hydrograph section separation

		K	P	Tl	F1	R_{sa}	NSE	RMSE	R_p	R_v
SCE-UA (for time-series)		23.70	0.75	4.60	0.35	167	0.725	47.790	-	-
SCE-UA (for time-series + HSS)	Rising Limb	24.900	0.550	4.500	0.500	124.00	0.799	15.941	-	0.088
	Crest	24.900	0.750	2.700	0.650	38.000	0.765	37.010	0.415	-
	Falling Limb	24.400	0.950	9.200	0.850	82.000	0.788	14.478	-	0.348

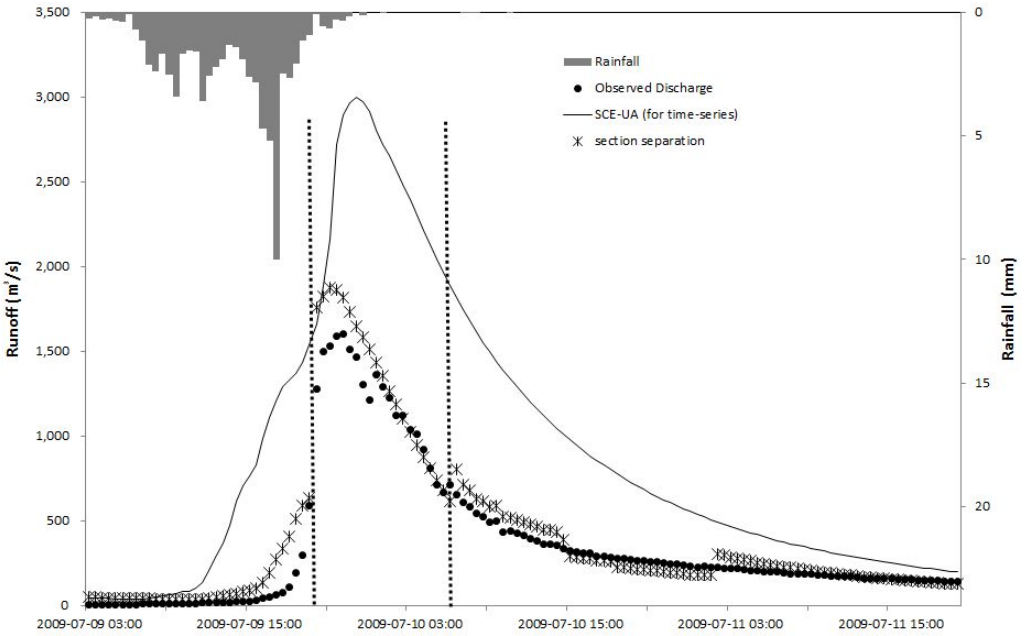

Figure 6.21 Parameter estimation by SCE-UA for time-series and HSS (2009/07/09 03:00-07/11 20:00)

Table 6.6 Efficiency of HSS (2009/07/09 03:00-07/11 20:00)

	NSE	RMSE	RE_p	RE_v
SCE-UA (for time-series)	-2.785	596.58	1.547	3.307
SCE-UA (for time-series + HSS)	0.765	43.231	1.212	1.536

However, a discretion occurred at the inflection point by synthesizing three separated sections into a hydrograph, so the time series of a hydrograph could not be illustrated smoothly. Despite this, the concern in the occurrence of a discretion was not a serious problem in estimating parameters, and instead, the efficiency of simulation was improved considerably.

In addition, in case of applying HSS to the event in July 2011 out of a verification, the NSE computed through HSS is 0.926, and the value is slightly improved from the NSE (0.879) that did not apply HSS (see Figure 6.22 and Table 6.7). In particular, the NSE value of the objective function in this research was largely increased.

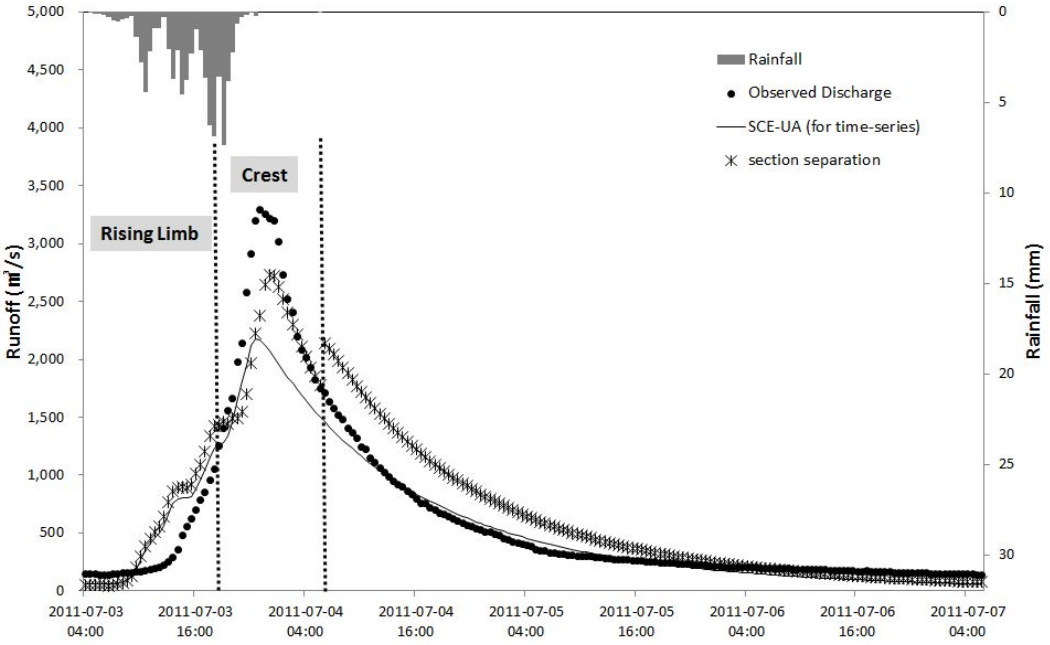

Figure 6.22 Parameter verification by SCE-UA for time-series and HSS (2011/07/03 04:00-07/07 05:30)

Table 6.7 Efficiency of HSS (2011/07/03 04:00-07/07 05:30)

	NSE	RMSE	RE_p	RE_v
SCE-UA (for time-series)	0.879	258.96	0.340	0.109
SCE-UA (for time-series + HSS)	0.926	81.983	0.171	0.153

6.2 Application to Flood Forecasting in Practical Use

By estimating parameters, it was expected that a global optimization methodology could make better results rather than the trial-and-error method intuitionally, and the point of this view was identified by actual results. Moreover, it was determined that flood forecasting by applying estimated parameters based on time-series data was more appropriate than by using parameters estimated based on each event of historical data. In addition, it was found that the parameters estimated by applying HSS, which could reflect the runoff properties of each hydrograph section derived better results. However, the HSS method can be applied only where a hydrograph exists. In this regard, there is a need to have views on a new methodology for future rainfall forecasting.

By applying a future forecasting method to the historical rainfall events that occurred in July 2011, its applicability was determined. To apply the parameter sets summarized in Table 6.5 to future rainfall events, each simulation is conducted at a predicted time by using the parameter set suggested (rising limb: set No.1; crest: set No.2; falling limb: set No.3) for each hydrograph section (rising limb, crest and falling

limb) (refer to Figure 6.23) . Then, by using each parameter set, the inflection point on a simulated hydrograph is found. According to the inflection point, the simulated hydrograph is divided into three sections. Only the part of the hydrograph prior to the inflection point is separated from the whole hydrograph simulated by the parameter set for the rising limb (set No.1). Then, likewise, only the part of the hydrograph between the inflection points on the rising and falling limbs is apart from the whole hydrograph by the parameter set for the crest (set No.2). Moreover, only the part of the hydrograph after the inflection point on the falling limb is separated from the simulated hydrograph by the parameter set for the falling limb (set No.3). Finally, these three separated sections are synthesized to generate a hydrograph for future rainfall prediction as shown in Figure 6.24.

In applying the proposed HSS method as described above to practical works for flood forecasting, the matter of most concern is the total time of simulation. First, it is necessary to determine the simulation time by applying SCE-UA.

Taking into consideration the existing forecasting system in Korea which simulates the large-scale watershed (e.g. the entire area Han River watershed) simultaneously, applying a global optimization method to the current system in practical

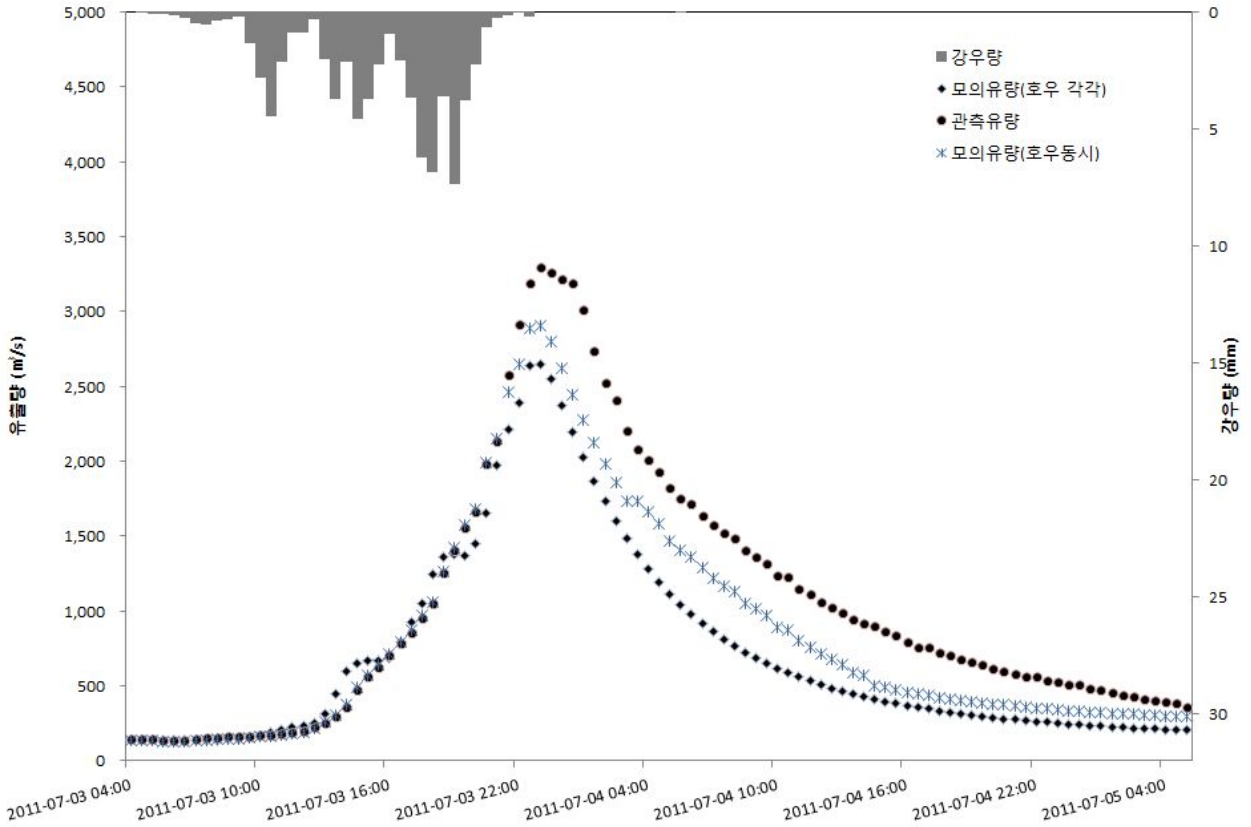

Figure 6.23 Simulation results with the parameter set in each section

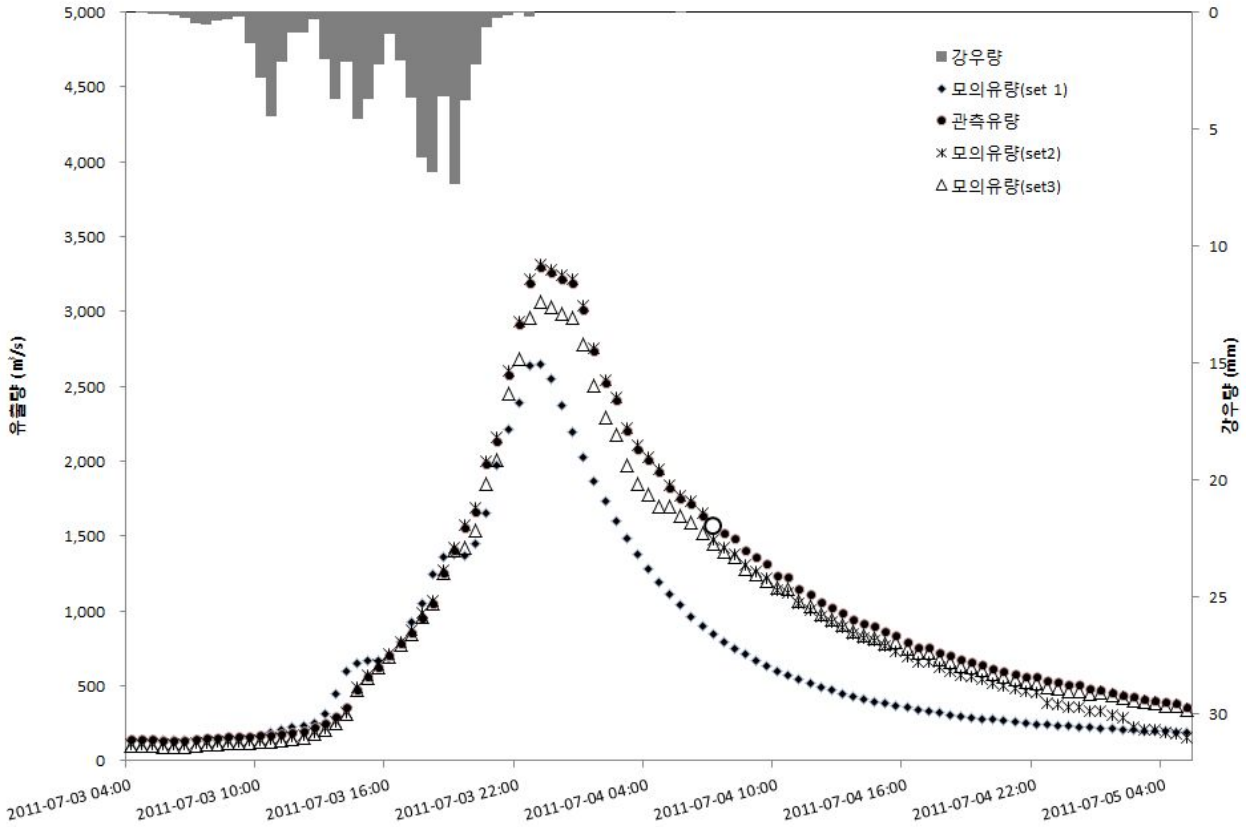

Figure 6.24 Combination of simulated hydrograph with the parameter set in each section

works might be doubtful because of its simulation time. It needs to find a global optimization technique that ensures a reasonable simulation time or proper ways to simplify it.

Moreover, it is necessary to operate an efficient hydrologic database to apply qualified time-series data. At this moment, a single integrated database system is being operated to manage data of the large-scale watershed; however, to estimate parameters based on time-series data, the flood forecasting system should be compatible with the database that contains the data in a scale of a unit watershed or a standard unit watershed.

Furthermore, it can be expected that both concerns in simulation time and hydrologic database management can occur when the HSS method is applied in practical works. It is expected that the efficient database management can contribute to the decrease in model simulation time.

In brief, high-performance computers and the efficient management of hydrologic database in a sub-basin scale can be key elements to the application of the proposed methodology in this research in practical works.

7. Parameter Estimation by Uncertainty Analysis

7.1 Computation of the Optimal Parameter Set

The uncertainty implied in a hydrologic model can be classified into four aspects as follows;

- Input data uncertainty
- Initial condition uncertainty
- Parameter uncertainty
- Model structure uncertainty

In this research, uncertainty analysis was conducted. In general, uncertainty analysis assesses the uncertainty by hypothesizing a probability distributed function (pdf) and computes the reliable range statistically according to the optimal simulation result. Moreover, there are a few methodologies of uncertainty analysis to assess the uncertainty by analyzing the statistical properties of the time-series errors of a rainfall-runoff model and to conduct iterative simulations using a resampling technique, such as the Monte Carlo simulation technique. In this research, GLUE, a resampling method,

was used to present the range of the optimal parameter by analyzing the error surface before and after executing HSS.

To apply GLUE, NSE was used as a likelihood measurement. First 1,000 sets of random number were generated, and this process was repeated 1,000 times to select the optimal parameter set. The number of response variable set (N) to the weight of the likelihood function was 1,000, and the optimal parameter set was estimated by giving a weight $[W_i = \frac{L(\theta_i)}{\sum_{k=1}^{N} L(\theta_k)}]$ to a set that had more than 0.6 of NSE, which is the likelihood function. Here, in calculating weight, θ_i is the value of the NSE of a set that satisfies more than 0.6 of NSE and $\sum_{k=1}^{N} L(\theta_k)$ is the sum of the NSE of 1,000 parameter sets. Finally, only a few parameter sets weighted by the likelihood function were selected out of the 1,000 parameter sets, and the optimal parameter set that has a 90% confidence interval were determined, except for the prediction with 5% of the upper and lower in a cumulative percentile.

The error surface among estimated parameters using a global optimization SCE-UA was analyzed, and the process of convergence to the optimal solution was examined. Moreover, the correlation among estimated parameters using GLUE was analyzed. The error surface of the most sensitive parameters K and Tl before and

after executing HSS was analyzed, and their results were compared. As shown in Figure 7.1 and 7.2, in case of applying SCE-UA after conducting HSS, parameter detectors are likely to move densely toward the optimal solution. Likewise, parameters estimated through GLUE show similar results (refer to Figure 7.3 and 7.4), but distinctive features in movement like SCE-UA are not visible.

Table 7.1 summarizes the results of estimating optimal parameters by applying SCE-UA and HSS. It highlights that there is a significant change in saturated rainfall R_{sa} after conducting HSS. Table 7.2 summarizes the optimal parameter set estimated by using the GLUE method. It can be seen that relatively the range of parameters for the falling limb is wider than the range for both the falling limb and the crest. Also, Figure 7.5 shows where the optimal parameter set estimated by using SCE-UA and HSS, respectively, is located within the range estimated through GLUE. In other words, Figure 7.5 shows whether the optimal parameter by using HSS is included within the range of optimal parameter set computed through the uncertainty analysis in parameters. As shown in Figure 7.5, saturated rainfall R_{sa} estimated without using HSS for all three sections (rising limb, crest and falling limb) is outside of the range of optimal parameter set. On the other hand, it is seen that all the parameters estimated by

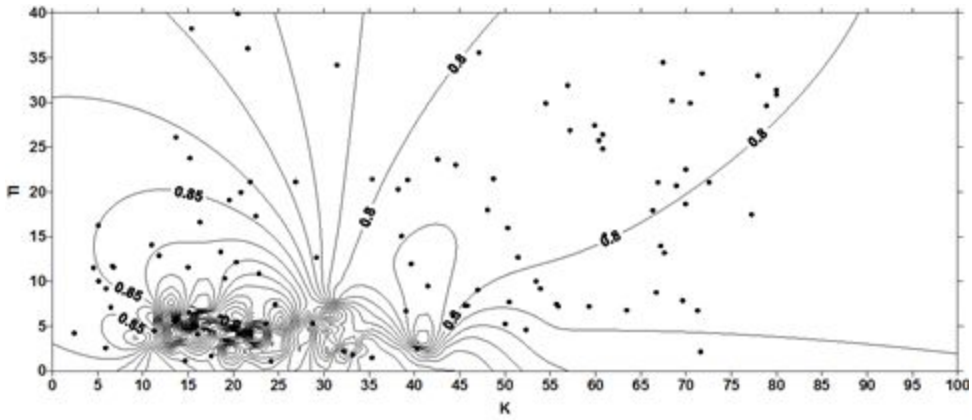

Figure 7.1 Response surface before HSS (SCE-UA)

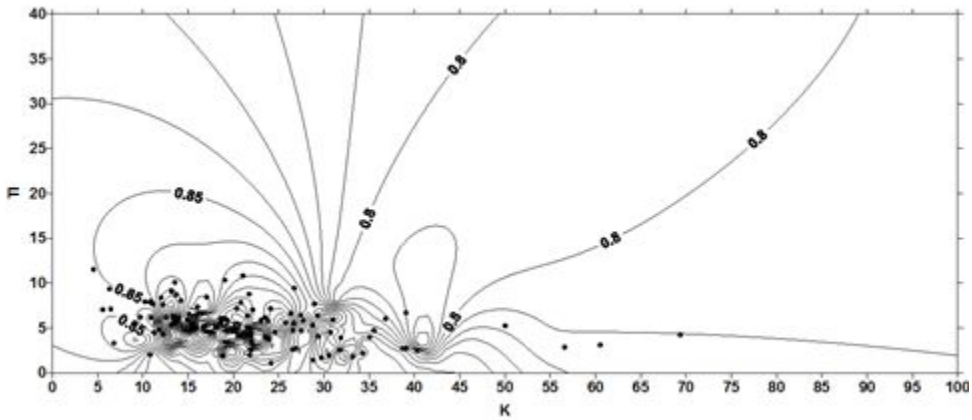

Figure 7.2 Response surface after HSS (SCE-UA)

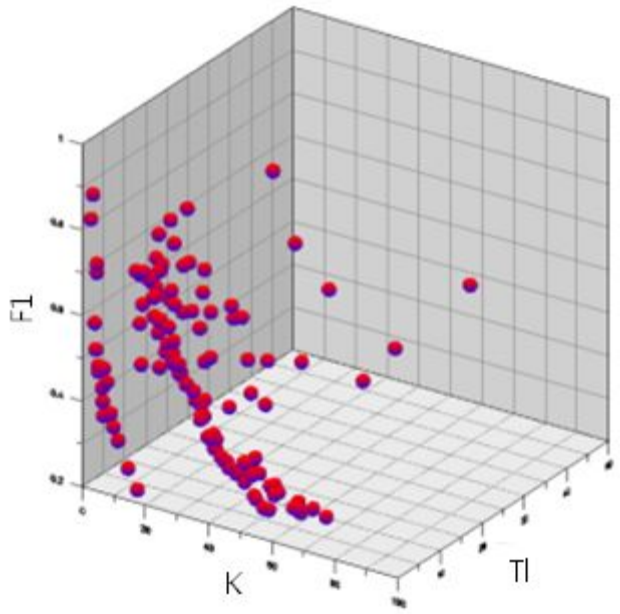

Figure 7.3 Response surface before HSS (GLUE)

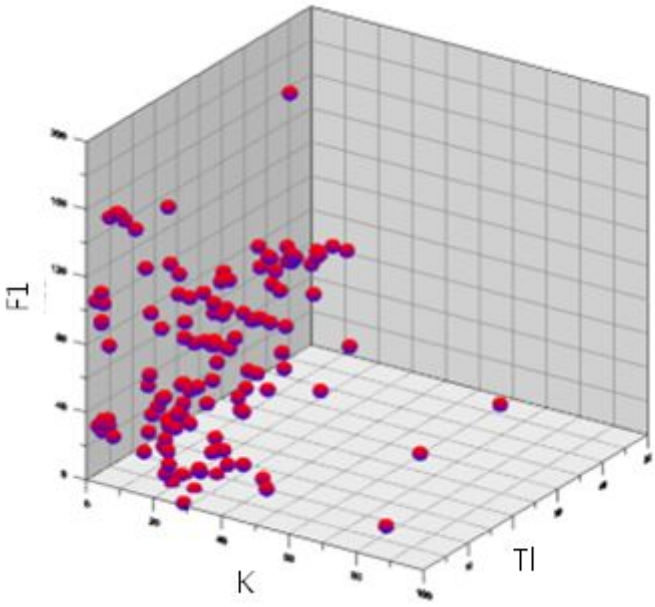

Figure 7.4 Response surface after HSS (GLUE)

Table 7.1 Optimal parameter set by SCE-UA

		K	P	Tl	F1	R_{sa}
SCE-UA (for time-series)		23.70	0.75	4.60	0.35	167
SCE-UA (for time-series + HSS)	Rising Limb	24.900	0.550	4.500	0.500	124.00
	Crest	24.900	0.750	2.700	0.650	38.000
	Falling Limb	24.400	0.950	9.200	0.850	82.000

Table 7.2 Characteristics of the optimal parameter set by GLUE

GLUE (for time-series + HSS)		K	P	Tl	F1	R_{sa}
Rising Limb	Minimum	3.30	0.06	0.44	0.11	32.15
	Median	19.40	0.50	4.67	0.32	60.45
	Maximum	45.79	12.00	10.00	11.00	132.11
Crest	Minimum	3.52	0.68	0.67	0.24	45.32
	Median	20.26	1.21	5.27	0.52	70.96
	Maximum	46.36	10.69	9.12	12.13	145.36
Falling Limb	Minimum	2.67	1.02	0.04	0.08	26.36
	Median	18.55	1.33	4.01	0.09	55.69
	Maximum	45.71	11.37	11.71	11.51	108.77

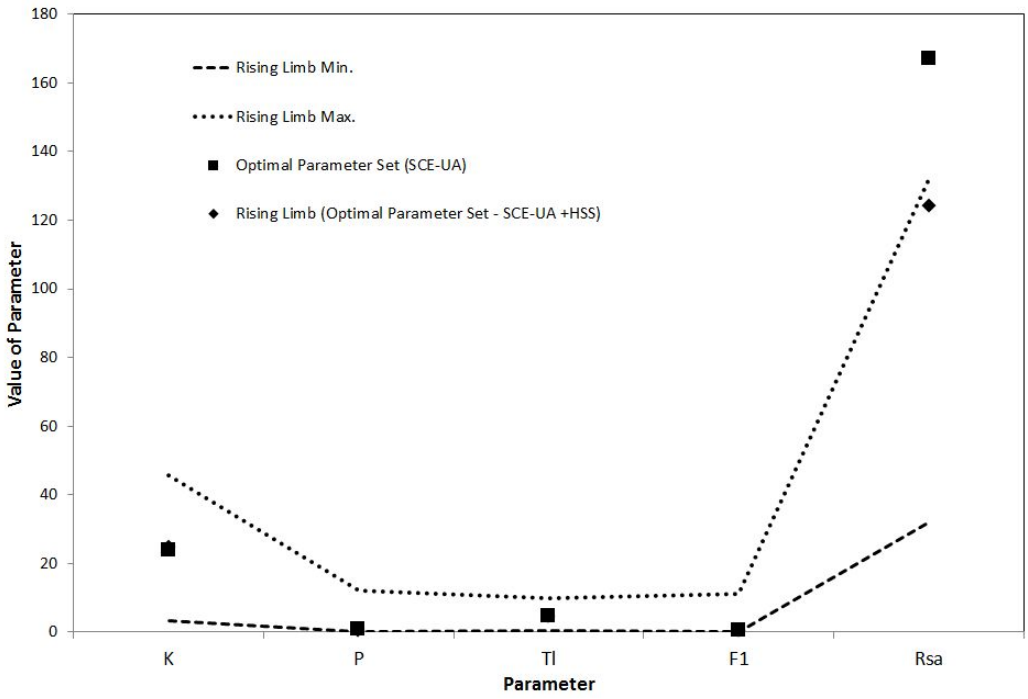

(a) Rising Limb

Figure 7.5 Optimal parameter set and range by SCE-UA, GLUE+ HSS

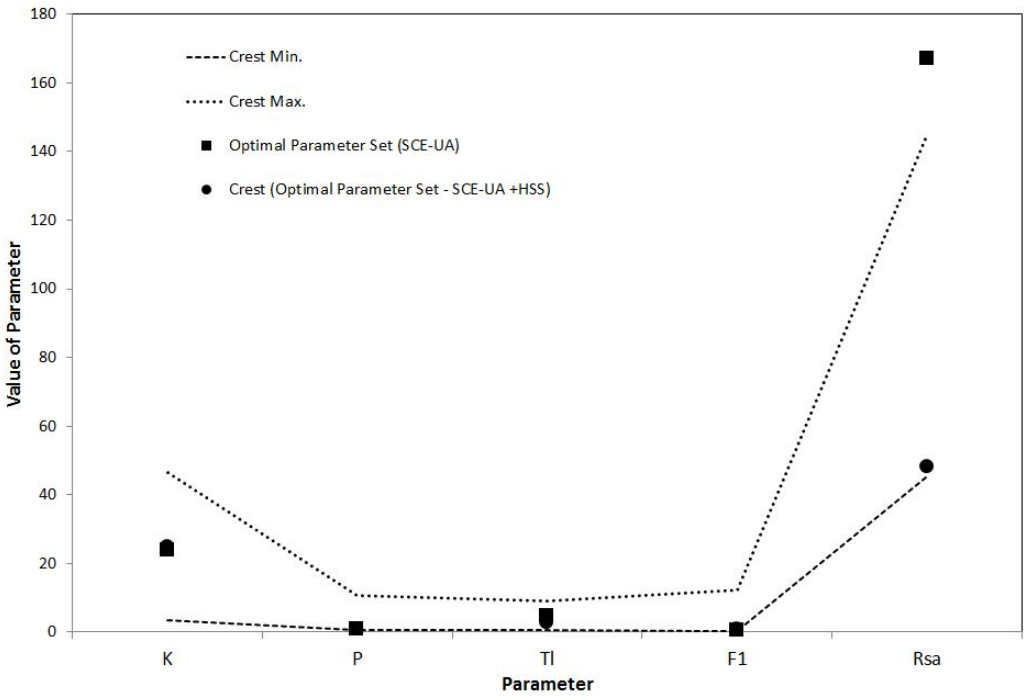

(b) Crest

Figure 7.5 Optimal parameter set and range by SCE-UA, GLUE+ HSS (continued)

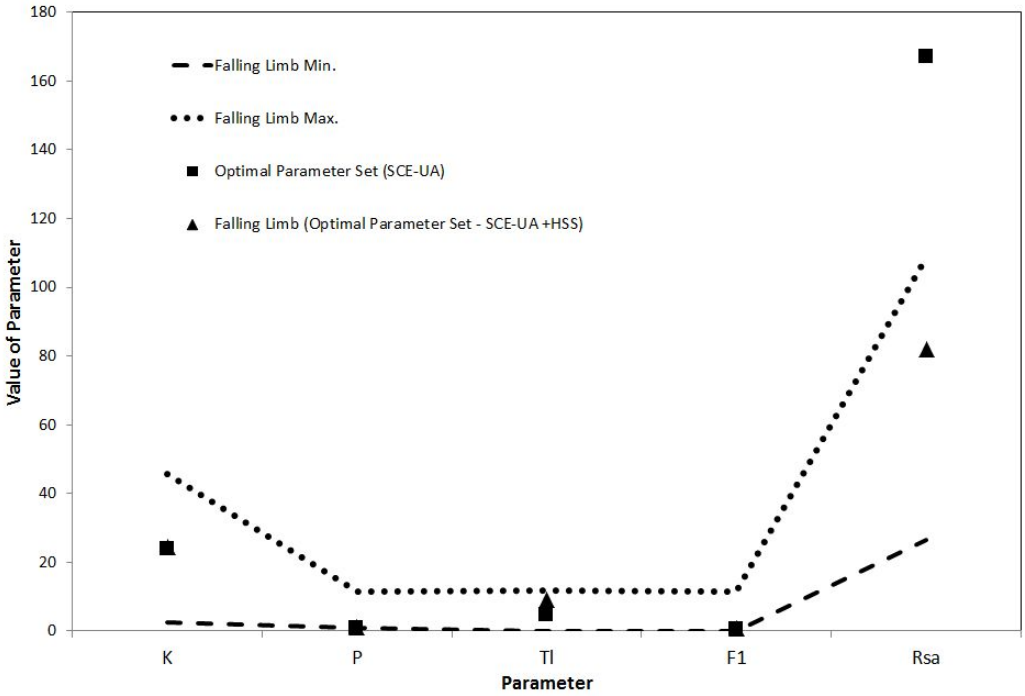

(c) Falling Limb

Figure 7.5 Optimal parameter set and range by SCE-UA, GLUE+ HSS (continued)

using the HSS method proposed in this research are located within the range of optimal parameter set. Ultimately, this results support the applicability of HSS.

Once the optimal parameter set and its range are determined, it is necessary to determine whether the initial parameter values that has been used in practice are located within the range of optimal parameter estimated by using HSS. Through this, it can be identified that which section of hydrograph includes the initial parameter values containing the largest error. As shown in Figure 7.6 and Table 7.3, except for storage constant K, all four parameters are outside of the range of optimal parameter set, and saturated rainfall R_{sa} is also beyond the range in all three sections (rising limb, crest and falling limb). In particular, it is seen that there are a number of parameters located outside of the optimal parameter set in the crest and it means there is a large difference between simulated results and observed data in the tail of hydrograph. Figure 7.7 shows the results in estimating the optimal parameter set and its range for an rainfall event with time-series from 03:00 on 9 July, 2009 until 20:00 on 11 July, 2009 by using SCE-UA, HSS, and GLUE in order.

Examining the hydrograph simulated with the optimal parameter set estimated, the range of the lower bound is slightly smaller than the range of the upper bound.

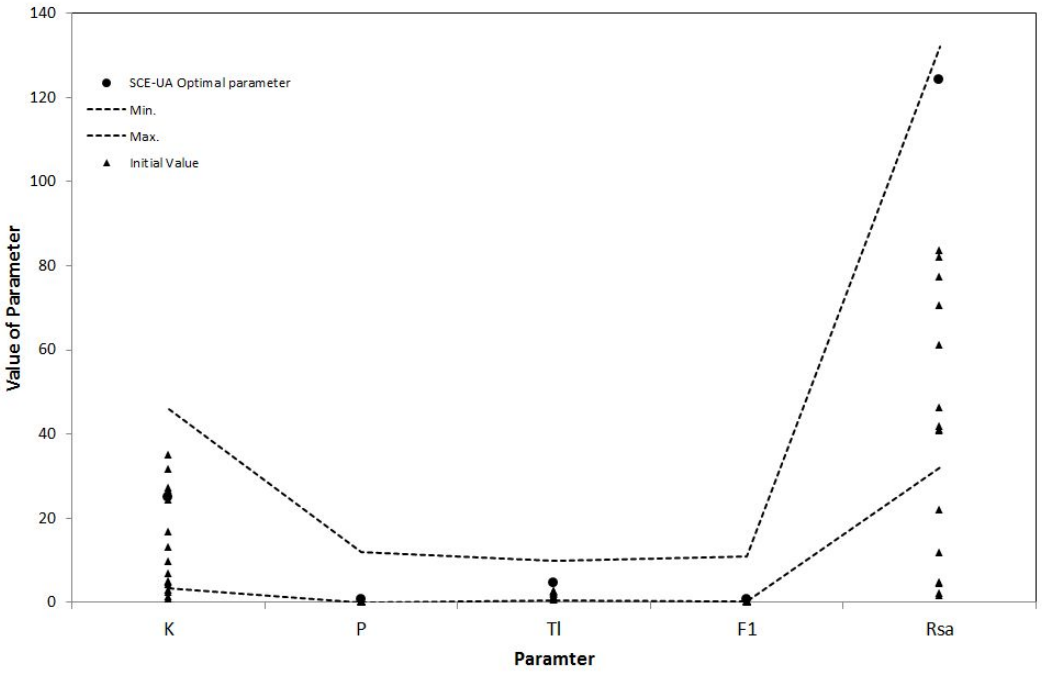

(a) Rising Limb

Figure 7.6 Comparison of initial value with the optimal parameter range

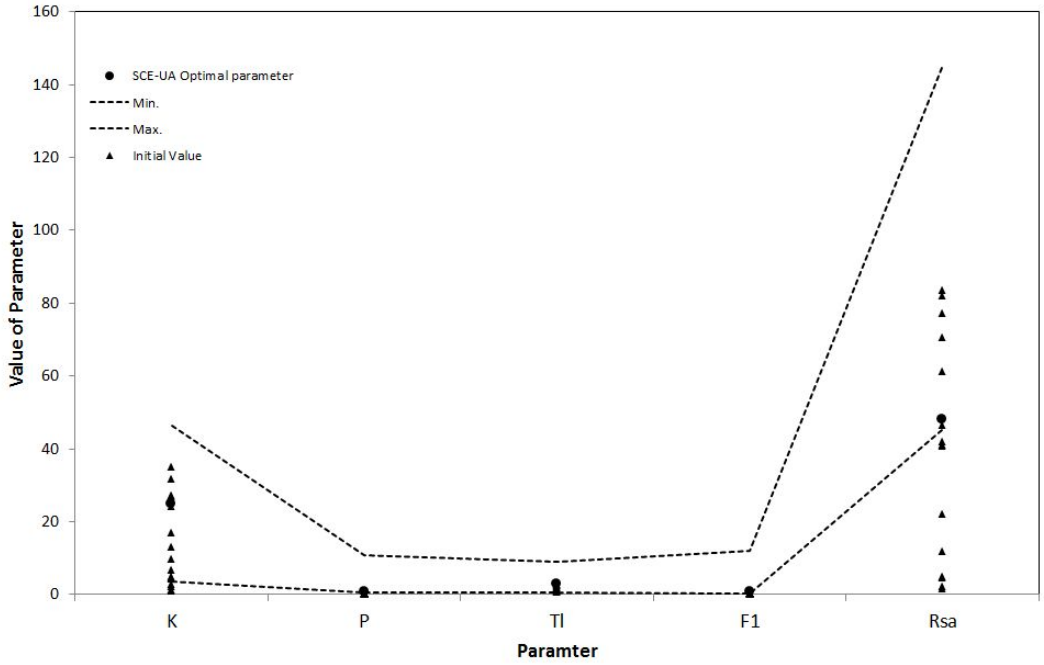

(b) Crest

Figure 7.6 Comparison of initial value with the optimal parameter range (continued)

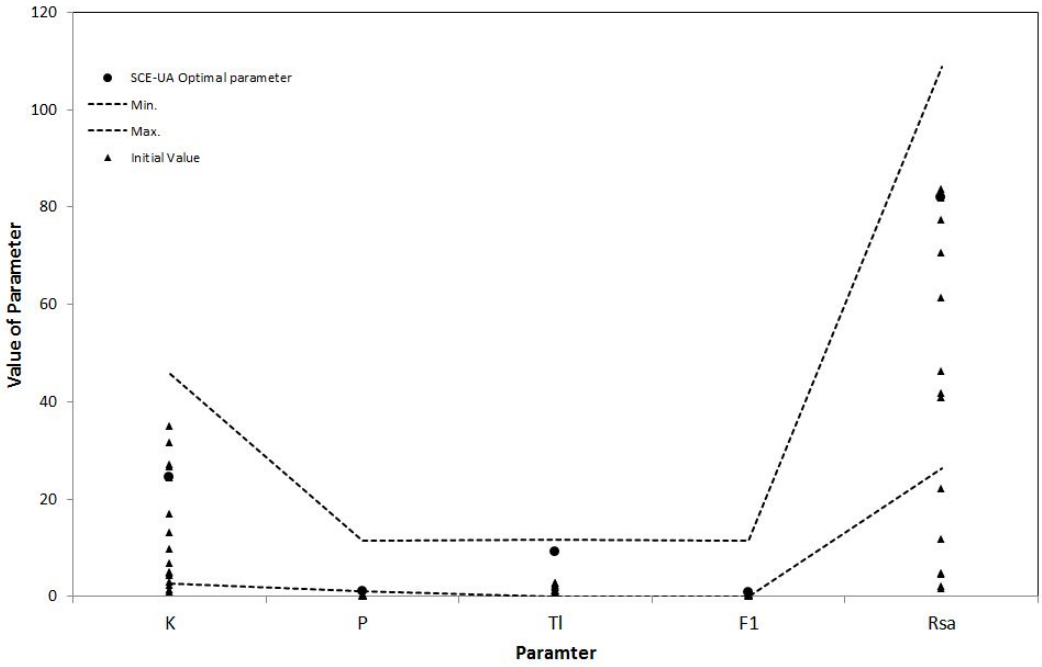

(c) Falling Limb

Figure 7.6 Comparison of initial value with the optimal parameter range (continued)

Table 7.3 Number of initial values included within an optimal parameter range

SCE-UA +GLUE (EP + HSS) / Initial Value	K	P	Tl	F1	R_{sa}
Rising Limb	17/18	15/18	15/18	14/18	9/18
Crest	17/18	13/18	14/18	10/18	4/18
Falling Limb	17/18	12/18	15/18	13/18	8/18

※ **/18: The number of initial values within the range / the number of total events

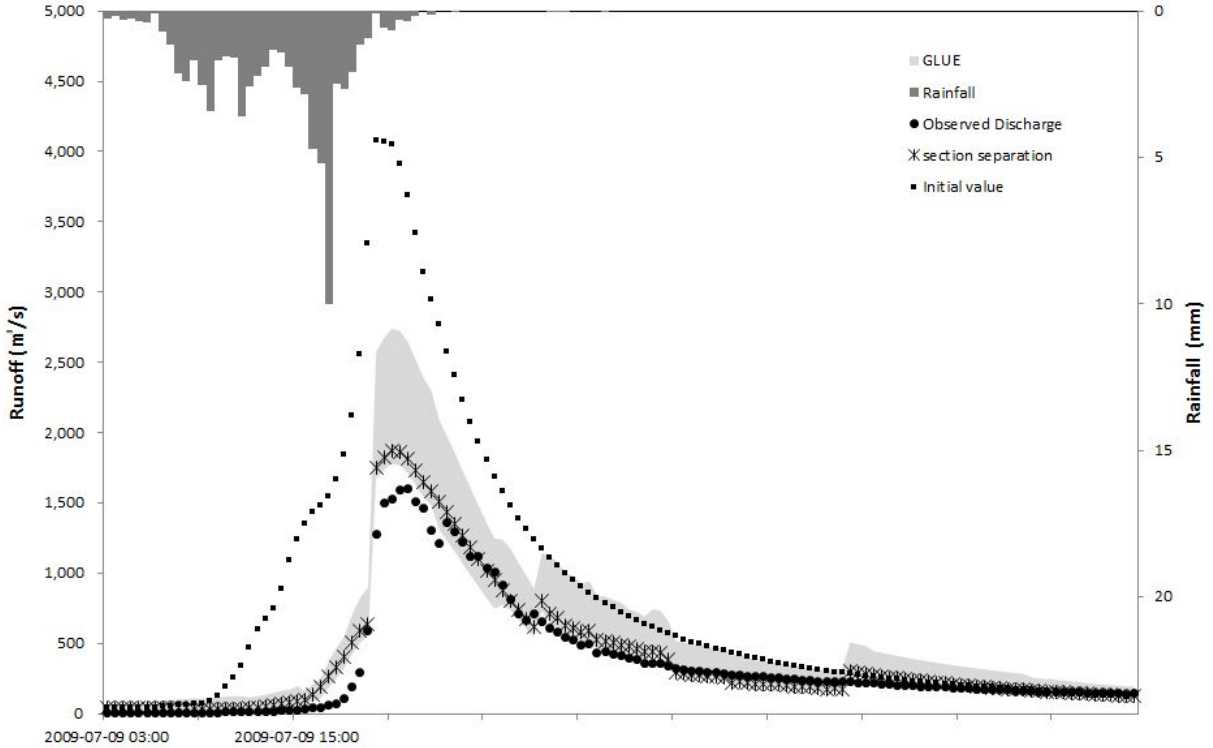

Figure 7.7 Optimal parameter set and range by SCE-UA and GLUE + HSS (2009/07/09 03:00 – 07/11 20:00)

In particular, the range width of the upper bound at the occurrence point of peak flow is larger. Here, the simulated runoff using the existing initial parameter values for each sub-basin shows a significant difference from the simulated results using the optimal parameter set estimated by the proposed methodology in this research. In the case of the existing initial parameter values that have been used in practice, it is determined that only some of which are included within the range of the optimal parameter set at the beginning phase and the falling limb of hydrograph partly.

7.2 Flood Forecasting Using a Parameter Set

The optimal parameter sets for each distinctive section of a hydrograph were estimated by applying SCE-UA and HSS based on the time series of historical data. At the same time, the range for its parameter set was determined by uncertainty analysis using GLUE to help model users in the selection of more preferable parameters within the optimal parameters according to the conditions as simulation.

By applying GLUE, the first 1,000 sets of random number were generated to have the initial value of parameters, and it was repeated 1,000 times. Then, the likelihood function was calculated to provide a weight, and the best sets of weighted parameters was collected. Among them, only selected parameter sets (a total of 1,940 sets) with a confidence interval of 90 % could be used for application in the study basin in this research.

In practical works, the initial values of the parameter estimated through the trial-and-error method are used to forecast future rainfall events. As the efficiency of simulation is lower than what is expected, randomly, the values of a few parameters

are likely to be modified to increase the efficiency. However, this approach can cause a local optimum, and it was not said that it uses optimal parameters.

To improve this limitation of the trial-and-error method, GLUE was applied to suggest the range of optimal parameters for a model user's reference as summarized in Table 7.4. Apart from the optimal parameter set suggested as a priority, a model user can select a proper parameter set from the range estimated by GLUE. In Table 7.4, the parameter set with the best value of NSE in the first column is used by priority for flood forecasting, but future rainfall events cannot be well simulated. It is because there are still uncertainties remaining. Although the results in Table 7.4 were optimized by taking a warming-up period for 1 year, a calibration period for 4 years, and a verification period for 2 years, it is impossible to excellently simulate future rainfall events. In this case, it is strongly recommended for a model user to select the set of parameter with the next priority instead of arbitrary changing any parameter according to his/her preference. It is expected that this approach can prevent a local optimum and contribute to the improvement of the reliability of flood forecasting results.

Table 7.4 Priorities in optimal parameters for the storage function model

SCE-UA (EP + HSS)		K	P	Tl	F1	R_{sa}	NSE
Rising Limb	Set1	24.900	0.550	4.500	0.500	124.00	0.891
	Set2	23.600	0.6000	4.0000	0.5500	153.00	0.891
	Set3	23.600	0.6000	4.0000	0.7000	8.00	0.890
	Set4	21.100	0.6000	4.7000	0.5500	147.00	0.886
	Set5	18.600	0.7000	4.3000	0.3000	153.00	0.883
	Set6	22.200	0.6500	3.5000	0.7000	162.00	0.881
	Set7	22.300	0.6500	3.5000	0.4500	63.00	0.881
	Set8	16.100	0.7500	4.0000	0.6500	7.00	0.879
	:	:	:	:	:	:	:
Crest	Set1	24.900	0.750	2.700	0.650	38.00	0.662
	Set2	24.100	0.750	3.700	0.550	40.00	0.661
	Set3	24.100	0.800	3.500	0.750	53.00	0.659
	Set4	24.200	0.800	2.800	0.600	50.00	0.659
	Set5	23.200	0.750	3.900	0.450	139.00	0.651
	Set6	23.500	0.850	2.900	0.700	37.00	0.649
	Set7	24.100	0.700	3.100	0.050	75.00	0.647
	Set8	24.500	0.800	2.200	0.700	133.00	0.647
	:	:	:	:	:	:	:
Falling Limb	Set1	24.400	0.950	9.200	0.850	82.000	0.682
	Set2	24.700	0.950	10.300	0.400	40.00	0.667
	Set3	24.900	0.850	7.600	0.200	158.00	0.659
	Set4	23.600	0.900	9.400	0.200	34.00	0.656
	Set5	24.400	0.900	10.100	0.150	109.00	0.656
	Set6	24.000	0.850	9.000	0.750	159.00	0.649
	Set7	22.700	0.950	9.600	0.350	79.00	0.639
	Set8	22.600	0.950	9.700	0.150	66.00	0.634
	:	:	:	:	:	:	:

8. Conclusions and Future Study

8.1 Conclusions

This research examined the validity of the existing parameter estimation approach used in domestic practice and raised a problem in relying on a single rainfall event rather than a time series. To improve the existing methodology, a global optimization method, SCE-UA was applied and its performance for parameter estimation was determined. Furthermore, HSS was newly proposed to conduct parameter estimation reflecting runoff properties for each separated section of hydrograph. The applicability of HSS was identified by assessing the efficiency of estimated parameters through HSS and the potential applicability of HSS to future rainfall events was also determined.

In summary, the findings of this research are summarized as follows:

(1) *Diagnosed problems in parameter estimation for flood forecasting used in domestic practice*

One of the problems in model parameter estimation for flood forecasting in domestic use is to use the mean value of parameters estimated from each rainfall event of the historical data. Parameter estimation based on each single event from the historical data is depending on the hypothesis that the soil in the watershed is fully saturated. However, it is determined that this assumption is improper for storage function model which is sensitive to precedent rainfall events and soil saturation. Rather than the NSE (-1.965) as using just a single event, the value of NSE (0.688) as applying time-series data is significantly improved

In general, the trial-and-error method, which has been widely used as estimating parameters, is likely to bring out a local optimum. It is because a case, which satisfies the objective function because of a change of only a single arbitrary parameter among the parameter set to be estimated, can occur.

(2) *Improved problems in parameter estimation used in practice*

The trial-and-error method is likely to generate a local optimum. Instead, it is strongly recommend to use a global optimization method, such as SCE-UA for parameter estimation. The mean value of NSE that applies parameter initial values

estimated by the trial-and-error method based on each rainfall event of historical data is just -1.965, which indicates a lower efficiency of model simulation. On the other hand, the value of NSE that applies SCE-UA based on each event is 0.659, which indicates an improvement in model efficiency.

By considering aspects of rainfall events, to increase reliability in parameter estimation, a time-series that covers the entire data period available should be used for long-term simulation rather than a fragmented parameter estimation based on each event of historical data. The value of NSE that applies SCE-UA based on a time-series data is 0.725, which also shows, an improvement in efficiency compared to that obtained by applying SCE-UA based on each rainfall event.

In consequence, it is identified that applying SCE-UA based on a time-series data shows much better results in the efficiency compared to the existing approach of applying the trial-and-error method based on each rainfall event.

(3) *Estimated parameters that reflect temporal runoff properties through HSS*

Despite the parameters estimated by applying SCE-UA based on a time series data were obtained, there were some cases in which the hydrograph generated based on

these estimated parameters could not reproduce time-series patterns of observed data. It was determined that this might be because estimated parameters could not sufficiently reflect runoff properties of hydrograph. In this regard, HSS was newly proposed in this research. In short, HSS is a new approach in parameter estimation that separates a hydrograph into three sections that represent different runoff characteristics.

To conduct HSS, first, the moving average method was applied to find the overlapping range between each first inflection point appearing at the left and right sides on the basis of occurrence time of peak flow. Then, finally the inflection point to separate each section on a hydrograph was obtained. The applicability of HSS was identified by reviewing various aspects such as the size of peak flow, rainfall duration, and patterns of time series. It is expected that this review and consideration of the various aspects available can somewhat contribute to overcome the limitation of this research, which shows a definitive result obtained from a single basin.

As the value of NSE that indicates the simulation efficiency was different between the rising limb and the falling limb of a hydrograph, a hydrograph was divided into three section: - rising limb, crest and falling limb - according to the inflection point on a hydrograph. Although a concern in which the number of the required parameter

should be tripled by applying HSS, it hardly affected the total running time of storage function simulation. Moreover, by applying the HSS method, the NSE showed much improved values, with 0.799, 0,765 and 0.788 for each section. It verifies that reliability was improved as well.

(4) Estimated the optimal parameter set through a global optimization and presented its reasonable range through uncertainty analysis

The optimal parameter set for storage function model by applying SCE-UA based on historical time series was presented. Even if the optimal parameter set was suggested, it is quite dangerous to assert that this parameter set will satisfy all the cases of rainfall in the future. Therefore, this research, also, presented both the optimal parameter set and its range to help model users select more appropriate parameters according to the conditions as simulation in the future.

In this research, the storage function model was simulated by using the initial parameter value that has used in flood forecasting practice for a long time and by using the optimal parameter estimated by applying the global optimization method, SCE-UA. Then, through the result comparison of each methodology, the efficiency in parameter

estimation by using SCE-UA was determined. In order to consider the uncertainty in parameter estimation, the GLUE method was used to compute the range of the optimal parameter. In addition, in order to improve the reliability in parameter estimation, the HSS method enabling to estimate the appropriate parameters regardless of the rainfall duration and the number of events was newly proposed and its applicability was identified through the application in the actual basin. It was determined that HHS could contribute to improve the accuracy in parameter estimation regarding various response patterns of hydrologic runoff.

8.2 Future Study

By considering the methodological aspects, to improve the accuracy of parameter sensitivity analysis it needs to analyze the relative sensitivity between parameters qualitatively. It would also be helpful to conduct quantitative sensitivity analysis of each parameter for the model. In addition, a stochastic approach for uncertainty analysis needs to be considered to be compared with the results of this results. Quantitative analysis of the proportion of the parameter uncertainty in the total

uncertainty generated during hydrological model simulation also needs to be considered in the future study.

By considering the application aspects, the hydrologic model, applied in this study is limited to only the storage function model used in domestic practice. To expand the applicability of the findings in this research, it might be necessary to apply more various types of hydrologic model with a wider variety of characteristics such as a distributed model. In this research, only the proposed methodology has been applied to a single sub-basin for the identification of applicability; however, additional studies are determined to assess the applicability of the proposed method in various basins and watersheds with a wider variety of hydrological and morphological characteristics.

Finally, for the newly proposed HSS method in this research, the concern in the disparate that occur in both axes of time and runoff when each sectional hydrograph (rising limb, crest, and falling limb) produced through HSS is synthesized needs to be improved. Furthermore, it is expected to determine the multiple utilization of the inflection point estimation method proposed in this research in comparison to the

existing hydrograph separation methods that focus on the separation of base flow from total volume.

REFERENCES

Ajami, N.K., Duan, Q., and Sorooshian, S. (2007). "An integrated hydrologic Bayesian multimodel combination framework: Confronting input, parameter, and model structure uncertainty in hydrologic prediction." Water Resource Research, Vol. 43, Issue 1, W01403.

Ajami, N.K., Gupta, H., Wagener, T., and Sorooshian, S. (2004). "Calibration of a semi-distributed hydrologic model for streamflow estimation along a river system." Journal of Hydrology, Vol. 298, Issues 1-4, pp. 112-135.

Bahremand, A., De Smedt, F., Corluy, J., Liu, Y.B., Poorova, J., Velcicka, L., and Kunikova, E. (2007). "WetSpa model application for assessing reforestation impacts on floods in Margecany-Hornad watershed, Slovakia." Water Resources Management, Vol. 21, Issue 8, pp. 1373-1391.

Bekele, E.G. and Nicklow, J.W. (2007). "Multi-objective automatic calibration of SWAT using NSGA-II." Journal of Hydrology, Vol. 341, Issues 3-4, pp. 165-176.

Beven, K. and Binley, A. (1992). "The future of distributed models: Model calibration and uncertainty prediction." Hydrological Processes, Vol. 6, Issue 3, pp. 279-298.

Beven, K. and Freer, J. (2001). "Equifinality, data assimilation, and uncertainty estimation in mechanistic modelling of complex environmental systems using the GLUE methodology." Journal of Hydrology, Vol. 249, Issues 1-4, pp. 11-29.

Beven, K.J. and Kirkby, M.J. (1979). "A physically based, variable contributing area model of basin hydrology." Hydrological Sciences Bulletin, Vol. 24, Issue 1, pp. 43-69.

Blasone, R.S., Vrugt, J.A., Madsen, H., Rosbjerg, D., Robinson, B.A., and Zyvoloski, G.A. (2008). "Generalized Likelihood Uncertainty Estimation (GLUE) using adaptive Markov Chain Monte Carlo sampling." Advances in Water Resources, Vol. 31, Issue 4, pp. 630-648.

Boyle, D.P., Gupta, H.V., and Sorooshian, S. (2000). "Toward improved calibration of hydrologic models: Combining the strengths of manual and automatic methods." Water Resources Research, Vol. 36, Issue 12, pp. 3663-3674.

Brath, A. and Rosso, R. (1993). "Adaptive calibration of a conceptual model for flash flood forecasting." Water Resources Research, Vol. 29, Issue 8, pp. 2561-2572.

Butts, M.B., Payne, J.T., Kristensen, M., and Medsen, H. (2004). "An evaluation of the impact of model structure on hydrological modelling uncertainty for streamflow simulation." Journal of Hydrology, Vol. 298, Issues 1-4, pp. 242-266.

Cho, H. and Olivera, F. (2014). "Application of multi-modal optimization for uncertainty estimation of computationally expensive hydrologic models." Journal of Water Resources Planning and Management, Vol. 140, Issue 3, pp. 313-321.

Cho, H., Kim, D., and Lee, K. (2014). "Efficient uncertainty analysis of TOPMODEL using particle swarm optimization." Journal of Korea Water Resources Association, Vol. 47, Issue 3, pp. 285-295. *(In Korean with English Abstract)*

Choi, S.H. (2004). "Introduction to global optimization techniques: deterministic and stochastic methods." ICASE MAGAZINE, Vol. 10, Issue 3, pp. 27-33. *(In Korean)*

Cho, I., Woo, H., Kim, J., and Lee, H. (2005). "Application of evolution algorithm for automatic calibration of water distribution models. " Proceedings of Fall Joint-Conference in 2005 by KSWW·KSWE, pp. 126-131. *(In Korean with English Abstract)*

Chow, V.T., Maidment, D.R., and Mays, L.W. (1988). Applied hydrology. McGraw-Hill.

Chung, G., Park, H.S., Sung, J.Y., and Kim, H.J. (2012). "Determination and evaluation of optimal parameters in storage function method using SCE-UA." Journal of Korea Water Resources Association, Vol. 45, Issue 11, pp. 1169-1186. *(In Korean with English Abstract)*

Doherty, J. and Johnston, J.M. (2003). "Methodologies for calibration and predictive analysis of a watershed model." Journal of the American Water Resources Association, Vol. 39, Issue 2, pp. 251-265.

Duan, Q., Sorooshian, S., and Gupta, V. (1992). "Effective and Efficient Global Optimization for Conceptual Rainfall-Runoff Models." Water Resources Research, Vol. 28, Issue 4, pp. 1015-1031.

Duan, Q., Sorooshian, S., and Gupta, V.K. (1994). "Optimal use of the SCE-UA global optimization method for calibrating watershed models." Journal of Hydrology, Vol. 158, Issues 3-4, pp. 265-284.

Eckhardt, K. and Arnold, J.G. (2001). "Automatic calibration of a distributed catchment model." Journal of Hydrology, Vol. 251, Issues 1-2, pp. 103-109.

Gan, T.Y. and Biftu, G.F. (1996). "Automatic calibration of conceptual rainfall-runoff models: Optimization algorithms, catchment conditions and model structure." Water Resources Research, Vol. 32, Issue 12, pp. 3513-3524.

Gong, Y., Shen, Z., Hong, Q., Liu, R., and Liao, Q. (2011). "Parameter uncertainty analysis in watershed total phosphorus modeling using the GLUE methodology." Agriculture, Ecosystems & Environment, Vol. 142, Issues 3-4, pp. 246-255.

Gupta, H.V., Sorooshian, S., and Yapo, P.O. (1998). "Toward improved calibration of hydrologic models: Multiple and noncommensurable measures of information." Water Resources Research, Vol. 34, Issue 4, pp. 751-763.

Gupta, H.V., Wagener, T., and Liu, Y. (2008). "Reconciling theory with observations: Elements of a diagnostic approach to model evaluation." Hydrological Processes, Vol. 22, Issue 18, pp. 3802-3813.

Haan, C.T., Storm, D.E., Al-Issa, T., Prabhu, S., Sabbagh, G.J., and Edwards, D.R. (1998). "Effect of parameter distributions on uncertainty analysis of hydrologic models." Transactions of the ASAE, Vol. 41, Issue 1, pp. 65-70.

Han River Flood Control Office, MOCT (1991). Improvement of Han River watershed runoff program. *(In Korean)*

Han River Flood Control Office, MOLIT (2011). Improvement of flood forecasting framework using a stochastic methodology. *(In Korean)*

Holland, J.H. (1975). Adaptation in natural and artificial systems. MIT Press, Cambridge, Mass.

Hope, A.S., Stein, A.K., and McMichael, C.E. (2004). "Uncertainty in monthly river discharge predictions in a semi-grid shrubland catchment." Proceedings of the British Hydrological Society International Conference - Hydrology: Science & Practice of the 21th Century, Vol. 1, pp. 284-290.

Hornberger, G.M. and Spear, R.C. (1981). "Approach to the preliminary analysis of environmental systems." Journal of Environmental Management. Vol. 12, pp. 7-18.

Huff, F.A. (1967). "Time Distribution of rainfall in heavy storms." Water Resources Research, Vol. 3, Issue 4, pp. 1007-1019.

Hughes, D.A., Kapangaziwiri, E., and Sawunyama, T. (2010). "Hydrological model uncertainty assessment in southern Africa." Journal of Hydrology, Vol. 387, Issue 3-4, pp. 221-232.

Hwang, K.S. (2003). Development of leak detection program for water distribution system using remoted meter-reading. Master thesis, Dong-A University, Korea. *(In Korean with English Abstract)*

Jang, S.W. (2012). Uncertainty analysis due to HEC-HMS model parameters in rainfall-runoff simulations. Master thesis, Seoul National University, Korea. *(In Korean with English Abstract)*

Joh, H.K., Park, J.Y., Jang, C.H., and Kim, S.J. (2012). "Comparing prediction uncertainty analysis techniques of SWAT simulated streamflow applied to Chungju dam watershed." Journal of Korea Water Resources Association, Vol. 45, Issue 9, pp. 861-874. *(In Korean with English Abstract)*

Jung, Y., Yeo, K.D., Kim, S.Y., and Lee, S.O. (2013). "The effect of uncertainty in roughness and discharge on flood inundation mapping." Journal of the Korean Society of Civil Engineers, Vol. 33, Issue 3, pp. 937-945. *(In Korean with English Abstract)*Kang, M.G., Park, S.W., Im, S.J., and Kim, H.J. (2002). "Parameter calibrations of a daily rainfall-runoff model using global optimization methods." Journal of Korea Water Resources Association, Vol. 35, Issue 5, pp. 541-552. *(In Korean with English Abstract)*

Kang, S., Kang, T., and Lee, S. (2014). "Application of the SCE-UA to derive zone boundaries of a zone based operation rule for a dam." Journal of Korea Water Resources Association, Vol. 47, Issue 10, pp. 921-934. *(In Korean with English Abstract)*

Kang, T. and Lee, S. (2014). "Modification of the SCE-UA to include constraints by embedding an adaptive penalty function and application: Application approach." Water Resources Management, Vol. 28, Issue 8, pp. 2145−2159.

Kang, T., Lee, S., Kang, S., and Park, J. (2012). "A study for an automatic calibration of urban runoff model by the SCE-UA." Journal of Korea Water Resources Association, Vol. 45, Issue 1, pp. 15-27. *(In Korean with English Abstract)*

Kavetski, D., Franks, S., and Kuczera, G. (2002). "Confronting input uncertainty in environmental modeling." Calibration of Watershed Models. AGU WSA Series.

Kavetski, D., Kuczera, G., and Franks, S.W. (2006). "Bayesian analysis of input uncertainty in hydrological modeling: 1. Theory." Water Resources Research, Vol. 42, Issue 3, W03407.

Khu, S.T. and Madsen, H. (2005). "Multiobjective calibration with Pareto preference ordering: An application to rainfall-runoff model calibration." Water Resources Research, Vol. 41, No. 3.

Kim, B.S, Kim, B.K., and Kwon, H.H. (2009). "Evaluation of the uncertainties in rainfall-runoff model using meta-Gaussian approach." Journal of Korean Wetlands Society, Vol. 11, Issue 1, pp. 49-64 *(In Korean with English Abstract)*

Kim, H.K., Kang, M.S., Park, S.W., Choi, J.Y., and Yang, H.J. (2009). "Auto-calibration for the SWAT model hydrological parameters using multi-objective optimization method." Journal of the Korean Society of Agricultural Engineers, Vol. 51, Issue 1, pp. 1-9. *(In Korean with English Abstract)*

Kirkpatrick, S., Gelatt, C.D., and Vecchi, M.P. (1983). "Optimization by Simulated Annealing." Science, Vol. 220, I 4598, pp. 671-680.

Klepper, O., Scholten, H., and Kamer, J.P.G. (1991). "Prediction uncertainty in an ecological model of the Osterschelde Estuary." Journal of Forecasting, Vol. 10, Issue 1-2, pp. 191-209.

Kuczera, G. (1994). A Bayesian nonlinear regression program suite, Version 1.00g. Department of Civil Engineering and Surveying, University of Newcastle, New South Wales.

Kuczera, G. (1997). "Efficient subspace probabilistic parameter optimization for catchment models." Water Resources Research, Vol. 33, Issue 1, pp. 177-185.

Kuczera, G. and Parent, E. (1998). "Monte Carlo assessment of parameter uncertainty in conceptual catchment models: the Metropolis algorithm." Journal of Hydrology, Vol. 211, Issue 3-4, pp. 69-85.

Kwon, H.H. and Moon, Y.I. (2005). "An analysis of the rainfall-runoff of natural watershed using the hydraulic routing method." Journal of Korea Water Resources Association, Vol. 38, Issue 7, pp. 555-564. *(In Korean with English Abstract)*

Kwon, H.H., Moon, Y.I., Kim, B.S., and Yoon, S.Y. (2008). "Parameter optimization and uncertainty analysis of the NWS-PC rainfall-runoff model coupled with Bayesian Chain Monte Carlo inference scheme." KSCE Journal of Civil Engineering, Vol. 28, Issue No. 4-B, pp. 383-392. *(In Korean with English Abstract)*

Lee, D.H. (2006). "Automatic calibration of SWAT model using LH-OAT sensitivity analysis and SCE-UA optimization method." Journal of Korea Water Resources Association, Vol. 39, Issue 8, pp. 677-690. *(In Korean with English Abstract)*

Lee, E. and Seo, D. (2011). "Flow calibration and validation of Daechung lake watershed, Korea using SWAT-CUP." Journal of Korea Water Resources Association, Vol. 44, Issue 9, pp. 711-720. *(In Korean with English Abstract)*

Lee, H., Jeon, M.W., Balin, D., and Rode, M. (2009). "Application of rainfall runoff model with rainfall uncertainty." Journal of Korea Water Resources Association, Vol. 42, Issue 10, pp. 773-783. *(In Korean with English Abstract)*

Lee, K.S. (2000). Fundamentals of Water Resource Systems. SaeRon Publishing Co.

Lee, K.T. (2011). Improving HEC-HMS model parameter estimation method. Master thesis, Seoul National University, Korea. *(In Korean with English Abstract)*

Lim, H.J., Kwon, H.J., Jang, C.H., and Kim, S.J. (2004). "Runoff hydrological analysis in Soyanggang-dam watershed using SLURP model." Proceeding of KWRA Annual Conference in 2004, pp. 1142-1146. *(In Korean with English Abstract)*

Liong, S.Y., Khu, S.T., and Chan, W.T. (2001). "Derivation of Pareto front with genetic algorithm and neural network." Journal of Hydrologic Engineering, Vol. 6, Issue 1, pp. 52-61.

Liu, Y.B. and De Smedt, F. (2005). "Flood modeling for complex terrain using GIS and remote sensed information." Water Resources Management, Vol. 19, Issue 5, pp. 605-624.

Loukas, A., Vasiliades, L., and Dalezios, N.R. (2002). "Climatic impacts on the runoff generation processes in British Columbia, Canada." Hydrology and Earth System Sciences, Vol. 6, Issue 2, pp. 211-228.

Madsen, H. (2000). "Automatic calibration of conceptual rainfall-runoff model using multiple objectives." Journal of Hydrology, Vol. 235, Issues 3-4, pp. 276-288.

Madsen, H. (2003). "Parameter estimation in distributed hydrological catchment modelling using automatic calibration with multiple objectives." Advances in Water Resources, Vol. 26, Issue 2, pp. 205-216.

MOCT and K-water (2004). Report on the status of comprehensive survey in the Han River watershed. *(In Korean)*

Montanari, A. and Brath, A. (2004). "A stochastic approach for assessing the uncertainty of rainfall-runoff simulations." Water Resources Research, Vol. 40, Issue 1, W01106.

Moore, C., Wohling, T., and Doherty, J. (2010). "Efficient regularization and uncertainty analysis using a global optimization methodology." Water Resources Research, Vol. 46, Issue 8, W08527.

Muleta, M.K. and Nicklow, J.W. (2005). "Decision support for watershed management using evolutionary algorithms." Journal of Water Resources Planning and Management, Vol. 131, Issue 1, pp. 35–44.

Oh, K.C. (1998). Uncertainty analysis of rainfall-runoff model through parameter estimation. Doctoral dissertation, Seoul National University, Korea. *(in Korean with English Abstract)*

Park, B.J., Cha, H.S., and Kim, J.H. (1997). "A study in parameters estimation of storage function model using the genetic algorithms." Journal of Korea Water Resources Association, Vol. 30, Issue 4, pp. 347-355.

SeonWoo, J.H. (2010). Hydrology. Dongmyung Publishing Co.

Singh, V.P. (1995). Computer models of watershed hydrology. Water Resources Publications.

Singh, V.P. and Woolhiser, D.A. (2002). "Mathematical modeling of watershed hydrology." Journal of Hydrologic Engineering, Vol. 7, Issue 4, pp. 270-292.

Sorooshian, S., Duan, Q., and Gupta, V.K. (1993). "Calibration of rainfall-runoff models: Application of global optimization to the Sacramento Soil Moisture Accounting Model." Water Resources Research, Vol. 29, Issue 4, pp. 1185-1894.

Spear, R.C., Crieb, T.M., and Shang, N. (1994). "Parameter uncertainty and interaction in complex environmental models." Water Resources Research, Vol. 30, Issue 11, pp. 3159-3169.

Sung, Y.K., Kim, S.H., Kim, H.J., and Kim, N.W. (2004). "The applicability study of SYMHYD and TANK model using different type of objective functions and optimization methods." Journal of Korea Water Resources Association, Vol. 37, Issue 2, pp. 121-131. *(in Korean with English Abstract)*

Tang, Y., Reed, P., and Wagener, T. (2006). "How effective and efficient are multiobjective evolutionary algorithms at hydrologic model calibration?." Hydrology and Earth System Sciences, Vol. 10, pp. 289–307.

Van Griensven, A., Francos, A., and Bauwens, W. (2002). "Sensitivity analysis and auto-calibration of an integral dynamic model for river water quality." Water Science and Technology, Vol. 45, Issue 9, pp. 325-332.

Vrugt, J.A., Gupta, H.V., Bouten, W., and Sorooshian, S. (2003). "A shuffled complex evolution metropolis algorithm for optimization and uncertainty assessment of hydrological model parameters." Water Resource Research, Vol. 39, Issue 8, SWC1-18.

Wagener, T. (2003). "Evaluation of catchment models." Hydrological Processes, Vol. 17, Issue 16, pp. 3375-3378.

Wagener, T. and Gupta, H.V. (2005). "Model identification for hydrological forecasting under uncertainty." Stochastic Environmental Research and Risk Assessment, Vol. 19, Issue 6, pp. 378-387.

Wheater, H.S., Jakeman, A.J., and Beven, K.J. (1993). Progress and directions in rainfall-runoff modeling. John Wiley & Sons, pp. 101-132.

Wohling, T., Vrugt, J.A., and Barkle, G.F. (2008). "Comparison of three multiobjective optimization algorithms for inverse modeling of Vadose zone hydraulic properties." Soil Science Society of America Journal, Vol. 72, Issue 2, pp. 305−319.

Yapo, P.O., Gupta, H.V., and Sorooshian, S. (1998). "Multi-objective optimization for hydrologic models." Journal of Hydrology, Vol. 204, Issue 1, pp. 83-97.

Yar, M. and Chatfield, C. (1990). "Prediction intervals for the Holt-Winters forecasting procedure." International Journal of Forecasting, Vol. 6, Issue 1, pp. 127-137.

Yoon, Y.N. (2009). Engineering Hydrology. Cheongmoongak Publishing.

초 록

수문곡선 구간분리와 불확실성 분석을 통한 수문 모형의 매개변수 추정 개선

강우-유출 모형을 이용한 모의과정에서 매개변수 추정은 필수적이며 모의결과에 가장 큰 영향을 미치게 된다. 그러나 현재까지 강우-유출 모형의 매개변수 추정을 위한 표준화된 기법이나 절차가 마련되지 못하였다. 매개변수의 불확실성과 변동성으로 인해 최적의 매개변수 추정 기법과 일반화된 추정 과정을 제시하는 것이 어렵기 때문에 매개변수 추정 과정은 선택한 모형, 적용된 강우사상, 모형 사용자에 따라 다르게 이루지고 있다.

강우-유출 모형의 매개변수를 추정할 때 목적함수가 명확하게 정의되지 못하거나 제한된 수의 강우 사상만을 고려하면 추정된 매개변수의 신뢰도가 낮아지는 문제가 발생한다.

따라서 매개변수간의 특성 및 상관관계를 고려할 수 있으며 선택된 수문모형과 모형 사용자 특성에 영향 받지 않고 일정한 값을 제시할 수 있는 방법이 필요하다. 또한 매개변수 추정 기법은 강우 규모와 유출 특성 등 개별적 강우 사상의 특성을 고려할 수 있어야 한다. 이는 각각의 강우 사상에 대한 모형별 반응양상이 매우 다채롭기 때문이다.

국내 실무에서 홍수예측시 사용하고 있는 매개변수 추정과정을 살펴보았다. 시행착오법을 통해 과거 홍수사상별로 추정된 매개변수를 초기값으로 사용하여 홍수사상을 예측하고 있다. 홍수예측의 신뢰성을 확보하기 위해 매개변수 추정과정을 개선해야 한다.

이러한 문제점을 개선하고자 본 연구에서는 과거 호우사상별 매개변수를 추정하는 것이 아니라 전기간을 대상으로 하는 장기 모의를 통한 매개변수 추정의 효율을 검토하였다. 또한 매개변수 추정기법으로 시행착오법이 아닌 매개변수 집합군을 추정하여 최적 매개변수를 제시하는 전역최적화 기법(SCE-UA, Shuffled Complex Evolution of University Arizona)을 사용한 결과를 비교, 분석하였다.

매개변수 추정시 유출 수문곡선의 유출특성을 반영하기 위해 수문곡선 구간 분리를 통해 구간별 매개변수 추정방법을 제시하였다. 수문곡선상의 변곡점(inflection point)을 기준으로 수문곡선을 세 구간(rising limb, crest, falling limb)으로 분리하여 각 구간별로 매개변수를 추정하여 효율을 검토하였다. 본 연구에서 제안하는 기법은 강우 사상과 유출 특성을 고려하여 발생하는 매개변수 추정의 변동성 문제를 개선하고자 한 것이다. 또한 불확실성 분석 방법 중 resampling 방법으로 GLUE(Generalized Likelihood Uncertainty Estimators)를 적용하여 최적 매개변수 집합뿐만 아니라 매개변수 범위를 함께 제시함으로써 매개변수 추정 결과의 신뢰도를 향상시키고 적용성을 강화하고자 하였다.

본 연구의 궁극적인 목적은 최적의 매개변수를 도출할 수 있는 매개변수 추정을 시도하는 것이며 제시된 기법은 강우-유출 모의시 첨두유량과 총유량을 모두 만족시킬 수 있으며 동시에 유출 규모와 유량 이동특성까지 반영할 수 있을 것으로 기대된다.

주요어 : 매개변수 추정, 전역최적화 기법, SCE-UA, 수문곡선 분리, GLUE, 최적 매개변수

학 번 : 2005-30253